ANALYSIS OF PI(3,5)P_2 THROUGHOUT MITOSIS

by

Cansu Dilege

A Dissertation Submitted to the
Graduate School of Sciences and Engineering
in Partial Fulfilment of the Requirements for
the Degree of
Master of Science
in
Molecular Biology and Genetics

KOÇ
UNIVERSITY

July 2022

ANALYSIS OF PI(3,5)P_2 THROUGHOUT MITOSIS

Koç University

Graduate School of Sciences and Engineering

This is to certify that I have examined this copy of a master's thesis by

Cansu Dilege

and have found that it is complete and satisfactory in all respects,
and that any and all revisions required by the final
examining committee have been made.

Committee Members:

Assist Prof. Ayşe Koca Çaydaşı (Advisor- Koç University)

Prof. Devrim Gözüaçık, MD PhD (Koç University)

Assist. Prof. Hüseyin Çimen (Yeditepe University)

Date: 19/07/2022

To my family, and my friends who always supported me

ABSTRACT

ANALYSIS OF PI(3,5)P_2 THROUGHOUT MITOSIS

Cansu Dilege

Master of Science in Molecular Biology and Genetics

July 19, 2022

Phosphatidylinositol 3,5-bisphosphate (PI(3,5)P_2) is a low abundant phosphatidylinositol derivative involved in several signaling and regulatory pathways such as membrane fusion/fission, Ca^{+2} signaling, vacuolar acidification, selective and bulk autophagy, stress response, Multi vesicular body (MVB) pathway and RNA granule transportation. Previous genetic screens in budding yeast identified upstream regulators of PI(3,5)P_2 which are *VAC7, VAC14* and *FAB1* among genes necessary for growth of mitotic exit defective cells, which suggest a novel role for PI(3,5)P_2 in mitosis, specifically during mitotic exit. In this thesis we aimed investigating the interplay between mitosis and PI(3,5)P_2. We first asked whether PI(3,5)P_2 synthesis is regulated by the cell cycle. To this end, we analyzed localization and levels of Atg18, a known PI(3,5)P_2 effector, throughout the cell cycle by using fluorescence live cell microscopy. Atg18-GFP localized to the vacuole membrane dependent on PI(3,5)P_2 and Vac7. We showed that Atg18-GFP predominantly localized at the periphery of the daughter vacuole rather than mother vacuole during mitosis. We next asked which proteins PI(3,5)P_2 interacts with during mitosis. We employed a pull-down approach using mitotic cell extracts and PI(3,5)P_2 coated beads. Net1, a nucleolar protein that binds the mitotic exit triggering phosphatase Cdc14, was pulled down with PI(3,5)P_2. In addition, several ribosomal and rRNA related proteins such as; RPS11B, RPL24A, RPL5, NSR1, RVB2 came out as hits of our assay.

Taken together, daughter specific localization of Atg18 and thus PI(3,5)P_2 may indicate a daughter-specific role in the asymmetric cell division of budding yeast. In addition, potential PI(3,5)P_2 interactors may be the link to the functions of PI(3,5)P_2 in mitotic exit, rRNA granule transportation and translation. Further studies such as using Western Blotting approaches, lipid strips, colocalization assays and growth assays will reveal the functional significance of the asymmetric PI(3,5)P_2 synthesis as well as the specificity and significance of identified novel PI(3,5)P_2 interactors.

ÖZETÇE

$PI(3,5)P_2$'NUN MİTOZ BOYUNCA ANALİZİ

Cansu Dilege

Moleküler Biyoloji ve Genetik, Yüksek Lisans

Temmuz 19, 2022

Fosfatidilinositol 3,5-bifosfat ($PI(3,5)P_2$), membran füzyonu/fisyonu, Ca^{+2} sinyali, koful asitliği, seçici ve genel otofaji, stres tepkisi, MVB yolu, RNA granül taşınması gibi çeşitli sinyalleme ve düzenleyici yolaklarda yer alan az miktarda bulunan bir fosfatidilinositol türevidir. Tomurcuklanan mayada gerçekleştirmiş önceki genetik araştırmalar *VAC7*, *VAC14* ve *FAB1* gibi $PI(3,5)P_2$ regülatörlerini mitozdan çıkışta görevli genlerin iyi çalışmadığı durumda hücre bölünmesi için gerekli genler arasında bulundu. Bu tezde mitoz ve $PI(3,5)P_2$ arasındaki etkileşimi araştırmayı amaçladık.

Önce $PI(3,5)P_2$ sentezinin hücre döngüsü tarafından düzenlenip düzenlenmediği soğulandı. Bu amaçla, florasan hücre mikroskobu kullanılarak hücre döngüsü boyunca bilinen bir $PI(3,5)P_2$ efektörü olan Atg18'in lokalizasyonu ve seviyeleri analiz edildi. Atg18-GFP'nin, PI(3,5)P2 ve Vac7'ye bağlı olarak koful zarına lokalize olduğu görüldü. Atg18-GFP'nin ağırlıklı olarak mitoz sırasında ana hücrenin kofulundan ziyade yeni oluşan hücre kofulunun çevresinde lokalize olduğunu görüldü. Daha sonra, mitoz sırasında $PI(3,5)P_2$ 'nin hangi proteinlerle etkileşime girdiği araştırıldı. Bunun için mitotik hücre pelletleri ve $PI(3,5)P_2$ kaplı boncuklar kullanarak presipitasyon yaklaşımı kullandık. Mitotik çıkışı tetikleyen fosfataz Cdc14'ü bağlayan bir nükleolar protein olan Net1, $PI(3,5)P_2$ kaplı boncuklar üzerinde tespit edildi. Ek olarak, presipitasyon deneyinin sonucunda ribozomal ve rRNA ile ilgili proteinler de elde edilmiştir.

Birlikte ele alındığında, Atg18'in yavru hücreye özgü lokalizasyonu ve dolayısıyla $PI(3,5)P_2$ tomurcuklanan mayanın asimetrik hücre bölünmesinde yavruya özgü bir rolü olduğunu gösterebilir. Ek olarak, potansiyel $PI(3,5)P_2$ efektörleri mitotik çıkış, rRNA granül taşınması ve translasyonda $PI(3,5)P_2$ 'nun görevleri olabilir. İlerleyen çalışmalar asimetrik $PI(3,5)P_2$ sentezinin fonksiyonel önemini ve ayrıca tanımlanan yeni $PI(3,5)P_2$ efektörlerinin özgüllüğünü ve önemini ortaya çıkaracaktır.

ACKNOWLEDGEMENTS

This study is funded by The Scientific and Technological Research Council of Turkey (TÜBİTAK grant no: 117Z232). I would like to give my thanks to TÜBİTAK for its support.

I would like to express my sincere gratitude to Assist Prof. Dr. Ayşe Koca Çaydaşı for her guidance and wisdom. She helped me through this process and directed me to the correct path. I would especially want to thank her patience throughout this process. And mostly I loved how we were able to discuss and troubleshoot. Other than hard work we had fun a lot.

Also, I would like to give my thanks to Assoc. Prof. Dr. Nurhan Özlü for her guidance and for being my co-advisor throughout my masters. I would also like to give my thanks to Assoc. Dr. Nurcan Tunçbağ for her assistance and guidance especially for bioinformatic analysis part.

I would also thank a lot to my family for supporting me through this process. It was not easy, and they were like an anchor for me. They listened to me and helped me a lot with everything. It was so helpful to share every stressful moment with them. Especially my sister Ece, who supported me through everything day and night, my mother Figen who always listened to me and loved me and my father Şükrü for his wisdom who always guided me through everything I need.

I would like to present my special gratitude to my friends. They were always here. I remember the fun nights we spent together gossiping and laughing about everything. It was also nice to know they were always here when I needed to cry and vent. I would like to thank a lot to Helin Gültekin, you will always be my sister whether you like it or not. We shared basically every stressful moment together and you were always there when I needed you; to Tuğçe Şahin I will always be with you and even though we did not know each other well in college I am so happy to get to know you when I did, I love you. You will always be my best friend and I sincerely hope to finish whatever educational step we have together; to Beste Senem, I will never forget your curly hair and smile. Thanks for being one of my best friends, and your endless love and support; Hüseyin Karabürk, I can say that you always made me laugh. I loved sharing my bench with you in the lab. I loved our singing times during the day, and I loved so much gossiping with you. You are missed a lot; to İdil Kırdök my twin in the lab. We started the same time in the lab, and I can’t express how much I enjoy working with you. I am following your footsteps.

See you in Europe! I would like to express my gratitude to Hakan Sevgili and Gökalp Bayram. You guys are the best people I have ever met, thanks for being in my life and supporting me. Also for Ilayda Koşağan and Barlas Çelik, thanks for being with me and enduring my psychological tantrums since high school, I love you guys.

I would also like to present my thanks to the present and former lab members of AKC lab. You helped me a lot, troubleshooting with you and laughing together made me feel “not alone” in this journey. Şeyma Nur, thanks for judging me whenever I needed to be shaking down, we shared a lot with you, and I am really glad that I got to know some as strong and independent as you. Mariam, you were always so understanding and compassionate towards me, whenever we hugged, I felt like my mom was holding me. Mukadder, in every depressive moment I had

we shared it together, I will always cherish that. I am leaving you my pipettes so may they bring some hope in you! Atakan, I can’t thank you enough for supporting me every time I needed, not to mention cheering me up in my down moments. Thank you for the memories. Sevilay, I loved how we rolled our eyes together when we “judge” something. You always understood me, it was such a nice experience to sit with you and glancing the stuff you watch every morning. I had a lot of fun with you. Barış, you knew just the right thing to say whenever I needed confidence boost, you are one of my best friends and I am glad to have known you. We will meet in Germany my friend! Betülceğizim, I missed you a lot but I loved our conversations and thank you for sometimes staying with me late at nights in the lab just to keep me company. You are wonderful human being.

Finally, I would like to thank to Can çocuk for standing by me through thick and thin you will be missed.

I might forget to mention few names but thank you all for guiding me, supporting me and enduring me. You will always be loved and cherished.

Table of Content

LIST OF TABLES

LIST OF FIGURES

ABBREVIATIONS

APS: Ammonium Persulfate

Atg18: Autophagy-Related Protein 18

CKI: Cyclin Dependent Kinase Inhibitor

DMSO: Dimethyl Sulfoxide

FEAR: Fourteen Early Release Pathway

GAP: GTPase Activating Protein

GEF: Guanine Exchange Factor

LC-MS/MS: Liquid Chromatography Mass Spectrometry

MEN: Mitotic Exit Network

MVB: Multivesicular Body

NET1: Nucleolar Silencing Establishing Factor and Telophase Regulator

$PI(3,5)P_2$: Phosphatidylinositol 3,5 bisphosphate

PI(3)P: Phosphatidylinositol 3 phosphate

SAC: Spindle Assembly Checkpoint

SDS-PAGE: Sodium Dodecyl Sulfate- Polyacrylamide Gel Electrophoresis

SPOC: Spindle Positioning Checkpoint

TCA: Trichloroacetic Acid

TORC1: Target of Rapamycin Complex 1

CHAPTER 1: INTRODUCTION

1.1.Phosphoinositides

Phosphoinositides (PPIs) are produced from the phosphatidylinositol, by phosphorylation of the inositol head at various hydroxyl groups with different combinations (Kim et al., 2011). With these different combinations, seven different PPIs are generated. These are PI(3)P, PI(4)P, PI(5)P which are the mono phosphorylated versions, $PI(3,4)P_2$, $PI(3,5)P_2$, $PI(4,5)P_2$ which are the bis-phosphorylated versions and finally $PI(3,4,5)P_3$ which is the triple-phosphorylated version (Falkenburger et al., 2010). Numbers in parenthesis indicate the position of the hydroxyl group at the inositol head that is phosphorylated in addition to the first position that is always phosphorylated in phosphatidylinositol. PPIs are synthesized by the action of PPI kinases and phosphatases (Auger et al., 1989).

Since PPIs are phospholipid molecules, they reside in membranes. PPIs are signaling lipids. They can locally and instantly modulate signaling pathways by recruiting other signaling molecules and thus regulating pathways. PPIs can directly and indirectly regulate the signaling and by binding directly to the cytosolic domains of membrane proteins they can initiate the signaling cascades. Localization of each PPI is unique which allows them to take charge in different cellular pathways. In addition to differences in their locations, differences in their hydrophobicity allow each PPI to have different sets of effector proteins to regulate different pathways (Junya Hasegawa et al., 2017) (Watt et al., 2002).Not only the different phosphorylation status of the PPI head group but also the acylation of their tail group plays an important role in their variation. Even the slightest difference may affect the interactor proteins of PPIs (Barneda et al., 2019). Size of these acyl chains differs the hydrophobicity of the PPI which causes them to be differently embedded in the membrane which eventually effects their functions.

PPIs regulate very crucial pathways including but not restricted to cell survival, membrane trafficking, transcription regulation, autophagy cell homeostasis. (Achiriloaie et al., 1999; Aikawa & Martin, 2005; Akhtar & Sah, 2020; Alcázar-Román & Wente, 2008; Ann et al., 1997; Balla, 2013). Owing to the diverse signaling pathways PPIs are involved in, loss of PPI homeostasis is associated with many disorders and disease formations such as cancer, neurological diseases, various cardiovascular disorders, diabetes, virulence efficiency, drug resistance, inflammation, tumor cell migration and metastasis, autoimmune diseases, embryonic development and obesity (Bakin et al., 2000; Hassan et al., 1998; Konopka, 2022;

Kunkl et al., 2017; Manna & Jain, 2015; McCartney et al., 2014; McCubrey et al., 2007; Ohashi, 2002; Watson, 2006; Waugh, 2012)

1.2.Phosphatidylinositol 3,5-bisphosphate (PI(3,5)P_2) synthesis

This thesis specifically focuses on one of the PPIs, namely the phosphatidylinositol 3,5-bisphosphate PI(3,5)P_2. PI(3,5)P_2 is the least abundant PPI (J. Hasegawa et al., 2017). Overall, it takes around 0.1% of total PPI levels (Ketel et al., 2016). Because of its low levels, PI(3,5)P_2 is especially difficult to investigate and monitor. It is known that, upon hyperosmotic shock of the yeast, PI(3,5)P2 levels increase up to 40 fold and then return to basal levels within 30 minutes (Jin et al., 2017). This spike is observed with insulin stress in mammals as well (J. Hasegawa et al., 2017).

PI(3,5)P_2 localizes to the vacuolar and late endosomal membranes and its turnover takes place in the vacuolar membrane. It has various cellular roles in maintaining homeostasis, nutrient sensing, stress signaling and multi vesicular body (MVB) sorting pathway, which will be further explained in the upcoming parts.

PI(3,5)P_2 is synthesized by a conserved phosphatidylinositol-3-phosphate 5-kinase named Fab1 in budding yeast, PIKfyve in human (Ho et al., 2015). This kinase phosphorylates PI3P at the fifth hydroxyl group of the inositol ring to generate PI(3,5)P_2. Thus, PI3P is the precursor for PI(3,5)P_2. PI3P is generated through phosphorylation of phosphatidylinositol by the phosphatidylinositol 3- kinase, which is known as Vps34 in yeasts and class III PI3K in human (Jaber & Zong, 2013).

PI(3,5)P_2 is converted back to PI3P by the phosphatase Fig4 (also known as Sac3), which hydrolyzes the phosphate at the fifth hydroxyl group of the inositol ring (Chow et al., 2009). Mammalians also have MTMR phosphatases which may act as a phosphatase to PI(3,5)P_2 other than Fig4 (Vaccari et al., 2011).

Other than phosphatidylinositol kinases and phosphatases that promote PI(3,5)P_2 synthesis and turnover, a regulatory protein group controls PI(3,5)P_2 levels by interacting Fab1 kinase. These proteins form a complex called PAS complex which is composed of Vac14 (ArPIKfyve in

mammalians), Vac7 (not conserved in mammalian), Atg18 (Autophagy-related protein 18) and Fig4 (Factor-induced gene) in addition to the Fab1 kinase (Choi et al., 2018). This PAS complex is localized to the membrane of vacuole/ lysosome in cell.

Vac7 is a vacuolar protein, and it is known to be required for normal vacuole structure. It is known that when *VAC7* is deleted in yeast (*vac7Δ*), vacuolar segregation cannot occur properly during the cell cycle (Bonangelino et al., 1997). Vac7 is also required for $PI(3,5)P_2$ production since it is a part of PAS complex. $PI(3,5)P_2$ levels diminishes in *vac7Δ* to cells, similar to *fab1Δ* cells (Gary et al., 2002).

Atg18 is a known autophagy related protein that takes part in generating the autophagosome (Rieter et al., 2013). Atg18 contains β-propeller domain which contains FRRG motif for high affinity recognition of $PI(3,5)P_2$ (Rieter et al., 2012). In mammalians, WIPI proteins (1-to-4) are homologues of Atg18, but they are not yet known to interact with $PI(3,5)P_2$ (Proikas-Cezanne et al., 2004). Atg18 binds to $PI(3,5)P_2$ and negatively regulates Fab1 activity in yeast (Dove et al., 2004). It is also known that Atg18 interacts with Fab1 and regulate organelle morphology via this interaction in a way that is independently of Fab1's ability to synthesize$PI(3,5)P_2$. When cells do not have effector Atg18, they exhibit enlarged vacuoles and elevated $PI(3,5)P_2$ levels (Bryant & Stevens, 1998). Atg18 localizes to the vacuolar membrane like Fab1, Vac7 and Vac14 however it is believed not to interact with neither of them. It is also showed that, Atg18 requires Vac7 to be recruited to vacuolar membrane again independent of Vac7's role in $PI(3,5)P_2$ synthesis (Efe et al., 2005). It is thought that Atg18 mechanism of $PI(3,5)P_2$ downregulation provides a negative feedback to decrease $PI(3,5)P_2$ amounts back to basal levels in response to increased $PI(3,5)P_2$ synthesis (Efe et al., 2007).

Fig4 (Factor induced gene) negatively regulates $PI(3,5)P_2$ formation through dephosphorylation of $PI(3,5)P_2$, however unexpectedly when Fig4 its depleted $PI(3,5)P_2$ production is impaired as well, suggesting that Fig4 has a dual role -negative and positive- in $PI(3,5)P_2$ synthesis (Botelho et al., 2008). Fig4 interacts with Vac14 and Fab1/PIKfyve and thereby promotes Fab1 activity (Botelho et al., 2008). Fab1's phosphorylating function is likely also dependent on Fig4 phosphatase activity since a catalytically impaired Fig4 mutant produces less $PI(3,5)P_2$ under hyperosmotic shock conditions compared to wildtype cells (J. E. Duex et al., 2006; Strunk et al., 2020).

In the absence of Vac14, $PI(3,5)P_2$ levels are diminished too (Alghamdi et al., 2013; Bonangelino et al., 2002).Vac14 acts as a scaffold to keep Fab1, Vac7, Fig4 and Atg18 along with Fab1 and thus enhances Fab1 activity (Jin et al., 2008).

Another control mechanism for $PI(3,5)P_2$ regulation occurs through an inverted BAR protein called Ivy1. Ivy1 acts as an inhibitor of Fab1 complex (C Malia et al., 2018). Ivy1 needs Ypt7 for its function (Numrich et al., 2015). Ypt7 binds $PI(3,5)P_2$ and through that Ivy1 binds to $PI(3,5)P_2$ and regulate Fab1 complex. When Ivy1 is overexpressed, it is shown to block Fab1 activity even in hyperosmotic shock conditions. It is believed that Ivy1 regulates Fab1 dependent $PI(3,5)P_2$ synthesis in stress conditions and regulates vacuole membrane environment.

1.3.Functions of $PI(3,5)P_2$ in budding yeast

$PI(3,5)P_2$ is known to be involved in membrane fusion/fission, Ca+2 signaling, endolysosome acidification, selective and bulk autophagy, stress response, Multivescular body (MVB) pathway. The effector proteins known to be involved in these processes are Yvc1, Atg18, RyRs, Ypt7-Kog1-Sch9, TRPML, Ent3p-mVps24, Atg21p-Hsv2p-Svp1p respectively (Fig1.1) (Bridges et al., 2012; Catimel et al., 2008; Choy et al., 2018; Han & Emr, 2011; Ho et al., 2012; Kotani et al., 2018; Liao et al., 2019; Miner et al., 2019; Nagano et al., 2019; Odorizzi et al., 1998; Puray-Chavez et al., 2021; Yamashiro et al., 1990) . Roles of $PI(3,5)P_2$ in these processes are explained below:

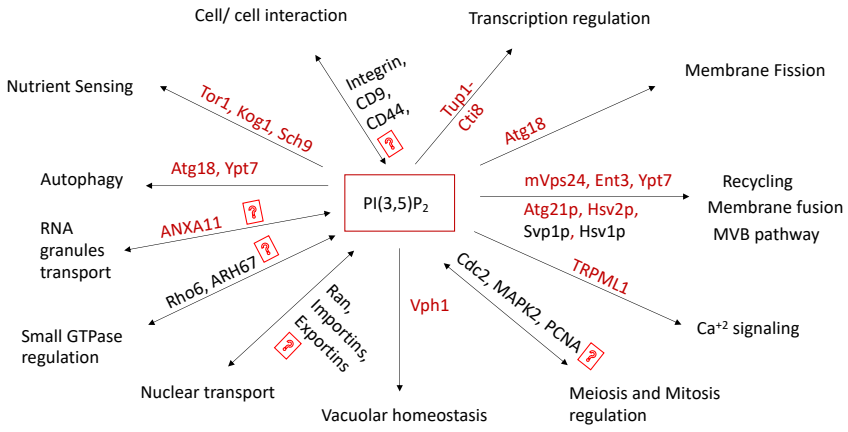

Figure 1. 1-The identified effector proteins and possible candidates of $PI(3,5)P_2$.
Single arrowed lines show $PI(3,5)P_2$ interactors that function in the indicated cellular process down stream of $PI(3,5)P_2$. Question mark indicates lack of knowledge on direct interaction.

1.3.1. Role in Endosomal Maturation and MVB Sorting

Endosomes are vesicles formed after internalization of macromolecules, plasma membrane components and other particles. They can fuse with vacuoles to degrade the internalized components (Huotari & Helenius, 2011). Endosomes' main aim is to target and internalize cargos. These vesicles bud from plasma membrane and at that phase they are called early endosomes. This stage is a transition state, where the internalized cargos can be recycled back to its origin, plasma membrane or move on with the endocytosis by their delivery to late endosomes. Through late endosomes they can get degraded by vacuoles/lysosomes. Even though the early endosome concept has not been completely illuminated, in yeast it is known that early-stage endosomes contain Vps21p (Rab5) and late-stage endosomes contain Ypt7p (Rab7). The maturation of early endosomes to late endosomes are achieved through Rab5 GTPase (Nagano et al., 2019). Multivesicular bodies (MVB) are late endosomes that sort ubiquitylated membrane proteins back to the plasma membrane for recycling, to the trans golgi network or to the vacuole or lysosomes to achieve protein turnover. For example, when vacuolar hydrolase carboxypeptidase S (pCPS) gets ubiquitinated, it is degraded in vacuolar lumen through MVB pathway (Katzmann et al., 2004; Odorizzi et al., 1998). The conversion of PI(3)P to PI(3,5)P2 by Fab1 kinase is essential for endosomal maturation. Cargo sorting which is regulated by the ESCRT complex also relies on PI(3,5)P since PI(3,5)P2 interacts with certain proteins in ESCRT complex (mVps24, Ent3p) (Ho et al., 2012). Thus, PI(3,5)P2 takes on an important role at the late endosomes /lysosomes /vacuoles and it sorts the cargo into MVBs (Wallroth & Haucke, 2018).

1.3.2. Role in Membrane Trafficking and Vacuolar Homeostasis

First, in the case where Fab1 fails to work properly yeast lysosomes (vacuoles) become extremely large (Rudge et al., 2004). Similarly, loss of Fab1/PyKfive activity causes very enlarged endo-lysosomal compartments in mammalian cells and mouse tissues (Choy et al., 2018). These suggest that PI(3,5)P2 has a role in maintaining vacuolar size, function, and fusion/fission events.

When vacuolar homeostasis is considered, PI3P is known to play inducing role against the fusion of vacuoles instead PI(3,5)P2 is known to promote vacuolar fission (Gary et al., 1998). Therefore, deletion or loss of function of Fab1 kinase results in lack of PI(3,5)P2 which causes very enlarged vacuole since fission pathway is inhibited. In addition, *atg18Δ* yeast cells fails to

fragment their vacuole under salt stress which indicates Atg18 and PI(3,5)P2 both work in membrane fission.

PI(3,5)P2 also interacts with V-ATPase V0 subunit of Vph1 to cause V-ATPase assembly which indicates PIP's role in proton release in case of hypertonic conditions (Miner et al., 2019). V-ATPase pump of vacuolar membrane lead to the acidification of vacuole (Yamashiro et al., 1990). Vacuolar acidification is highly important because it has a great role in protein/cargo selection and maintenance of overall intracellular pH, the zymogen activation completely relies on vacuolar acidification.

Ca^{+2} is known as the key regulator during neurotransmission. Other than that, it is involved in membrane trafficking too. How Ca^{+2} is released from the lumen of organelles and vesicles? The answer to that relies on the interaction of PI(3,5)P2 with TRPML1 (Mucolipin Transient Receptor Potential) which are localized in the late endosomes and lysosomes. By interacting with TRPML1 channel, PI(3,5)P2 regulates Ca^{+2} release which eventually regulates vacuolar fission, vacuolar, pH, cargo sorting, membrane trafficking (Shen et al., 2012).

1.3.3. Role in Nutrient Sensing and TORC function

For a cell to grow and exhibit healthy metabolic regulations, mTOR (mechanistic Target of Rapamycin) function is highly important. mTOR is conserved and consists of TORC1 and TORC2 complexes. In budding yeast, TORC1 complex is formed by Tor1, Tor2 and Kog1 along with Lst8 and Tco89 (Loewith & Hall, 2011). TORC1 is known to regulate the cell growth by balancing out the autophagy and protein synthesis. One can say that it acts as a switch, when there is nutrient the protein synthesis is positively regulated along with the cell growth and autophagy pathway is negatively regulated (Sancak et al., 2008). In the case of starvation or Rapamycin (the inhibitor of TORC1), "the switch" is off and TORC1 complex cannot promote cell growth and autophagy becomes more dominant rather than cell growth. TORC1 complex is known to localize to the vacuole membrane in yeast and in mammalians it localizes to lysosomes and late endosomes. This vacuolar localization is known to be very crucial for yeast viability (Zurita-Martinez et al., 2007). TORC1 complex has many regulators such as EGO complex (Ragulator in mammalian) (Dubouloz et al., 2005). It is known that, through its WD-40 domain, Raptor (Kog1 in yeast) interacts with PI(3,5)P2 and it is believed that through that interaction Kog1 is being translocated in vacuolar membrane to regulate TORC1 function. In the meantime the deletions of Fab1, Vac14, Fig4 caused defects in TORC1 phosphorylating ability therefore its function (Bridges et al., 2012). When all this information

considered, it was a possibility that PI(3,5)P2 works as an upstream regulator of TORC1. Later, it was found that, one of the TORC1 substrate Sch9 (in mammalians S6K) is recruited to the vacuolar membrane to TORC1 complex for TORC1 to be able to phosphorylate it. PI(3,5)P2 is the one that is responsible for Sch9 and Kog1 recruitment to the vacuolar membrane. This suggests that vacuoles may work as scaffolds for TORC1 activation (Takeda et al., 2018) . PI(3,5)P2 also helps regulate the TORC1 dependent phosphorylation of Npr1 and Atg13 as well which results in negatively regulated autophagy. Also, it was seen that PI(3,5)P2 helps degrading autophagic bodies (Jin et al., 2014). All of these finding suggest that PI(3,5)P2 has a role in nutrient sensing in the aspect of triggering TORC1 and by inhibiting autophagy via various direct and indirect ways (Fig1.2).

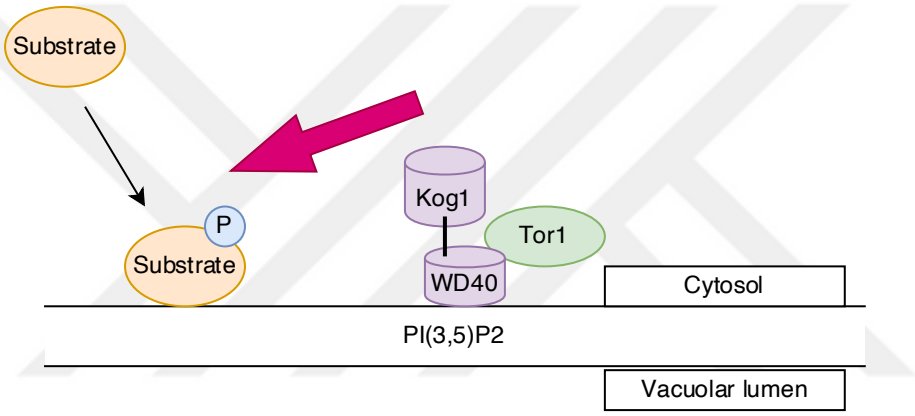

Figure 1.2: Demonstrates the PI(3,5)P_2 dependent activation of TORC1 which indicated that PI(3,5)P_2 is an upstream regulator of TORC1 (figure is inspired from Jin et al,. 2014)

1.3.4. Role in Autophagy and Autophagosome Formation

Autophagy is known as "self-eating". Its balance is extremely important to maintain cellular homeostasis. It is a pathway used for degrading proteins and organelles. Autophagy can arise with various of reasons such as nutrient deprivation, infection, lack of growth factors. When talking about autophagy one can mention bulk autophagy and selective autophagy (Yorimitsu & Klionsky, 2005). Autophagy occurs through several steps such as induction of autophagy, membrane formation followed by autophagosome formation and maturation then fusion of autophagosome with lysosome and cargo delivery into the lysosome for degradation (Colacurcio et al., 2018) (Dooley et al., 2014). It is known that together all PPIs are known to have a function in different steps of these. PI(3,5)P2 activates TORC1 via Sch9 recruitment and therefore it plays a role in TORC1 dependent inhibition of autophagy (Bridges et al., 2012). On the other hand, PI(3,5)P2 is also required for autophagosome fusion with lysosome by helping with the docking site with the help of Rab7 (mentioned above which is localizes in late endosomes and interacts with PI(3,5)P2) which tethers the autophagosome to lysosome (Baskaran et al., 2012). In addition, degradation of the autophagosome in lysosome requires acidic pH of vacuole/lysosome lumen, which is also regulated by PI(3,5)P2 . Futhermore, yeast Rab family GTPase Ypt7 which is a known effector protein of PI(3,5)P2 is being recruited to the autophagosomes along with Pleckstrin homology domain-containing protein family member 1(PLEKHM1) and LC3 recruitment to lysosomes. Ypt7 induces the recruitment of HOPS complex (Homotypic fusion and protein sorting) (Balderhaar et al., 2010). Thus, through different pathways and interactions PI3,5P2 affects autophagy both negatively and positively (Kotani et al., 2018). Atg18, an established effector and regulator of $PI(3,5)P_2$ is also essential for autophagy and vacuolar morphology too. Atg18 (along with Atg2) helps with the elongation stage of the autophagosome through its interaction with PI3K. Atg18's interaction with PI(3)P was thought to be the only important interaction for autophagy regulation and activity (Obara et al., 2008). Nevertheless, this view is challenged now with the findings that Atg18 negatively regulates $PI(3,5)P_2$ production while $PI(3,5)P_2$ positively regulates TORC1 activation (Jin et al., 2014). This contradictory may be the result of $PI(3,5)P_2$'s homeostatic role in cell. One might hypothesize that, with the rising level of $PI(3,5)P_2$ the TORC1 gets stimulated as described above, which causes certain autophagy related proteins to be phosphorylated and silenced by TORC1. In the meantime, Atg18 starts to negatively regulate $PI(3,5)P_2$ which eventually leads to TORC1 inactivation which causes autophagy related proteins to be activated. In cell, especially the formation of the autophagosome and selective autophagy is really important for efficient protein turnover, and it is quite possible that the interaction of

Atg18- PI(3,5)P_2 helps to maintain that protein turnover and serves to maintain cell in a balanced state (Fig1.3).

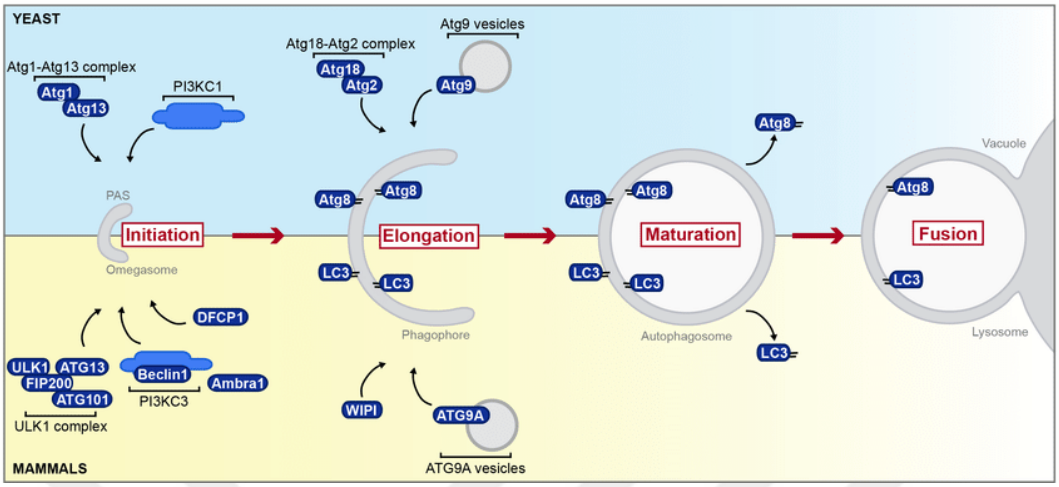

Figure 1.3: Autophagosome formation in yeast and mammalians and depiction of how they fuse with vacuole/lysosome (figure is adapted from (Kohler et al., 2020))

1.3.5. Role in Transcription in Budding Yeast

PI(3,5)P2 is also shown to have a role in transcription regulation. One of the enlightened pathways that require PI(3,5)P2 is transcriptional reprogramming from glycolysis to gluconeogenesis. Under normal conditions, glucose is turned into pyruvate through glycolysis process then the pyruvate is again metabolized further through mitochondrial oxidative phosphorylation (aka TCA cycle) (Martínez-Reyes & Chandel, 2020). It is seen that when glucose is rich in the environment, Gal1 (identified PI(3,5)P2 dependent transcriptional regulatory mechanism) is being repressed by a complex of Mig1-Cyc8-Tup1 (Wong & Struhl, 2011). In the absence of glucose however the Gal4 is activating GAL1 transcription is being activated by the conversion of Cys8-Tup1 repressor to Cti6-Cyc8-Tup1 activator. Recent studies showed that, PI(3,5)P2 presence is essential for Gal1 transcription activation (Wong & Struhl, 2011). PI(3,5)P2 binding to Cti6 and Cyc8-Tup1 converts the transcriptional repressor complex Mig1-Cyc8-Tup1 to the transcription activator Cti6-Cyc8-Tup1 complex (Han & Emr, 2011). Thus, PI(3,5)P2 dependent Tup1 (human homologue is TLE proteins) conversion is crucial for switching from glycolysis to glucogenesis (Malave & Dent, 2006). It is hypothesized that, glucose starvation affects the vacuolar luminal pH, as well as its content which can affect PI(3,5)P2 production so that it can stimulate PI(3,5)P2 dependent Tup1 conversion. It is also

well established that during nutrient depletion mTORC1 is activating transcription factor EB at the lysosome membranes so that transcriptional adaptations occur concerning lysosomal biogenesis (Han & Emr, 2011). Since mTORC1 is active in nutrient rich environment it is blocked in nutrient poor environment and when it is not active it cannot suppress autophagy (Takeshige et al., 1992).

1.3.6. Transport of RNA granules by Lysosomes via Their Interaction With PI(3,5)P_2

Other than its indicated roles, PI(3,5)P_2 is also involved in translocation of RNA granules. Proteins are usually translated at their usage site instead of being trafficked around the cell(Kindler et al., 2005) Since this "on-point translation" is preferred, RNA must be also transported from the nucleus to the preferred cite of local tranlation. For membrane- bound organelles interacting with membrane proteins to enable transport is somehow easy but in the case of RNAs since the membrane usually don't exist, they must organize themselves in RNA granules with RBPs (RNA binding proteins) (Weber & Brangwynne, 2012). The mutations of RBPs cause RNAs to not form into granules which causes the loss of local translation which results in various diseases mostly neurological ones (Chevalier-Larsen & Holzbaur, 2006). It has been recently illuminated that one of the ways which cargos get transported is docking near membrane-bound organelles such as endosomes. This is called "hitchhiking" (Guimaraes et al., 2015). It has seen that RNA granules perform this hitchhiking act for long-distance transportation as well (Liao et al., 2019). It has been shown that RNA granules interact with lysosomes through the RNA granule-associated protein Annexin A11 (ANXA11). RNA granules interact with ANXA11 on lysosomes only when both Ca^{+2} and PI(3,5)P_2 is present on the lysosome (Liao et al., 2019). It was described above that, PI(3,5)P_2 interacts with TRPML1 which is the Ca^{+2} regulation channel in vacuoles/lysosomes (Dong, Wang, et al., 2010). So it is believed that the RNA granules docking to lysosomes or late endosomes the ANXA11 protein is working with PI(3,5)P_2.

1.4.Disease and Disfunctions Related to PI(3,5)P_2

Due to its diverse cellular roles, defects in PI(3,5)P2 production are associated with many human diseases. Because of its role in Ca^{+2} signaling it is associated in many neurological disorders. Charcot-Marie-Tooth type 4j is one example for that and it is caused in heterogenous or homozygous mutations leading to reduced expression in Fig4 (phosphatase of PI(3,5)P2) (Lenk et al., 2019; Rivero-Ríos & Weisman, 2022) also other disorders caused by Fig4 mutation is ALS (Amyotrophic lateral sclerosis), Biallelic Vac14 variants cause Yunis-Varon syndrome

(Lines et al., 2017). Mutations in Fab1 kinase results in Congenital cataract, Francois-Mouchetee, Fleck corneal dystrophy diseases among others(Li et al., 2005). Mutation in Vac14 is associated with childhood onset striato-nigral degeneration (Stutterd et al., 2017).

Other than established links between diseases and PI(3,5)P2, it is observed that the inhibitor of Fab1, Apilimod which is an anti-inflammation drug halts the infection against SARS-CoV-2. It is believed that, by altering $PI(3,5)P_2$ production through Fab1, the acidity of the vacuoles/lysosomes can be decreased. During the MVB sorting, late endosomes fuse with vacuoles/lysosomes to eliminate the cargo and these cargos can also be viruses. However certain viruses known to avoid termination by elevating the pH of lysosome/vacuole. Because apilimod can counteract this elevation of lysosomal pH, it is now being considered as a treatment option for COVID-19 (Ou et al., 2020; Puray-Chavez et al., 2021).

1.5.Conclusive Remarks and Future Directions

$PI(3,5)P_2$ is one of the seven phosphatidylinositol which is involved in various of pathways from sensitive stress signaling to transcription regulation. The tight regulation of PI(3,5)P2 with PAS complex exhibits itself in maintaining cell homeostasis. Any type of mal regulation can lead to disruption in cascades which results in different diseases. Having said that, PI(3,5)P2 is still poorly understood. We only know few proteins interacting with PI(3,5)P2. and for the future its interactome should be characterized more so its role can be illuminated in other pathways as well. Right now, its involvement in viral infections and cancer formation is widely studied due to its role in lysosomal acidification. Is PI(3,5)P2 involved in other vital pathways such as cell cycle? These questions among others might be answered through a comprehensive transcriptomic and proteomic research.

1.6.Budding Yeast as a Model Organism

Model organisms are invaluable tools for life sciences. They share certain common traits such as reflecting and representing larger populations, easy manipulation, overcoming ethical issues, easy handling and availability of established methods (Hartwell et al., 1974). *Saccharomyces cerevisiae* is one of the well-established model organisms for the study of cell biology (Hanson, 2018). It is also known as the budding yeast and brewer's yeast. *S. cerevisiae* is a single celled eukaryotic organism. The genome of the budding yeast was the first eukaryotic genome that was sequenced (Goffeau et al., 1996; Lennon & Lehrach, 1992). Although diverged millions of years ago from others, budding yeast shares commonalities with higher eukaryotic cells with

respect to basic cellular processes, including but not restricted to cell division cycle, organelle biogenesis, translation, transcription, DNA replication, aging and autophagy (Foti et al., 1999; Schmitt & Clayton, 1993; Wu & Malkova, 2021). Conservation of cell biology from yeast to mammals and genetic malleability of the budding yeast makes it an ideal model for cell biology studies. When budding yeast decide to divide, a visible bud (hence the name, budding yeast) emerges on the pre-existing (mother) cell. Bud (daughter cell) grows during cell cycle and detaches from the mother at the end of the division. Thus, budding yeast cell cycle is trackable morphologically by observing the bud. This feature of the budding yeast makes it a good model for cell cycle studies (Hartwell et al., 1974). Also, there are two types of division; asymmetric cell division, where two daughter cells have different characteristics and symmetric cell division, two daughter cells share the same fate (Lew & Reed, 1995). Budding yeast demonstrates asymmetric cell division. Yeast is inherently polarized along the mother-daughter cell axis. Actin cables and mitotic spindle is oriented in this direction to carry organelles, chromosomes, and biomolecules. Mother and daughter cell differs in terms of age, protein, mRNA content and organelle number and quality. This makes budding yeast is a good model organism in studying cellular aging and asymmetric cell division (Harrison et al., 2009). The budding yeast is famous for it is genetic power. It is relatively easy to edit the genome of yeast owing to the high homologous recombination rates (Orr-Weaver et al., 1981). High homologous recombination rates enable knock-in and knock-out of genes/sequences by providing the yeast with DNA fragments that contain the desired modification. These fragments can be obtained by very well-established cassette PCR techniques (Knop et al., 1999). Another reason that makes yeast famous for genetic studies is its life cycle. Yeast can grow as diploid and haploid. In its third chromosome, yeast carries its mating-type identity. In haploid yeast cells this can either be type a (MATa) or type α (MATα). Cells can divide in their haploid state. Under necessary conditions two haploid yeast cells mate and generate diploid MATa/ MATα cells (Throm & Duntze, 1970). These diploid cells undergo mitotic cell cycle similar to haploid cells and when exposed to harsh conditions they generate the haploid spores by going through meiosis (Hartwell, 1974; Hartwell et al., 1974) (Fig1.3). It is more efficient to do genome editing in haploid cells because they have single copies of genes. Furthermore, haploid state of yeast allows generation of mutants by random mutagenesis when necessary. One example for that is the temperature sensitive mutants of essential genes in yeast. Such mutations can be obtained in haploid yeast cells, because they have single copy of each gene, and they can be put into complementation groups by mating with each other taking advantage of the diploid state

(Hartwell, 1967; Hutchison & Hartwell, 1967). Overall, these traits make yeast a very important and useful model organism.

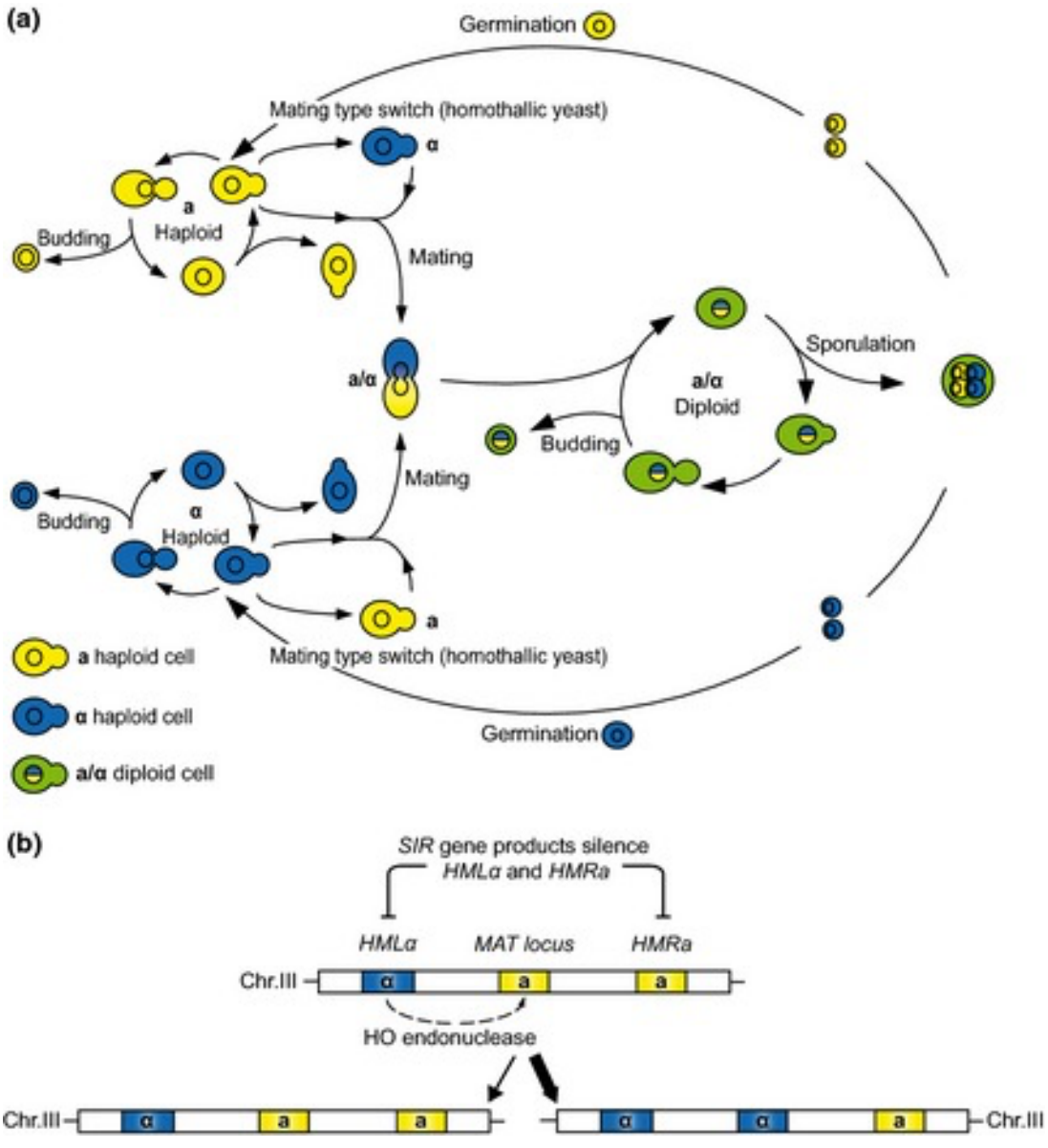

Figure 1.4: Life cycle of budding yeast. This figure is adapted from (Steensels et al., 2014)

1.7. The Cell Cycle of *S. cerevisiae*

Budding yeast divides asymmetrically which results in one mother cell and one daughter cell. Daughter cell emerges as a bud, grows in size then detaches from the bud site and becomes an independent cell throughout the cell cycle (Hartwell & Unger, 1977).

Like other eukaryotes, budding yeast cell cycle consists of two parts: (1) interphase which consists of G1-S-G2 where the cell grows, prepares for division, replicates its genome and centrosomes; (2) Mitotic phase (M) where nuclear division occurs (Alberghina et al., 1986; Hartwell et al., 1974). In G1 phase cells gets bigger in size, and once it passes a critical size, cell commits itself to cell cycle (Johnston et al., 1977) by moving to the S phase where cell duplicates its genome. In G2 stage, cell continues growing and DNA damage is monitored (Following G1, cells progress into the M phase, where chromosomes are segregated to the opposing poles of the cell. All these cell cycle stages in yeast correlate with the bud size: in G1 phase, there isn't any bud formation, but bud site is determined (Johnston et al., 1979). In S phase, bud emerges as a tiny protrusion on the mother. In G2, the bud becomes larger however still smaller than the mother (Mayhew et al., 2017). Bud continues growing until late M phase where the bud is almost as large as the mother (Chant & Pringle, 1995).

1.7.1. Mitosis

Mitosis happens under four main stages followed by a fifth final step where cytokinesis occurs (Hartwell & Unger, 1977). Also, in budding yeast there is no nuclear envelope disappearance, so it is going through a closed mitosis which is not the case for a mammalian cell (Newport & Forbes, 1987). The four stages of mitosis are prophase, metaphase, anaphase, and telophase. These stages happen in an ordered fashion however cytokinesis begins around anaphase and continues throughout the telophase (Novak & Tyson, 1993). During prophase, DNA condensation occurs, and they become the condensed chromosomes. In metaphase, microtubules bipolarly attach themselves to kinetochores (Hartwell & Unger, 1977; Liu et al., 2005) and cell is then ready to move to the anaphase. This transition from metaphase to anaphase is a very critical step for cell cycle and does not happen until all chromosomes are correctly attached to the mitotic spindle. For anaphase to start, the Cohesin complex that holds the sister chromatids together must be cleaved so that the sister chromatids can separate. For this, an enzyme called Separase (Esp1) cleaves cohesin from the Scc1 (Kleisin subunit of cohesin) (Michaelis et al., 1997; Vinod et al., 2011). The reason why separase is not cleaving the cohesin until anaphase is another protein called Securin (Pds1 in yeast). This protein keeps

the Separase inactive until all chromosomes are correctly attached. Securin then gets degraded by APC/Cdc20 complex so that Separase gets activated and removes the cohesion between sister chromatids(Ciosk et al., 1998; Siller & Doe, 2009). This process is assured by the spindle assembly checkpoint, it is highly sensitive and tightly regulated. Sister chromatids are pulled to the opposite poles during anaphase until telophase. In telophase everything that happened in prophase reverts such as, chromosomes start to decondense, mitotic spindle disassembles. Then finally, cells split from the site where the bud emerged earlier in the cell cycle (Fig1.4). Cytokinesis is regulated by independent mechanisms, one of which is actomyosin ring constriction which can be compared with the cleavage furrow in mammalian cell. In addition to actomyosin ring constriction, for yeast cells to separate the cell wall forms at the site of cytokinesis by septum formation (Wloka & Bi, 2012).

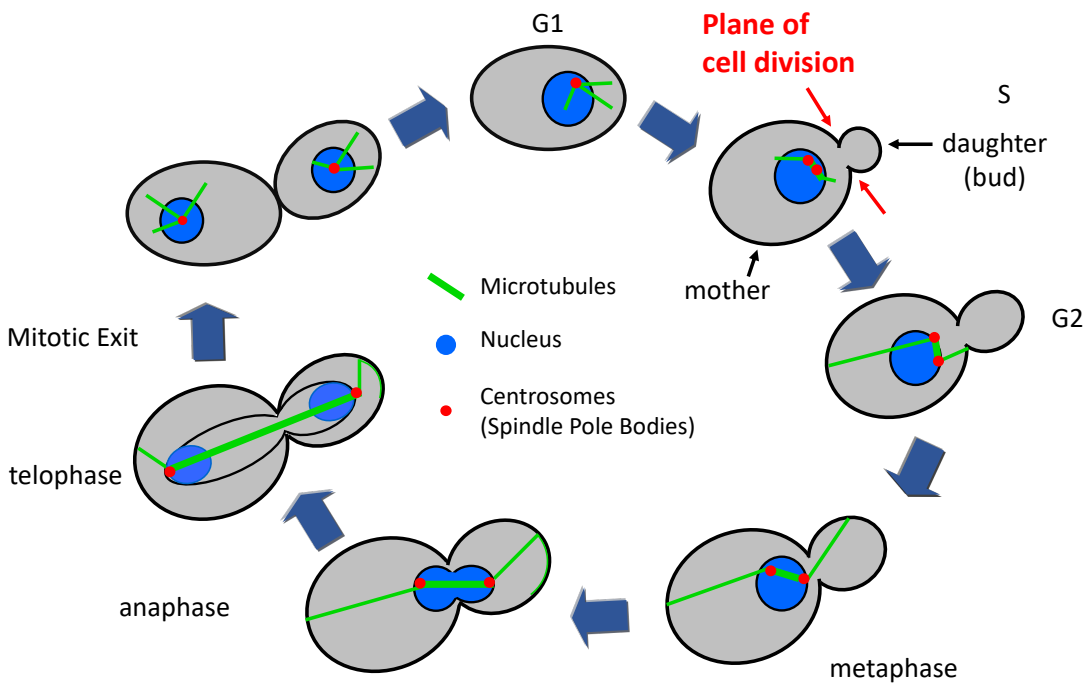

Figure 1.5: The cell cycle progress of budding yeast. (This figure is adapted from Ayşe Koca Çaydaşı)

1.7.2. Cell cycle Control Mechanism

Cyclin-dependent kinases (CDKs) are the key protein family that drive the cell cycle. CDKs are kinases and they phosphorylate serine/threonine residues that are followed by a proline (S/T-P) (Ding et al., 2020). CDKs regulate activity of several proteins that mediate phase specific events such as DNA replication, chromosome condensation and mitotic spindle formation (Morgan, 1995). In budding yeast, the key CDK is Cdc28 (Cdk1 in fission yeast and human) (Murray, 2004). CDKs require interaction with proteins that are named cyclins to get activated (Beach et al., 1982; Nurse & Thuriaux, 1980). CDK protein levels are kept in stable amount during the cell cycle whereas the cyclin levels oscillate through stages of the cell cycle(Malumbres & Barbacid, 2009). Cyclins are transcribed and degraded in a cell cycle phase dependent manner, which accounts for the oscillations in their levels. Cyclins can be grouped according to the phases their levels increase and thus they can form complexes with Cdk: G1-cyclins (Cln3 in budding yeast), G1/S-cyclins (Cln1,2 in budding yeast), S-cyclins (Clb5,6 in budding yeast), M-cyclins (Clb1,2,3 in budding yeast) (Figure 1.4) (Andrews & Measday, 1998). Each phase specific cyclin-CDK complex promote activation of the next and inhibition of the previous cyclin-CDK to provide directionality of the cell cycle (Fig1.5).

Interaction with cyclins is necessary for CDKs activation but not enough. CDKs are also regulated through phosphorylation by other kinases (such as CAKs and Wee1) (Pavletich, 1999). Furthermore, proteins that are named CDK inhibitors (CKIs) inhibit CDK-cyclin interaction and/or activity (Morgan, 1995).

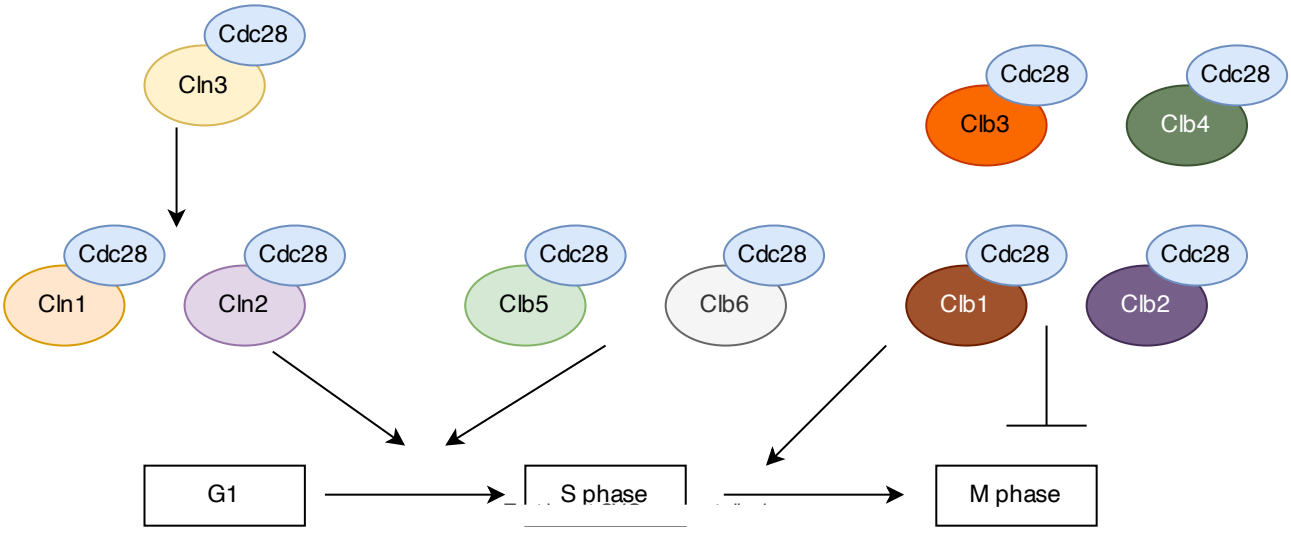

Figure 1.6. CDK-cyclin regulation throughout the cell cycle. This figure is inspired from (Bloom & Cross, 2007)

For cell cycle to work error-free there are checkpoint mechanisms to oversee this fidelity of key events. These checkpoints monitor key processes and stop the cell cycle until the problem is fixed (Bloom & Cross, 2007). G1/S checkpoint (START) sense if the cell has grown enough to divide and if the environment is favorable for a division. Without favorable conditions G/S and S phase cyclins are not transcribed (Pellicioli et al., 2001). DNA damage checkpoint monitor DNA damage and replication problems before entry into M phase. Upon DNA damage Cdk is inactivated. One of the most important checkpoints arise in M-phase. It is called Spindle Assembly Checkpoint (SAC) (Musacchio & Salmon, 2007). During M phase, to achieve successful segregation of each and every chromosome to the opposing poles, the mitotic spindle coming from opposing poles must attach to the kinetochores of chromosomes in a bipolar manner (Sironi et al., 2002). SAC works in that aspect, if there is problem with spindle-kinetochore attachments it pauses anaphase onset until the correction is achieved. Normally, while cells move on to anaphase Securin (Pds1) gets degraded so that Separase (Esp1) can be free to cleave Scc1 subunit from the Cohesin complex (Hornig et al., 2002). This is achieved by APC/C activation. (Anaphase Promoting Complex/Cyclosome). During SAC, until ideal conditions are achieved, APC/C is blocked thus Separase is not activated until all chromosomes are correctly attached to the microtubules. In order to keep cells arrested at SAC, there is a highly regulated molecular mechanisms which involves Mad2 in its closed version, Cdc20. Closed- Mad2 is recruited to the unattached kinetochores with the help of Mad1. Then closed-Mad2 converts to its open form to bind Cdc20 (so Cdc20 would not bind to APC/C) (Agarwal & Cohen-Fix, 2002). Not only Cdc20 is kept, but it also gets degraded by APC/C to ensure SAC is in progress and cell cycle does not proceed the anaphase (Irniger et al., 1995). When there are problems occurring in maintaining SAC, cells are divided with unequal number of chromatids since the separation is not correct (Qiao et al., 2016).

Another checkpoint is called SPOC (Spindle Position Checkpoint), its aim is to ensure spindle is elongated in mother-daughter axis, thus chromosomes are segregated in the mother-daughter direction (Burke, 2009). SPOC prevents mitotic exit of the cells with oriented spindles by inhibiting exit from mitosis through inhibition of the Mitotic Exit Network (MEN) (Fig1.6).(Caydasi et al., 2012).

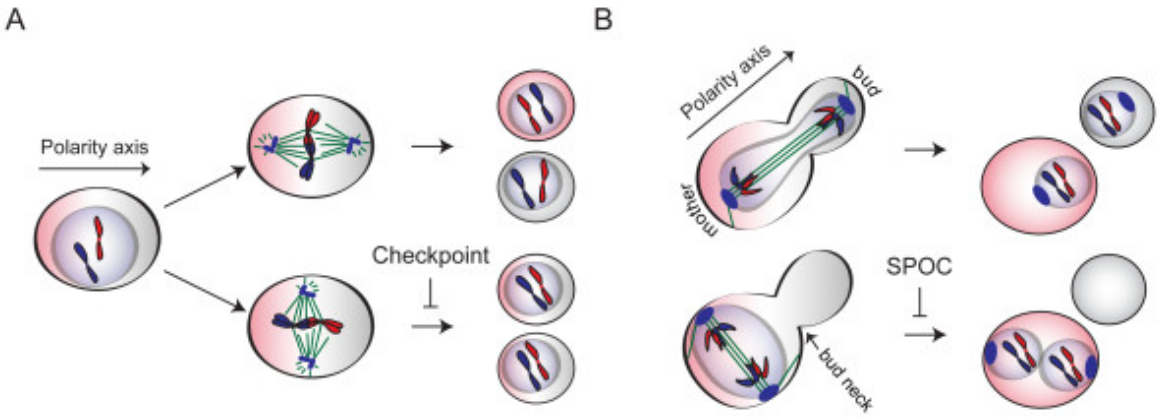

Figure 1. 7: SAC and SPOC checkpoints. A) Depiction of the spindle assembly checkpoint, when the spindles are not assembled correctly the checkpoint interferes. B) Depiction of spindle positioning checkpoint, when spindle is not positioned in the correct polarity axis the checkpoint interferes (Caydasi et al., 2010)

1.7.3. Mitotic Exit in Budding Yeast

In order for mitotic exit to take place, the M-cyclin-CDK complexes which were generated to induce mitosis needs to be inhibited. The E3 ubiquitin ligase APC in complex with its regulatory subunit of Cdc20 and Cdh1 is important for destruction of M-phase cyclins, and thus inhibition of Mitotic CDK activity (Renicke et al., 2017).

In budding yeast, Cdc14 phosphatase drives exit from mitosis (Yellman & Roeder, 2015). This phosphatase dephosphorylates M-cyclin-CDK substrates and inhibit M-cyclin-CDK complexes. For example, Cdc14 dephosphorylate Cdh1 to promote APC-Cdh1 formation. In budding yeast complete degradation of M-cyclins is managed by APC-Cdh1 rather than APC-Cdc20. Another target of Cdc14 is, Sic1 (CKI) which is the ultimate inhibitor of Cdk1 in yeast. The third protein to get dephosphorylated by Cdc14 is Swi5. Swi5 is a transcription factor and its being dephosphorylated causes it to move into the nucleus which then triggers Sic1 transcription (Visintin et al., 1998).

For Cdc14 to cause these adjustments happens by Cdc14 release. Until the metaphase to anaphase transition, Cdc14 localizes in the nucleolus. When the SAC permits cell to move on to anaphase Cdc14 is partially released in the nucleoplasm. To ensure Cdc14 does not get active prematurely, Net1 forms a complex with Cdc14 in nucleolus, so Cdc14 does not get release and get activated. Around the time where metaphase to anaphase transition occurs, Net1 gets

phosphorylated by M-cyclin-CDKs which causes Cdc14 to partially release. Before this, Net1 is kept in that dephosphorylation form by PP2A/Cdc55 phosphatase. This partial release of Cdc14 is regulated by the Cdc Fourteen Early Release (FEAR) pathway. However, FEAR is not essential for mitotic exit (Shou et al., 1999).

A signaling pathway named the Mitotic Exit Network (MEN) is essential for triggering mitotic exit. The SPOC checkpoint inhibits the MEN by inhibiting the small GTPase name Tem1. Tem1-GTP initiates the MEN. During SPOC and before anaphase Bfa1-Bub2 GTPse Activating Protein (GAP) complex inactivates Tem1 by keeping it in its GDP bound form. When the spindle is correctly positioned Cdc5 (polo kinase) phosphorylates Bfa1 and hence inhibits Bfa1-Bub2 GAP activity, thus Tem1 is active and the MEN initiates. With the activation of Tem1, Cdc15 gets activated which then phosphorylates Dbf2/Mob1 complex which in turn causes Cdc14 full release. The FEAR released Cdc14 is blocking M-Cyclin-CDKs so that they cannot inhibit the Cdc15 and phosphorylated Dbf2/Mob1(Komarnitsky et al., 1998) . Therefore, the partial release of Cdc14 is extremely crucial but without the full release of Cdc14 in MEN, the exit from mitosis would not have happened.

The MEN cascade is highly regulated by many pathways including FEAR, SPOC and cell polarity. The Hippo pathway in higher eukaryotes is the homologous pathway to the MEN (Justice et al., 1995) (Han, 2019; Harvey & Hariharan, 2012) . Failure of MEN regulation causes aneuploidy and multiploidy and chromosomal instability in yeast, whereas failure of Hippo pathway regulation in animals cause cancer and setbacks in development (Pan, 2010). Therefore, understanding mechanisms of MEN control in yeast is also relevant to the mammalians and figuring out disease mechanisms as well (Fig1.6).

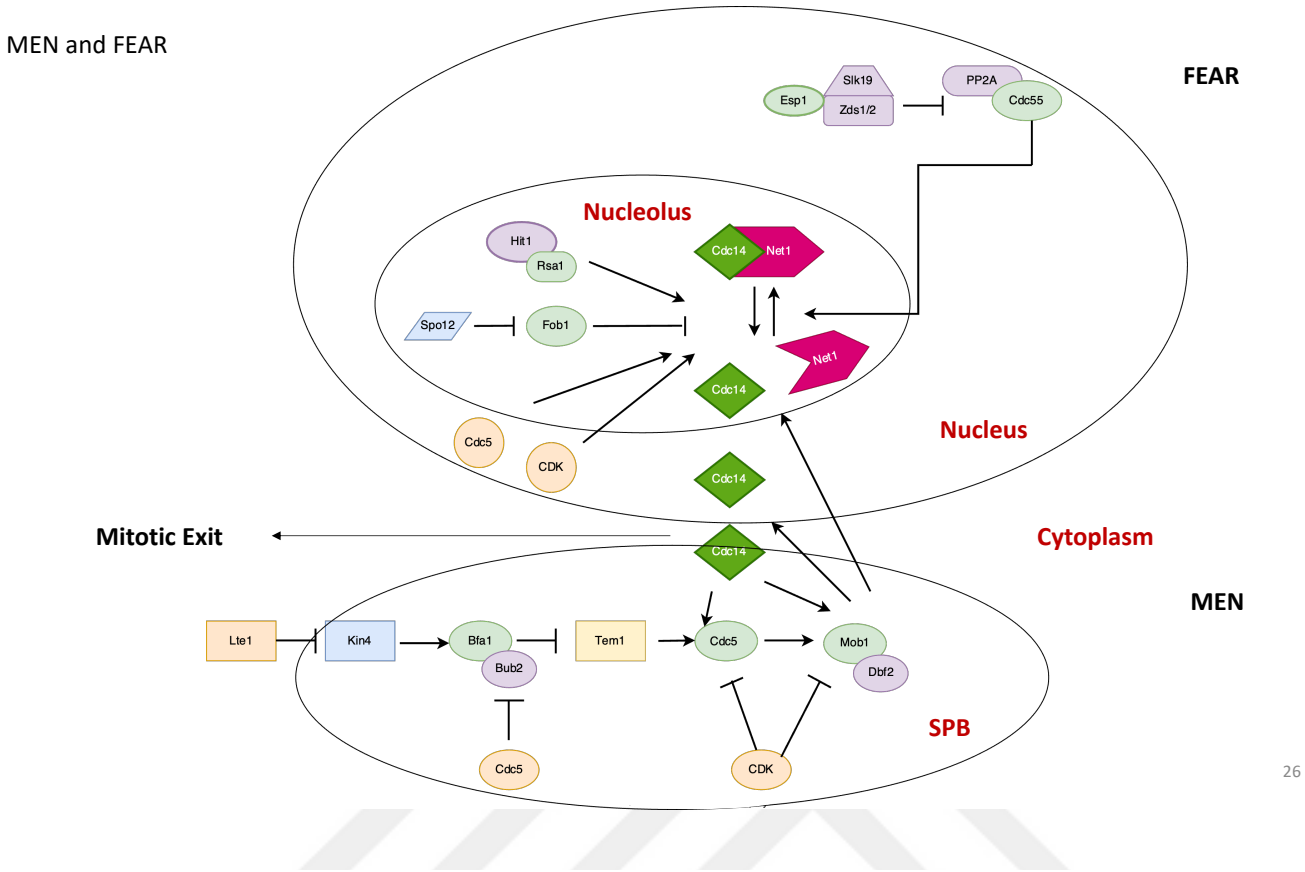

Figure 1.8: **MEN with FEAR. Cdc14 is being released from the nucleolus by Net1 to cytoplasm through FEAR. This initiates the mitotic exit network and full release of Cdc14 ensures the mitotic exit network.**

1.8. Vacuole Segregation During Cell Cycle

Yeast cells contain a huge organelle which is called vacuole. Its function is like lysosomes in mammalian, and it is highly acidic for its purpose it contains enzymes to break down molecules as well. How this organelle's segregation among other organelles happens? In yeast since the division is asymmetric which requires organelle transition from mother to bud (Fagarasanu et al., 2007). The transport of vacuole starts at G1 phase, and it is monitored during the cell cycle progression. During cell cycle, daughter gets a piece of vacuole from mother cell (Weisman et al., 1987). Mother sends a piece of the vacuole by the vacuole transport complex which consists of Vac8 (vacuole membrane anchored protein), Vac17 (adaptor protein) and motor Myo2 (Wang et al., 1998). Segregation of the vacuole starts at G1 with the help of Cdk1/Cdc28 and to end the vacuole segregation with the end of cell cycle Vac17 gets ubiquitylation. It is also seen that, even during the absence or malfunction of vacuole segregation pathway the vacuole synthesis may occur in the new daughter cell (Jin & Weisman, 2015). Even though when

vacuole segregation is halted it is seen that the cell survival is not being affected. However, the vacuole is required for cell growth. It is seen that, cell-cycle required proper vacuole segregation and proper vacuole function. It has been seen that along with *tor1*Δ and *vac17*Δ shows synthetic growth defects (Zurita-Martinez et al., 2007). Also, *tor1*Δ and *vac17*Δ deletion resulted in cells arresting at G1 phase. However even with this double deletion, the new vacuole is generated which indicates TOR1 being active in the new vacuole, and from the daughter vacuole it is needed for cell cycle progression. Overall, it was concluded that, functional vacuole is highly crucial for cell- cycle progression in G1 to S transition and TORC1 (with Sch9) also invests in this control mechanism. This generated the hypothesis that maybe there is another checkpoint at G1-S when certain organelles -maybe only vacuole- function is absence (Jin & Weisman, 2015).

Chapter 2: MATERIAL AND METHODS

2.1.*Saccharomyces Cerevisiae* Methods

The descriptions and components of the media, buffers and reagents are listed in Appendix Table 6.4.

2.1.1. Yeast Strains and Plasmids

S288C isogenic yeast strains were used in this study. Strains and plasmids used are listed in Table 6.1 and Table 6.2 Cassette PCR genome editing method was used for genetic manipulations of yeast which involves deletion and C- or N- terminal tagging. These techniques are based on homologues recombination. If the genetic manipulation is deletion the confirmation of the strain was done by yeast colony PCR or PCR from yeast chromosomal DNA. For N- or C-terminal tagging, confirmation was done by microscopy and Western Blotting if the tag was fluorophore or only by Western Blotting if the tag was an epitope such as HA. For obtaining strains with Atg18-Sloop and Atg18-FGGG mutations, cassette strategy was used to replace *atg18*Δ locus in CDY53 with Atg18-Sloop-GFP-klTRP, Atg18-FGGG-GFP-klTRP and as a control with Atg18-GFP-klTRP PCR cassettes obtained using pCD001, pCD002i and pCD003 plasmids as template and Atg18-XmaI-Fw and Atg18-SacII-Rev2 as primers

2.1.2. Yeast Growth

Yeast strains were grown at 30 °C and in sterile YPAD media if not stated otherwise. Filter sterilized SC media was used for microscopy experiments. D-(+)-Glucose (BioFroxx, #1191GR500) was used as the sole carbon source unless stated otherwise. For strains that require galactose for their growth, 2% galactose and 3%raffinose were used as carbon source. Agar plates were prepared with 20g per Liter Agar (Carl Roth #5210.2). All media and agar plates were sterilized.

Prior to the experiments, cells were transferred from -80°C glycerol stocks to appropriate solid agar plate. Then from the solid agar, cells were transferred into the respective liquid medium. To obtain logarithmically growing culture (log-phase), first the liquid culture was left to grow overnight (12-18h) so that they reach the stationary phase. Then, stationary culture's optical density (OD) was measured at 600nm. Spectrophotometer (PG Instrument, T60 Visible Spectrophotometer) was used for spectrophotometric measurements. Next, it was diluted to

OD600 0.15-0.2 in fresh medium. Diluted cultures were then grown until it reaches the OD600 value of 0.8-1.0, which corresponds to ~2.5 doubling.

2.1.3 Yeast Competent Cell Preparation and Transformation

Logarithmically growing 50 ml of culture were transferred to sterile centrifuge tubes and centrifuged at 3200 rpm 2 minutes. All centrifugations in this protocol were performed at room temperature. Later, supernatant was discarded, and the pellet of cells were washed with 20-25 mL sterile of dH_2O. Then cells were resuspended in 20-25 mL LISORB. Then, the pellet is centrifuged once more without adding any reagents to remove the excess LISORB. The excess LISORB is aspirated to ensure there is only pellet left. As a final step, pellet was resuspended in 300 µl LISORB and 50 µl denatured salmon sperm DNA. The amounts of LISORB and salmon sperm DNA were adjusted according to the OD600 and volume of the log-phase culture. To denaturate the salmon sperm DNA, it was heated at 95 °C for 5 minutes followed by 5 min incubation on ice until usage. Obtained competent cells were freshly used for transformation, if not they were stored at -80 °C and thawed at room temperature prior to transformation.

Competent cells were transformed with cassette PCR products or linearized integration plasmids or circular plasmids dependening on the experiment. Commonly 5 µl of PCR product with desired genetic manipulation or 5 µl of integration plasmid or 1-2 µl of circular plasmid was used for high efficiency. For transformation, casette PCR product or the plasmid was mixed to the competent cells and cells are left at room temperature approximately around 15 minutes. Afterwards, 300 µl LIPEG was added to the cells. Competent cells were vortexed well and inculbated at room temperature for another 15 minutes. Next, 35 µl DMSO (Fisher Scientific #BP231-1) was added to the mixture, vortexed and immediately incubated at 42°C water bath for exactly 15 minutes. After the incubation cells were centrifugated at 3200 rpm for 2 minutes at room temperature and supernatant was removed by aspiration. As a final step, cell pellet was resuspendend in 200 µl 1X sterile PBS and transferred to respective selective agar plate (according to the marker) and plated out. The plating out happened immediately if the marker is an auxotrophic marker however if the selective marker is an antibiotic resistance, the cells are left to grow overnight at respective temperature in YPAD for recovery and then plated out to antibiotic containing agar plate. After transformation, plates were incubated at 30 °C.

2.2. Molecular biology Methods

2.2.1. Cassette PCR

All PCRs were conducted using Biometra Tadvenced Twin Analytik Jena PCR machine. To conduct gene deletions; S1/S2 primers were used. For C-terminal and N-terminal tagging S2/S3 primers and S1/S4 primers were used respectively. 50 µl cassette PCR reaction was prepared each time; 5 µL (20 ng/µL) plasmid as template, 3.2 µL forward S1 or S3 primers (10 µM), 3.2 µL reverse S2 or S4 primers (10 µM), 5 µL 10X PCR Buffer 8.75 µL dNTPs (NEB #N0446S), 0.6 µL enzyme mix (2X Taq polymerase (NEB #M0273L) + 1X Vent polymerase (2U/ µL, NEB #M0254S) and 24.25 ddH_2O were added together.

The PCR condition changed depending on the expected size of the PCR product however the common cycles were; 2 min at 95 ºC (Step 1), 30 sec. at 95 ºC (Step 2), 30 sec at 52 ºC (Step 3), X min at 68 ºC, (X is calculated as 1 minute per 1000 bp of the expected product size) (Step 4). Steps 2 to 4 are repeated for 9 times before going through step 5. 30 sec at 95 ºC (Step 5), 30 sec at 52 ºC (Step 6), X min with an increment of 20 sec per step at 68 ºC (Step 7). Steps 5 to 7 are repeated 19 times. When the reaction is down, it was held at 4 ºC. To check the PCR product, 0.8% (unless stated otherwise) agarose gel electrophoresis is run.

2.2.2. Yeast Colony PCR

Colonies were picked from agar plates and added in 50 µL Sarkosyl/NaOH solution (0.01% Sarkosyl in 0.02 NaOH), vortexed vigorously, and boiled at 95 ºC for 15 minutes. To ensure the lysis and increase the lysis efficiency after boiling the mixture was frozen and thawed before usage. The PCR cycle conditions differed according to the desired final product, the general conditions were 5 min at 95 ºC (Step 1), 30 sec at 95 ºC (Step 2), 30 sec at 54 ºC (Step 3), X min at 68 ºC (Step 4), (X is calculated as 1 minute per 1000 bp of the expected product size). Steps 2 to 4 are repeated for 30-35 times. 3 minutes at 68 ºC (Step 5). After the PCR, the products were run on 0.8 % agarose gel electrophoreses prepared in 1X TAE buffer. To test gene deletions, WT PCR products were used as control.

2.2.3. Yeast DNA Isolation by %6 SET Buffer

The yeast cells were inoculated in 5-10 ml YPAD media, and they were kept overnight to ensure stationary phase. Then, 3ml culture was collected by centrifugation at 3200 rpm for two minutes. After removing the supernatant, 300 µl %6 SET buffer was added to the pellet. The

mixture was vortexed and incubated at 65 ºC with shaking for 15 minutes. Then the mixture was transferred onto the ice. On top of that, 150 µl of PI was transferred. This time the mixing was done with invert rotating and the mixture was incubated on ice for 15 minutes. When the incubation finished, the mixture was centrifuged at 14000rpm for 10 minutes. When centrifuge is over, the supernatant was transferred to new Eppendorf tubes and 500 µl isopropanol was added. The Eppendorf was mixed with invert rotate. It was centrifuged for 1 minute at 14000rpm. Then the supernatant was poured and 200 µl cold %70 ethanol was added. The centrifuge was done once more, and the supernatant was poured. The mixture was left to air dry until the ethanol completely evaporates. The isolated DNA pellet was resuspended in 50 µl TE+ 1 µl 1mg/ml Rnase A or pre warmed ddH_2O. The DNA pellet was stored at -20 ºC.

2.2.4 MiniPrep (Plasmid Isolation with Manual Method)

First, an *E. coli* was streaked on the appropriate marker containing TY plate with appropriate antibiotics, then a single colony is inoculated into 3 mlthe liquid TY media with appropriate antibiotics and left to grow overnight at 37 °C with shaking (12-18h). From that culture, 1.5-2 mL culture was taken and centrifugated at 6000 rpm for 5 minutes at RT. Supernatant was aspirated. Then, 300 µl P1 buffer was added on the pellet and vortexed. Next 300 µl of P2 buffer was added and mixed gently by invertion-rotation rapidly. Then immediately 300 µl P3 buffer was added and mixed by invertion-rotation. Then, the mixture was centrifugated at 14000 rpm for 10 minutes. After the centrifuge, the supernatant was transferred into a new Eppendorf tube that contains 500 µl Isopropanol (ACS #0312.2500), mixed by invertion-rotation and centrifugated at 14000 rpm around 15-20 minutes. The supernatant was discarded and 500 µl 70% molecular Ethanol was added to the pellet. Then to get rid of the ethanol, the isolated plasmid is centrifugated at 14000 rpm for 5 minutes. The supernatant was discarded and centrifugated once more to make sure all the ethanol is gone. The supernatant was discarded again, and the pellet was left to air dry until all the Ethanol completely evaporate. As a final step, plasmid was dissolved in 30µl pre-heated (at 65 °C) ddH_2O. The concentration of the isolated plasmid was measured by the NanoDrop device, and the plasmid DNA is stored at -20 °C.

2.2.4. Site-Directed Mutagenesis

A) Atg18-FGGG and Sloop Mutations

Chromosomal DNA isolation was done to Atg18-eGFP containing strains. Then by using 1 µL of the isolated chromosomal DNA, with 250 µL total amount of PCR was set. For that, Atg18-XmaI-Fw (TCCCCCCGGGGCGCTTGTCTATGGACAC) and Atg18-SacII-Rev (TCCCCGCGGCGCGTGAAGTTAACTCTTCCG) were used. After the PCR, the product will run on agarose gel and then it was purified. The purified product was be digested with XmaI and SacII and again it was run on gel and purified. In the meantime, prs315 (the backbone) is also digested with one of the restriction enzymes (XmaI), it was run on gel and purified. Then it was digested with the second restriction enzyme (SacII) and it was run on gel and purified. To the cut insert and cut backbone T4 ligation was applied. After the ligation, the product was PCR product is transformed to *E. coli DH5α* competent cells along with a control which doesn not contain insert. 12 colonies were selected from insert + backbone plate. Each colony were digested with the restriction enzymes of XmaI and SacII. Also, they were cut with NheI (has a cut site only in backbone) and Blp1 (has a cut site only in insert). With this double check we have selected three colonies which were successfully cloned as Atg18-eGFP-klTRP1. Then for Atg18-FGGG site directed mutagenesis, Atg18-FRRG was modified as R285G, R286G. For Atg18-Sloop these modifications Y367K,D369M,K373Y,M375D were done. Primers were designed accordingly to include these modifications (Gopaldass et al., 2017). Site directed mutagenesis is performed to obtain a desired mutation in a plasmid DNA. To perform Atg18-FRRG to FGGG and Atg18-Sloop this method is used.

PCR reaction control	5 µL (5 ng/µL) plasmid	40 µL ddH_2O	10X Turbo PFU Buffer

50 µL mutagenesis PCR	5 µL (5 ng/µL) plasmid	4 µL (2 mM) dNTPs (NEB #N0446S)	1.5 µL forward primer (10 µM)	1.5 µL reverse primer (10 µM)	1.5 µL Turbo PFU DNA Polymerase (Agilent #600250)	5 µL 10X PFU Turbo Buffer	and 31.5 µL ddH_2O

The PCR conditions are set as; 30 sec at 95 ºC (Step 1), 30 sec. at 95 ºC (Step 2), 1 min at 54 ºC (Step 3), X min at 68 ºC (Step 4), (X is calculated as 2 minutes per 1 kb of the expected vector size). Steps 2 to 4 are repeated for 16 times. After the PCR, 2 µL DpnI (Thermo Fisher Scientific #ER1705) is added to the PCR mixture and left to incubate at 37 ºC at least 10 h.

Followed incubation, 3 µL PCR product is transformed to *E. coli DH5α* competent cells to amplify the plasmid. From the forming colonies plasmid isolation was done and sent for sequencing for confirmation. Confirmed colonies were transformed to Atg18Δ strains.

2.3.Biochemical Methods

2.3.1. TCA Total Cell Protein Extraction

The desired cell culture was brought to log phase, and cell pellets were obtained after centrifugion at 14000 rpm for 2 minutes and aspiration of the supernatant. rCell pellets were then resuspended in 800 µl cold ddH_2O and immediately 150 µL of 1.85M NaOH (Merck, #106498) was added and vortexed. Then the mixture was kept on ice for no longer than 5 minutes. 150 µL of 55 % (w/w) TCA (Trichloroacetic acid, Merck #100807) was added to the lysate, vortexed and incubated on ice for 10 minutes. Then the samples were spinned at 14000 rpm for 15-20 minutes at 4 °C. After the centrifuge, the supernatant was sucked by aspiration. The protein pellets were then centrifugated once more without adding anything at 14000 rpm for 1-2 minute at room temperature and the supernatant was once more aspirated all the way. The remaining pellet was resuspended in HU-DTT according to OD600of the culture. For an abundant protein of interest 1ml OD600 starting culture corresponded to 150 µL HU-DTT. If the protein of interest is less abundant 75 µL of HU-DTT was used. After the HU-DTT addition, to neutralize the solution if needed 1-2 µL of 2M Tris-HCI was also added to the mixture. As a final step, the protein samples were boiled to denaturate at 65 °C for 15 minutes and stored at -20 °C if not immediately used for SDS-PAGE.

2.3.2 SDS- PAGE

SDS-PAGE was performed using Biorad Mini-Protean II gel system. The polyacrylamide gels consisted of two parts: separating gel (see table x) and stacking. After separating gel solution was poured , isopropanol (ACS #0312.2500) was added on the gel to cut air contact and align the gel. For the second part of the gel, isopropanol was poured out and the stacking gel was prepared as described in table x. The comb was placed for defining wells. Prior sample loading, the samples were centrifugated at 14000 rpm for 2 minutes. Gels were run in x buffer, at xx mA until…

2.3.3 Western Blotting

After the SDS-PAGE, the blotting was done in semi-dry manner using nitrocellulose membrane (Merck, GE10600002) and 1X Blotting Buffer for 1.5hours at 0.1 A constant with Bio-Rad

Mini-Trans-Blot transfer apparatus. To check if the transfer was successful, Ponceau S staining was applied after each transfer. For blocking, the membrane is blocked with either 5% non-fat dried milk (AppliChem, # A0830) prepared with 1X PBS-T for 1 h at room temperature or overnight at 4 °C or with 5%BSA (SIGMA, A7906) in 1X PBS-T for 1 h at room temperature or overnight at 4 °C. After the blocking, the primary antibody incubates steps followed. Primary antibodies were used multiple times with 3 % non-fat dried milk or %3 BSA containing 1XPBS-T. For HA antibody (mouse) 1:1000 was used and for GFP antibody (rabbit) 1:4000 was used. The membrane is either incubated 1h in RT or overnight at 4 °C. After incubation, the membrane is washed with PBS-T solution 5 minutes for at least 3 times in RT. Then for indirect imaging to occur, the secondary antibody incubation is initiated in of 3 % non-fat dried milk or %3 BSA with 1:1000 concentration. Secondary antibodies used are goat-anti-mouse, goat-anti-rabbit (Advansta #R-05062-500) both are conjugated with HRP (Horse Radish Peroxidase). The imaging is done at Chemidoc (BioRad) using home-made ECL (enhanced chemiluminescence).

2.3.4 PI3,5P2 Pull-Down Assay

A. Small scale test:

Atg18-6HA bearing strain were grown in YPAD until log phase and pellets were collected through centrifugation at 3000 rpm for 2 min at +4°C. Cell pellet coming from a total of 200 ml log-phase culture of 1 OD600 was divided into two screw cap lysis tubes and kept at -80 until lysis. 300 µl ice cold lysis buffer (10mM HEPES pH 7.5, 150mM NaCl, 0.25% NP40, protease inhibitors (2mM Benzamidine, 1mM PMSF, 2,5X Roche protease inhibitor cocktail mix) , phosphatase inhibitors (10mM Sodium ortovanadate, 100mM beta-glycreophosphate, 50mM Sodium Fluoride) were added on each pellet containing lysis tube. Acid washed glass beads (Sigma-G8772) were added on top, until no liquid is visible. Cells were lysed with the help of cell homogenizer (SpeedMill Plus, Analytic Jena), the lysis process was done 13 times and each lysis took 20 sec on and 30 sec resting time at +4°C . Lysis was checked by observing 2 µl from lysates under a compound microscope. Lysed cells look like ruptured empty cells under the microscope with pieces of membranes seen all around. Later, a small cut was made on the cap of lysis tubes using a scalpel. Tubes were placed upside down in 15mL centrifuge tubes and centrifuged at 4000 rpm at +4 ºC for 2min. Then, the lysis tubes were removed, and all cell lysate was collected in another falcon tube. Afterwards, the cell lysate was divided into Eppendorf tubes and spined at 14000rpm for 2 min at +4 ºC. This time only the supernatants

were collected in another tube. 2 µl was taken for protein concentration measuring and 10 µl was taken as total extract. Protein concentration was measured using Bradford Assay (Bio-Rad, 500-0006) and approximately each experiment yielded 15-20mg/ml protein. For Pull Down Assay, two beads were used: One is $PI(3,5)P_2$ covered (P-B035A, Echelon) and control beads (P-B000, Echelon). To get the beads properly the pipette tip was cut and appropriate amount was taken smoothly. Beads were washed at least 5 times. For washing 1ml of 1X wash buffer (10mM HEPES pH 7.5, 150mM NaCl, 0.25% NP40) was used and the beads were centrifuged at 1000rpm for 2 min at +4 ºC. After each centrifuge before removing the supernatant, the beads were left on ice at least 30 sec. After the final wash, the 1X washing buffer was completely removed with the aid of a loading tip. 15 µl (bead bed volume) control beads were added to the cell extract coming from 200 OD x mL cells and incubated for 1.5h in +4°C. This step was necessary to remove sticky proteins that bind to beads unspecifically.

Then the supernatant was taken and divided in two equal amounts and incubated with 15µl (bead bed volume) of either $PI(3,5)P_2$ covered or empty beads for 2h in +4°C. After the incubation beads were washed at least 5 times with 1X wash buffer. After final wash, 1X wash buffer was completely removed from the beads using a gel loading tip and 15µl HU-DTT (0.15g added high Urea buffer solution) was added on the beads and samples were eluted from beads by boiling for 15 min at 65°C. Samples were analyzed by Western Blotting and using anti-HA mouse primary antibody with anti-mouse secondary antibody and by using HRP reaction with ECL solution via ChemiDoc.

B. Large scale experiments:

Two different samples were collected: Metaphase arrested, and anaphase arrested samples.

To achieve anaphase arrested cells, Gal1-Tem1-Upl strain was used, and cells were grown in YP-Raf/Gal medium. When they reached OD600 1, they were centrifuged at 3200 rpm at RT for 2 min and the supernatant was thrown. The pellet was washed at least 2 times with YPAD medium, then the cell pellet was transferred in the YPAD medium for arrest to happen. Approximately, 3h were required for an efficient arrest (around 98%), and to check the arrest cells were checked under the microscope. If large-budded cells are seen around 98% the cells, they were collected. To achieve metaphase arrested cells, Gal1-Cdc20-Upl strain was used and cells were grown in YP-Raf/Gal medium. When they reached 1 OD600 , they were centrifuged at 3200 rpm at RT for 2 min and the supernatant was thrown. The pellet was washed at least 2 times with YPAD medium, then the cell pellet was transferred in the YPAD medium for arrest

to happen. Approximately, 3h were required for an efficient arrest (around 98%), and to check the arrest cells were checked under the microscope. If large-budded cells are seen around 98% the cells, they were collected.10L of 1 OD600 culture pellet was collected for each experiment and divided into 100 lysis tubes to have 100ml x 1 OD600 culture pellet in each tube. Pre-incubation with empty beads followed by pulldown. Protocol was same as the small scale experiment except following: For preclearing the amount of empty bead bed volume was 75µl per experiment. For pulldown the amount of each bead bed volume was 62.5µl. At the end, samples were boiled in 62.5 Hu-DTT. After loading the samples to the gel (by using 9-welled, 1,5mm thick SDS-PAGE gels, entire lysate was able to be loaded), they were stained with PAGE BLUE and given to LC-MS/MS facility in Koç University (KUPAM).

2.3.5 Analysis of the LC-MS/MS analysis

After sending the gels to LC-MS/MS facility in Koç University (KUPAM), their raw file was processed with MaxQuant (Cox & Mann, 2008; Tyanova et al., 2015). LFQ (label free quantification) was chosen and "match between runs" were set. For identification fasta file of yeast genome was uploaded to the software and for digestion Trypsin was selected. The generated "txt" file after the analysis was uploaded to Perseus software (Tyanova et al., 2016) for comparing LFQ values of control and experiment and performing comparison significance analysis. First all the "contaminant", "identified by one site" and "revertants" were excluded from the file. Then the log2(x) of taken for LFQ values. Which resulted in NaN in several values, all the row which contained at least one value were kept but if all the values in one row is NaN it was eliminated. For each NaN, an imputation was done. For determining the significance and enriched proteins in samples the student's t-test was used (S0:0.1 and FDR (false discovery rate) :0.05). With using Perseus, volcano plot is drawn with "Log2(x)" on -y axis and" LFQ experiment -LFQ control" on -x axis. The right, upper side of the volcano plot is indicated as our significant protein list which are enriched in experiment.

2.4 Microscopy-based Methods

The fluorescent microscopy experiments were done using Carl ZEISS Axio Observer 7 motorized inverted epifluorescence microscope equipped with Colibri 7 LED light source, Axiocam 702 Monochrome camera, 100X and 63X Plan Apochromat immersion oil objective lenses, Filter sets 95 (GFP/Cherry), 20 (Rhodamin), FITC and DAPI, and an XL incubation and climate chamber. Each analysis was done with 63X Plan Apochromat immersion oil objective.

2.4.1 Live Cell Imaging

Samples for timelapse experiments were prepared as following: 200µl 6% Con A (Concanavalin A) was spread on the glass surface of Glass bottom petri dishes (WvR 10810-054 Matsunami). After 10 min incubation at room temperature, the Con A was collected back and the glass surface was washed 5-6 times with ddH_2O. Then 200µl log phase culture (in SC-complete filter sterilized media) was transferred on to the glass center. Cultures were incubated on the dish for 30-40 min at 30 °C. Then the glass surface was washed with at least 5 times with the appropriate medium to get rid of the cell debris. The petri dish was transferred to microscopy chamber (pre-heated to 30°C) and the areas of interest were designated. Glass bottom petri dishes containing the cells were kept in the microscope chamber at least for 30 min before imaging for equilibration. Time-lapse experiments were done by using mCherry (led intensity %5 and exposure time 30ms) and FITC (led intensity %30 and 65ms) and FITC channels (63x and 2x2 binning , 1.5min (Fig3.2A),1 min time interval (Fig3.2.B)) with 13 z-stacks).

For still image experiments, cells were grown in appropriate medium at 30 °C. When they reach log phase (0.8-1 OD600), 1ml of each sample were taken and centrifuged at 3200rpm 2min at RT. The supernatant was removed and 20µl of 1XPBS was used to dissolve the pellet. Then to a slide, 2µl of sample was placed, and the cover slide was placed gently without any air bubble. The images were taken at 63x, with mCherry (led intensity %5 and exposure time 30ms) and FITC (led intensity %30 and 65ms) channels. From one slide, only 5 images were taken to avoid the effect of photobleaching. For salt induction assays, 2µl samples were mixed with 2µl 1.8M NaCl on the slide and the cover slide was placed gently. It was waited 10 min before taking the photos. The images were again taken 5 images max and to visualize the effect of salt the imaging was done between 10 min to 15 min following salt addition.

2.4.2. Image Analysis

All microcopy-based image analysis were performed using Image J. For each analysis" max z-projection" was applied. Vacuole localizations were determined by eye, depending on colocalization of Atg18-GFP signal with Vph1-3xmCherry signal. Colocalization was also confirmed using the plot profile function of the ImageJ. Briefly a line of 3 pixel thickness was drawn from inside of the vacuole to the outside of the vacuole perpendicularly to the Vph1-3mcherry signal. Mean fluorescence intensities of GFP and Cherry signals along the line was measured. For each channel, the background was subtracted from the signal to correct for the

background and the obtained corrected signal was divided to the whole cell mean fluorescence intensity (Efe et al., 2007).

For measurement of Atg18-GFP and Vph1-3xmCherry intensities from the time lapse experiments; time frame which the Atg18-GFP signal was not yet seen is taken as a start point and for each channel the mean fluorescence intensity was measured by drawing a circle around the vacuole periphery until after the Atg18-GFP signal is gone. This was done with keeping the area fixed and the circle was moved with the dynamic vacuole. For each channel, another area near the cell of interest was selected as reference area and both the area and its background were also measured. Then for each time point and each channel, fluorescence mean intensity of the background for the cell of interest was subtracted, obtained value was divided by the fluorescence mean intensity of the reference area from which its background was also subtracted.

2.4.3 Statistical Analysis

Graphs were plotted and statistical analysis was performed using Prism 8.0.1 (GraphPad, La Jolla, CA). One-way Anova, and unpaired t-test were used to determine the significance of Atg18-GFP localization on vacuole membrane. ($p < 0.05$ was indicated with * and if or > 0.05 (ns) not indicated on graphs)

AIM OF THE THESIS

$PI(3,5)P_2$ is a low abundance phosphatidyl inositide derivative that takes roles in various of pathways such membrane fusion/fission, Ca^{+2} signaling, endolysosome acidification, selective and bulk autophagy, stress response, MVB pathway (Jason E Duex et al., 2006; Falkenburger et al., 2010; Junya Hasegawa et al., 2017; Li et al., 2014; Odorizzi et al., 1998; Rieter et al., 2012).Although no role has been suggested for $PI(3,5)P_2$ in mitotic exit regulation, proteins involved in $PI(3,5)P_2$ synthesis (*VAC7*, *VAC14* and *FAB1*) were identified among genes required for mitotic exit in the absence of known mitotic exit controllers in multiple independent genome-wide genetic screens(Caydasi et al., 2017; Costanzo et al., 2019; Ye et al., 2005). Using different approaches in our laboratory, mitotic promoting role of $PI(3,5)P_2$ were confirmed (unpublished data), it has not been unraveled how $PI(3,5)P_2$ promotes mitotic exit at the molecular level.

Thus, the aim of this thesis to understand whether $PI(3,5)P_2$ has a role in mitotic exit, and whether $PI(3,5)P_2$ production is under any control of the cell cycle. For this purpose, the following approaches were followed:

1. Monitoring $PI(3,5)P_2$ throughout the cell cycle since cell cycle dependent changes in $PI(3,5)P_2$ levels and /or localization would indicate a possible cell cycle dependent regulatory mechanism on $PI(3,5)P_2$ synthesis. A known $PI(3,5)P_2$ effector protein, Atg18 as an *in vivo* sensor has been monitored throughout the cell cycle.
2. Identifying potential $PI(3,5)P_2$ effector proteins in the mitosis stage of the cell cycle would dissect the functional link between $PI(3,5)P_2$ and mitotic exit. To execute this aim, a pull-down approach has been employed using $PI(3,5)P_2$ covered beads followed by mass spectrometry analysis.

RESULTS

3.1. Atg18 localizes to the vacuole periphery depending on PI(3,5)P_2 and Vac7 dependent way

To understand whether PI(3,5)P_2 levels change during cell cycle, we sought to monitored PI(3,5)P_2 in living cells. There is no available dye or antibodies that specifically bind PI(3,5)P_2. The most ideal candidate as a PI3,5P2 sensor is the Atg18 protein which is a known effector protein of PI(3,5)P_2, (Dove et al., 2004; Efe et al., 2007; Gopaldass et al., 2017; Takatori et al., 2016). Although Atg18 can bind both PI(3,5)P_2 and PI3P, there is evidence that affinity of Atg18 to PI(3,5)P_2 is much higher than its affinity to PI3P (Dove et al., 2004; Gopaldass et al., 2017). Atg18 localizes to the vacuole membrane in a Fab1 dependent manner and to a punctuate compartment in the vicinity of vacuoles independently of Fab1 (Dove et al., 2004), suggesting that the vacuole membrane localization of Atg18 is its interaction with PI(3,5)P_2. Although Fab1 and Atg18 physically interacts (Efe et al., 2007) vacuole localization of Atg18 is unlikely to be via its interaction with Fab1 as Atg18 vacuole membrane localization also depends on Vac7 and Vac14 (Efe et al., 2007)both of which are required for PI(3,5)P_2 synthesis. These data yet do not rule out the possibility that Atg18 vacuole membrane localization may be directly through Atg18 interaction with the Vac7-Vac14-Fab1 complex.

In order to understand whether Atg18 can be used as an *in vivo* sensor for PI(3,5)P_2 we first analyzed how Atg18-GFP localization at the vacuole membrane changes when PI(3,5)P_2 levels increase but Vac7-Vac14-Fab1 complex protein levels stay unchanged. Membrane localization of Fab1, Vac7 and Vac14 do not change upon hyperosmotic shock while PI(3,5)P_2 levels increase(Csikász-Nagy et al., 2006; J. E. Duex et al., 2006). Thus, we made use of hyperosmotic shock to increase PI3,5P2 levels without affecting the Vac7-Vac14-Fab1 complex levels. Hyperosmotic shock increased the percentage of wild type cells that displayed Atg18-GFP on their vacuole membrane (Fig3.1A and B). Thus, elevated levels of PI(3,5)P_2 results in increased Atg18 vacuole membrane localization. As expected, deletion of *VAC14* , *VAC7* and *FAB1* *i*mpaired Atg18 localization (Fig1C-H). Salt treatment caused an increase in Atg18-GFP vacuole membrane localization in *vac14*Δ cells (Fig1C and D), but not in *vac7*Δ (Fig1E and F) and *fab1*Δ (Fig1G and H) cells, which is consistent with previous data that hyperosmotic shock triggered PI(3,5)P_2 production in *vac14*Δ cells, albeit at a low level, but not in *vac7*Δ cells (Jason E Duex et al., 2006). These experiments support that PI(3,5)P_2 vacuole membrane

localization correlates with the PI3,5P2 levels rather that PAS protein levels at the vacuole membrane.

Next, we made use of a hyperactive Fab1 allele (*fab1-hyp*) (J. E. Duex et al., 2006) to increase $PI(3,5)P_2$ levels as an alternative method to hyperosmotic shock(J. E. Duex et al., 2006) . *fab-hyp* expression increased the percentage of wild type and *vac14*Δ cells that displayed Atg18-GFP on their vacuole membrane (Fig1A and B). Although *fab1-hyp* rescues $PI(3,5)P_2$ levels in *vac7*Δ cells(J. E. Duex et al., 2006; Gary et al., 2002) it did not affect Atg18-GFP vacuole membrane localization in *vac7*Δ cells (Fig1C-D). Taken together these data suggest that $PI(3,5)P_2$ localization at the vacuole membrane requires both the presence Vac7 and $PI(3,5)P_2$ but not Vac14.

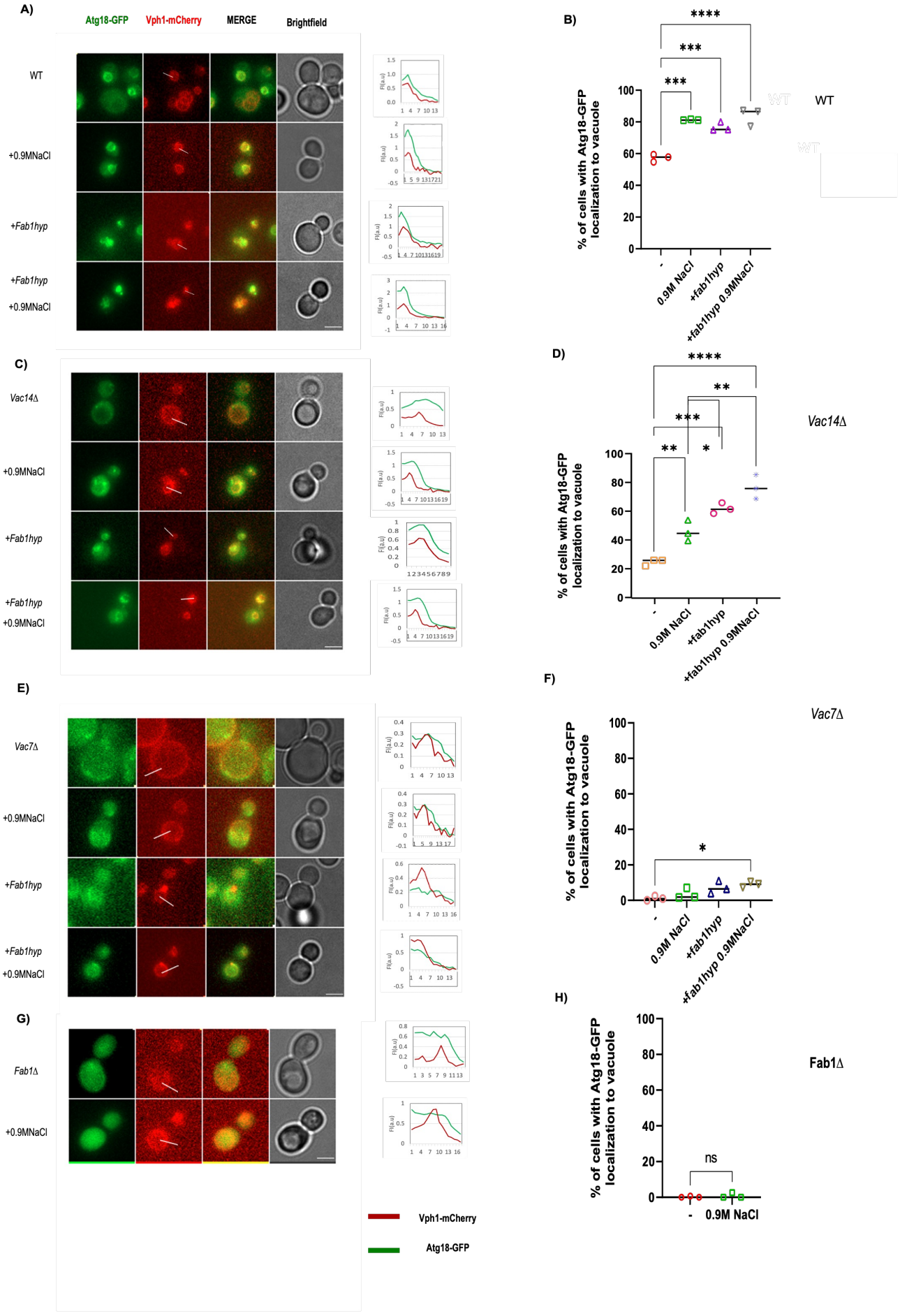
A)
Atg18-GFP
Vph1-mCherry
MERGE
Brightfield
WT
+0.9MNaCl
+Fab1hyp
+Fab1hyp
+0.9MNaCl
B)
% of cells with Atg18-GFP localization to vacuole
WT
0.9M NaCl
+fab1hyp
+fab1hyp 0.9MNaCl
C)
Vac14Δ
D)
Vac14Δ
E)
Vac7Δ
F)
Vac7Δ
G)
Fab1Δ
H)
Fab1Δ
ns
Vph1-mCherry
Atg18-GFP

Figure 3. 1. Atg18 localizes to the vacuole periphery depending on PI(3,5)P_2 and Vac7
Representative still images and quantification of Atg18 vacuole membrane localization in WT (A-B), *vac14*Δ (C-D), *vac7*Δ (E-F) and *fab1*Δ (G-H) cells. The experiments were conducted in basal conditions (marked with a hyphen), under hyperosmotic shock (0.9 M NaCl), in the presence of the fab1 hyperactive allele in the cell (+*fab1hyp*) and both hyperosmotic shock and fab1 hyperactive addition (+*fab1hyp* 0.9 M NaCl). Log phase cultures of Atg18-GFP and Vph1-3xmCherry bearing strains were analyzed by microscopy. Vph1-3xmCherry serves as a vacuole marker. Atg18-GFP localization around the vacuole periphery was considered as vacuole membrane localization. Scale bar= 2 μm.
Graphs show data from three independent experiments. Standard deviation and means are indicated. At least 100 cells were counted from each cell condition in each experiment. One-way Anova was performed for comparison of localization, where; *: p<0.05:, **:p< 0.002, ***: p= 0.0001 and ****: p < 0.0001. Co-localization of Vph1-3xmcherry and Atg18-GFP is shown by plotting the corrected mean fluorescence profiles (Image J) of both signals along the indicated line in A, C and E. Signal intensity correction was performed for the medium background and the cytoplasm as: (FI_{ROI}- FI_{ROI} backround)/$FI_{cytoplasm}$) (Efe et al., 2007).

3.2. Atg18 significantly localizes to the daughter vacuole periphery more than the mother vacuole periphery

Considering the low levels of PI3,5P2 under basal conditions, we were intrigued by Atg18-GFP presence at the vacuole membrane of more than 50% of cells without hyperosmotic shock (Fig3.1B). We noticed that when Atg18-GFP was detected in such cells, it was found mostly on the vacuole that resided in the bud (Fig3.1A). To examine this more carefully, we quantified vacuole membrane localization of Atg18-GFP in cells that already segregated their vacuole to the daughter (bud) cell compartment. We scored five different categories of Atg18-GFP signal at the vacuole: mother and daughter vacuole periphery localization, only daughter periphery localization, only mother periphery localization, punctuated localization on the vacuole, and no signal (Fig3.2A). Atg18 localized at the daughter vacuole whereas the localization of only mother vacuole and both vacuoles were significantly lower (Fig3.2A-B). Upon *fab1-hyp* expression, Atg18 at the daughter vacuole was not significantly changed, whereas Atg18-GFP at both mother and daughter compartment increased (Fig3.1C).

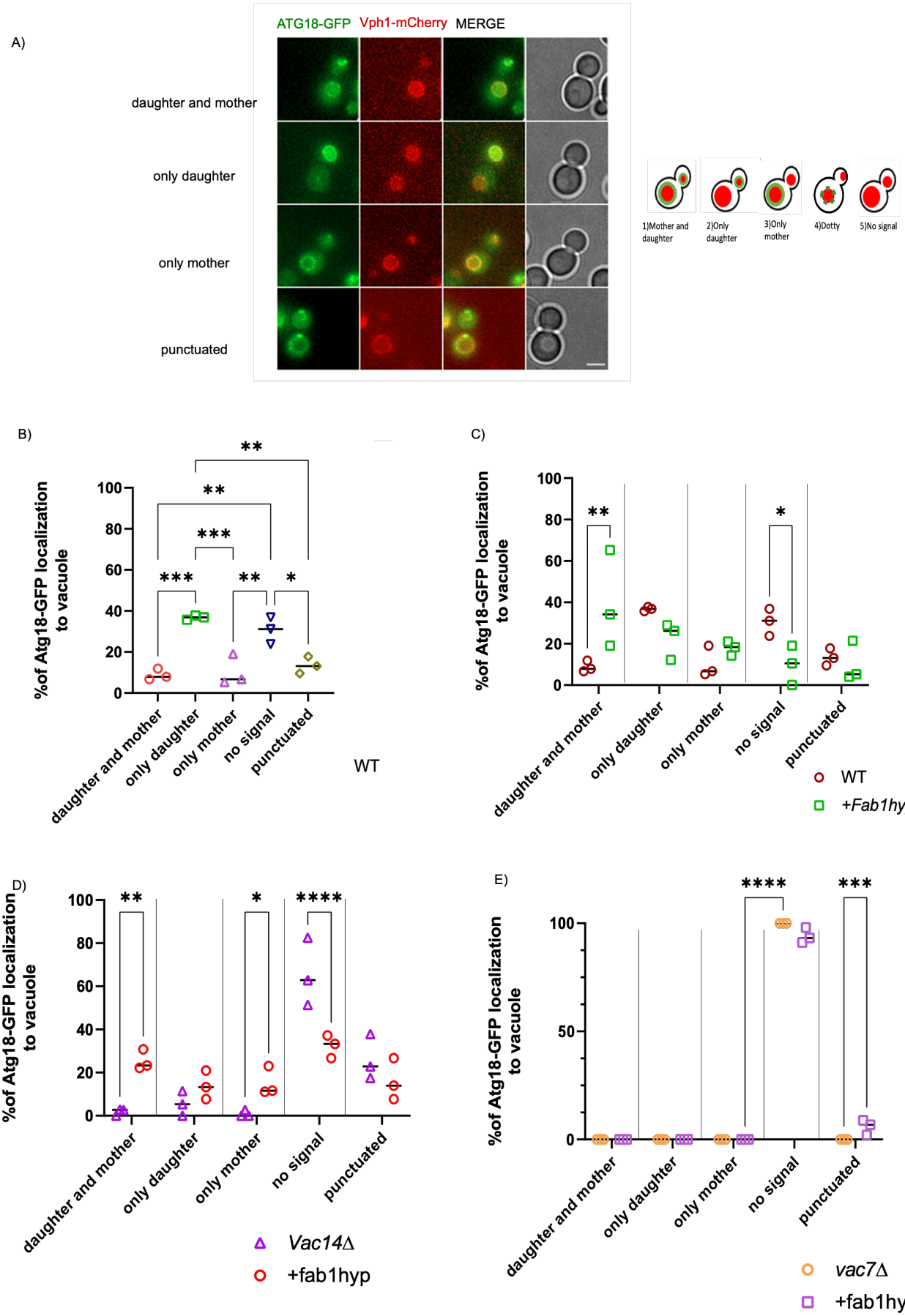
A)
ATG18-GFP
Vph1-mCherry
MERGE
daughter and mother
only daughter
only mother
punctuated
1)Mother and daughter
2)Only daughter
3)Only mother
4)Dotty
5)No signal
B)
%of Atg18-GFP localization to vacuole
daughter and mother
only daughter
only mother
no signal
punctuated
WT
C)
%of Atg18-GFP localization to vacuole
WT
+Fab1hyp
D)
%of Atg18-GFP localization to vacuole
Vac14Δ
+fab1hyp
E)
%of Atg18-GFP localization to vacuole
vac7Δ
+fab1hyp

Figure 3. 2. Atg18-GFP localizes predominantly to the daughter vacuole of unperturbed cells that had segregated their vacuole

Atg18-GFP localization in cells with segregated vacuoles. **A.** Representative still images for indicated type of vacuole localization in WT cells. Scale bar= 2 µm. Atg18 localization in (B) WT cells, (C) *WT* cells with and without *fab1-hyp*, (C) *vac14*Δ cells with and without *fab1-hyp*, (D) *vac7*Δ cells with and without of *fab1-hyp*. WT data shown in B comes from the same experiment as in C, and thus are identical.
Graphs show data from three independent experiments. Standard deviation and means are indicated. At least 100 cells were counted from each cell condition in each experiment. One-way Anova was performed for comparison of localization, where; *: p<0.05:, **:p< 0.002, ***: p= 0.0001 and ****: p < 0.0001.

When only considering cells with segregated vacuoles, *vac14*Δ cells had less Atg18-GFP vacuole localization overall, but about 10% of cells had Atg18-GFP only at the daughter vacuole (Fig3.2D). *fab1-hyp* introduction to *vac14*Δ increased Atg18-GFP at both vacuoles (Fig3.2D). Atg18-GFP at the vacuole was lost in *vac7*Δ cells independently of presence of fab1-hyp (Fig3.2E), consisted with previous data. These data suggest that $PI(3,5P)_2$ levels may be specifically high at the vacuole that has segregated to the daughter.

3.3. Atg18 localizes to the daughter vacuole during mitosis

In order to understand the timing of Atg18-GFP daughter vacuole localization under basal conditions, we performed time-lapse experiments. Vph1-3xmCherry was used as a vacuole marker. Cells in which vacuole segregation were observed during the time-lapse experiment were categorized according to Atg18-GFP localization at the vacuole membrane. Three independent timelapse experiments were conducted. Each timelapse lasted 90 min with 1.5 min time resolution. In average 50 cells were counted from each timelapse experiment to make 160 total number of dividing cells where vacuole segregation was observed. About 50% of such cells had Atg18-GFP at only their daughter vacuole and a small fraction had Atg18 at the mother vacuole or both vacuoles (Fig3A and B). Atg18 signal was not detected at the vacuole membrane, or a punctuated signal was observed in about 20% of cells (Fig3A and B).

Next, we calculated the persistence of Atg18-GFP localization at the vacuole periphery in these cells. Atg18-GFP signal stayed on average 10 minutes on daughter vacuole (Fig3C) and 5 minutes on the mother vacuole (Notice the low number of cells in which Atg18 localization

was restricted to the mother vacuole alone). We then asked the timing of Atg18-GFP signal appearance on the mother or daughter vacuole membranes with respect to the timing of vacuole segregation. The start of pinching-off of the mother vacuole towards the daughter cell is considered as the "start of the segregation". When the link between mother vacuole and daughter vacuole is disconnected, it is considered as the "end of vacuole segregation". Daughter vacuole membrane localization started in average 10 min after vacuole segregation finished (Fig3.3D). However, this localization appeared mostly before vacuole segregation when Atg18 localization was restricted to the mother vacuole alone (Fig3.3D).

Then, we asked when Atg18-GFP appears at the daughter vacuole with respect to the cell cycle. For this, mCherry-Tubulin was used as a cell cycle marker. Onset of anaphase was determined by the start of fast tubulin elongation and tubulin breakage marked the mitotic exit. Using anaphase onset, spindle breakage and the entrance of one spindle pole to the daughter cell compartment as reference points, we analyzed the timing of Atg18-GFP signal appearance at the daughter vacuole (Fig3.3E). Atg18-GFP appeared on the daughter vacuole in average 5 min before anaphase onset (tubulin elongation start) and 17 min before anaphase ends (spindle breaks). This timing coincided well with the entrance of one spindle pole to the daughter cell (Fig3.3F).

To sum up, Atg18 appeared at the daughter vacuole shortly before anaphase onset and persisted for about 10 min. These data suggest that, in cells which are not under hyperosmotic shock, $PI(3,5)P_2$ may specifically be synthesized in mitosis at the vacuole that segregated to the daughter cell compartment, or interaction of Atg18 with Vac7 or Fab1 may specifically be promoted in this compartment during mitosis.

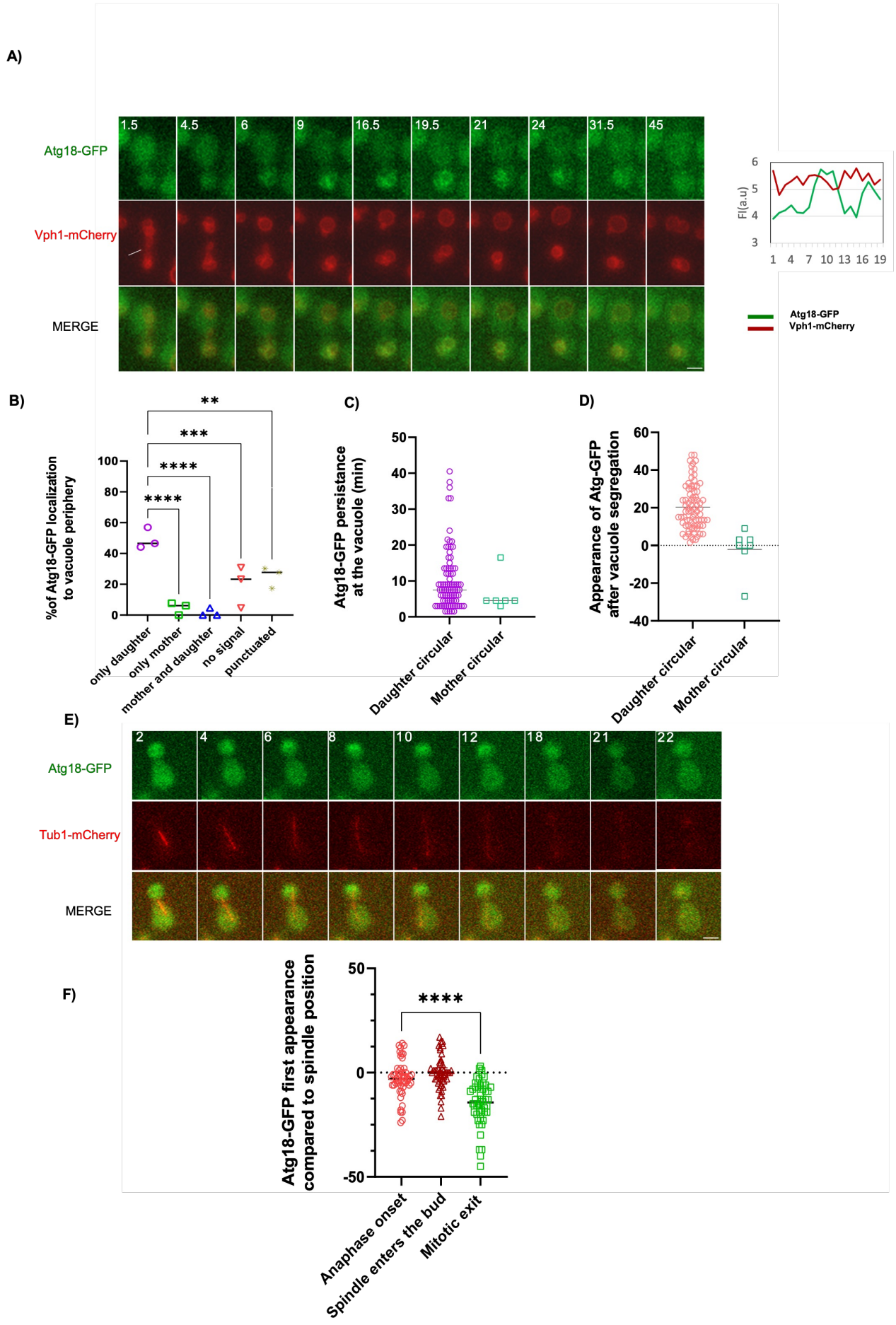
A)
Atg18-GFP
Vph1-mCherry
MERGE
1.5
4.5
6
9
16.5
19.5
21
24
31.5
45
FI(a.u)
Atg18-GFP
Vph1-mCherry
B)
%of Atg18-GFP localization to vacuole periphery
only daughter
only mother
mother and daughter
no signal
punctuated
C)
Atg18-GFP persistance at the vacuole (min)
Daughter circular
Mother circular
D)
Appearance of Atg-GFP after vacuole segregation
Daughter circular
Mother circular
E)
Atg18-GFP
Tub1-mCherry
MERGE
F)
Atg18-GFP first appearance compared to spindle position
Anaphase onset
Spindle enters the bud
Mitotic exit

Figure 3. 3. Atg18-GFP localizes predominantly to the daughter vacuole of cells in mitosis. **A.**Selected time points from the time-lapse series of Atg18-GFP Vph1-3mCherry cells (left panel) and quantification of Atg18-GFP and Vph1-3mCherry signals on the daughter vacuole. Timepoints (in minutes) are indicated on the top row of images and on the x-axis of the graph. B. Dot plot showing percentage of Atg18-GFP localization at the vacuole membrane, based on timelapse data coming from three independent experiments. Time resolution of the time-lapse were 1,5 min. Only the cells in which vacuole segregation were observed during the time-lapse experiment were quantified. The number of cells quantified in each experiment were: 65, 43 and 52. Atg18 localization in such cells were categorized as "no signal" when Atg18-GFP was not detected at the vacuole membrane; as "punctuated" when Atg18-GFP was not present all around the vacuole membrane but at some small puncta around the vacuole at least one time frame; as "only mother" when Atg18-GFP signal was seen only around the mother cell vacuole at least for one time frame; as "only daughter" when Atg18-GFP signal was seen only around the daughter cell vacuole at least for one time frame; as "daughter and mother" when Atg18-GFP signal was seen around the daughter cell vacuole and around the mother cell vacuole at the same time or at different time points from the start of vacuole segregation until the end of the timelapse. (Note that in only one cell, the signal appeared at the daughter cell vacuole first and then this signal was converted to a punctuated signal. This cell was counted in both categories separately). **C**.Dot plot showing the duration of Atg18-GFP signal at the daughter and mother vacuole. Each dot represents an individual cell that came from the sum of three independent experiments which were also used in B. It was seen that, Atg18-GFP persisted longer (on average 10min) on daughter vacuole compared to mother vacuole (on average 5min). There are times which Atg18-GFP signal appeared again after getting disappeared for the first time. Their total duration was calculated in those cases. **D.** Dot plot showing the first appearance of Atg18-GFP signal at the daughter and mother vacuole compared to the start of vacuole segregation. Each dot represents an individual cell that came from the sum of three independent experiments which were also used in B and C. It was seen that, when Atg18-GFP localization to the daughter vacuole periphery is observed on average 20 min after the vacuole segregation start. Whereas, Atg18-GFP localization to mother vacuole periphery is observed around or before the vacuole segregation starts. **E.** Selected time points from the time-lapse series of Atg18-GFP mCherry-Tub1 cells and quantification of Atg18-GFP mCherry-Tub1 which Atg18-GFP is seen on daughter **cells.** Timepoints (in minutes) are indicated on the top row of images and on the x-axis of the graph. **F.** Dot plot showing the percentage of Atg18-GFP signal

at the daughter cell. Each dot represents an individual cell. Time resolution of the time-lapse were 1min. Cells were analyzed according to the tubulin elongation. First reference point was taken as tubulin elongation start which indicates the anaphase onset, second reference point was taken as the time where tubulin enters the bud, and the third reference point was taken as spindle breakage time which indicates the mitotic exit. Only the cells which all three reference points seen are counted. Scale bar is 2 μm. One-way Anova was performed for comparison, **where;** *: $p<0.05$:, **:$p< 0.002$, ***: $p= 0.0001$ and ****: $p < 0.0001$.

3.4 Atg18 localization at the daughter vacuole is independent of it is PI3P binding

Atg18 has WD-40 repeats that fold into a beta propeller structure with seven blades(Dove et al., 2004), through which it binds to PI3P and $PI(3,5)P_2$. FRRG sequence present in between 5^{th} and 6^{th} blades is important for Atg18 binding to PI3P and $PI(3,5)P_2$. Accordingly, mutation of this sequence to FTTG or FGGG decreases its affinity to both PI3P and $PI(3,5)P_2$more than 40-fold(Dove et al., 2004; Gopaldass et al., 2017). Another mutant where the alpha-helix structure is disrupted (Atg18-SlooP) mutant only binds to $PI(3,5)P_2$but not PI3P(Gopaldass et al., 2017). Previous reports showed that Atg18-SlooP but not Atg18-FGGG localizes to the vacuole periphery under osmotic stress(Gopaldass et al., 2017). To understand the nature of vacuole localization of Atg18 under basal conditions, we analyzed Atg18-Sloop localization in cycling live cells without osmotic stress. Atg18-SlooP mutant localized to vacuole membranes whereas Atg18-FGGG mutant did not (Fig4A). Atg18-Sloop localization increased upon salt treatment whereas ATG18-FGGG did not (Fig4A). This data indicates that Atg18 vacuole localization under basal conditions is mostly through its interaction with $PI(3,5)P_2$ rather than P3P.

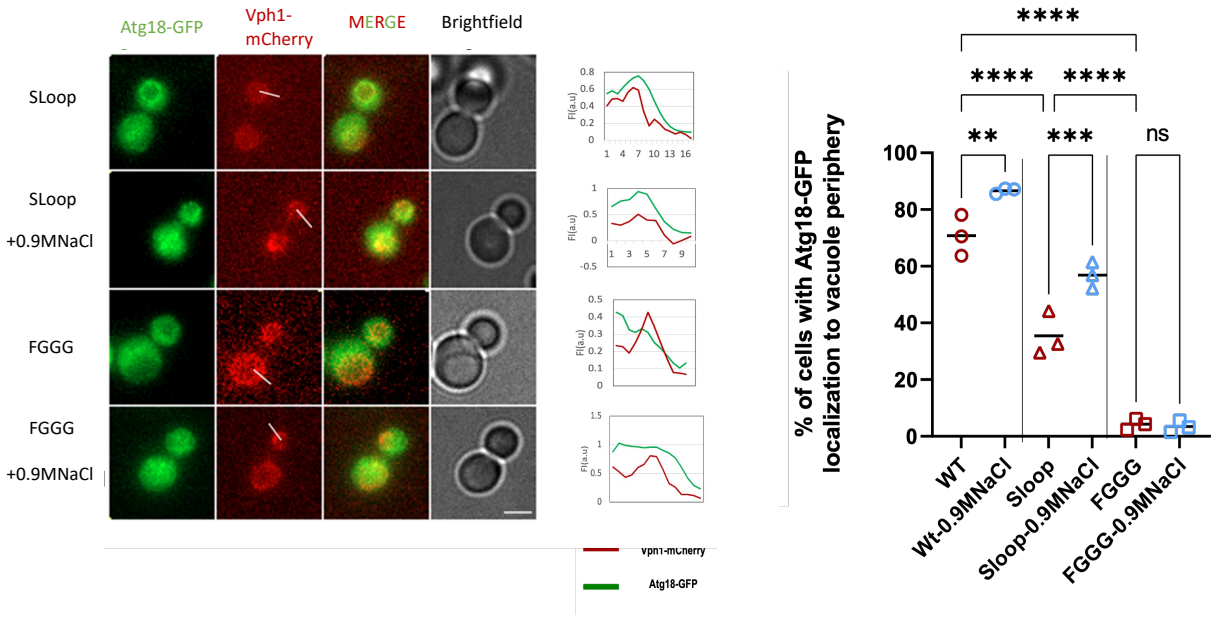

Figure 3. 4. Atg18-Sloop-GFP localizes predominantly to the vacuole of unperturbed cells

A) Still images of Atg18-Sloop-GFP and Atg18-FGGG-GFP Vph1-3mCherry cells with and without 0.9MNaCl and quantification of Atg18-GFP localization to Vph1-3mCherry signals on vacuole periphery. **B.** Dot plot showing percentage of Atg18-GFP, Atg18-Sloop-GFP and Atg18-FGGG-GFP localization with or without 0.9MNaCl (respectively) at the vacuole membrane, based on three independent experiments. WT Atg18-GFP exhibits nearly 70% localization without salt and more than 80% localization with salt. Atg18-Sloop-GFP exhibits around 35% localization to vacuole without salt and the localization increased up to 60% with salt. Atg18-FGGG-GFP showed no localization to vacuole periphery with or without salt. not detected at the vacuole membrane; as "punctuated" when Atg18-GFP was not present all around the vacuole membrane but at some small puncta around the vacuole at least one time frame; as "only mother" when Atg18-GFP signal was seen only around the mother cell vacuole at least for one time frame; as "only daughter" when Atg18-GFP signal was seen only around the daughter cell vacuole at least for one time frame; as "daughter and mother" when Atg18-GFP signal was seen around the daughter cell vacuole and around the mother cell vacuole at the same time or at different time points from the start of vacuole segregation until the end of the timelapse. Note that, Atg18-Sloop-GFP signal was localized mostly on the daughter

vacuole, but the signal was fader than the Wt. The significance analysis is done by one-way Anova. (Overall $p<0.05$ gives significance, *<0.05, ** < 0.002 - *** = 0.0001 - **** < 0.0001)

Taken together, our data shows that Atg18 localizes to the daughter vacuole of cycling cells mostly during metaphase-anaphase and this localization is dependent on its binding to $PI(3,5)P_2$ (not PI3P) and Vac7.

Since $PI(3,5)P_2$ is scarce *in vivo*, it is less studied compared to other PPIs. So far only few effector proteins are identified. To determine potential effector proteins of $PI(3,5)P_2$ we took a pulldown approach followed by mass spectroscopy (MS). For this purpose, briefly, we incubated yeast cell lysates with $PI(3,5)P_2$ covered beads (P-B035A, Echelon) in addition to empty beads (P-B000, Echelon) as control. Proteins bound to beads were identified by MS.

To optimize the pull-down method, we used Atg18 as a known effector of PI3,5P2. To avoid non-specific bindings, all lysates were pre-incubated with control beads prior to pull down. Then, lysates of Atg18-6HA carrying yeast strains were incubated with control beads and $PI(3,5)P_2$ covered beads and analyzed for the presence of Atg18-6HA on beads through western blotting (Fig6A). Atg18 came along with the $PI(3,5)P_2$ covered beads but not with control beads (Fig6A). After this initial proof of principle experiment, we performed large scale experiments where we used cells arrested in anaphase and metaphase. For anaphase arrest we used Gal1-UPL-Tem1 strains which arrest as large-budded cells with segregated DNA (based on microscopy with DAPI staining) in glucose containing media upon depletion of Tem1, which is an essential protein for mitotic exit (Valerio-Santiago & Monje-Casas, 2011). For metaphase arrest we used Gal1-UPL-Cdc20 strains which arrest as large-budded cells with unsegregated DNA (based on microscopy with DAPI staining) in glucose containing media upon depletion of Cdc20. Lysates were incubated with beads, beads were washed with lysis buffer and boiled in HU-DTT sample buffer. Samples were then run on %10 SDS-PAGE and stained with Page Blue dye (Figure 6C-F). Each lane was divided in 5 fractions and was given to mass spectrometry facility (Koc University, KUPAM) for LC-MS-MS analysis. Each experiment were done as two independent biological replicates and LC-MS-MS was performed in 2 technical replicates for each independent experiment.

For determining the significant hits that specifically bind PI3,5P2 coated beads but not to empty beads, MaxQuant software (Cox & Mann, 2008) was used. In MaxQuant, LFQ (Label free quantification) option was chosen along with "match between runs". Then the generated data by MaxQuant was loaded into Perseus.exe (Tyanova et al., 2016) for comparison and significance analysis. After removing the "contaminants", "revertants", and "only identified by one site proteins"; the LFQ intensity values were transformed by log2(x). Then, each control LFQs were assigned as LFQ control group and each $PI(3,5)P_2$ LFQ intensity was assigned as LFQ sample. For significance analysis, Student's two sample t-test was applied with (S0: 0.1 and FDR: 0.05). The volcano plot for each biological replica was generated. In volcano plots the names of the common proteins were written. (Fig5A and D).

We then compared the proteins that came significantly in each group and biological replicate (among two anaphase and two metaphase biological replica) (Fig 8). When we look at the diagram, it is seen that biological replicas of metaphase arrested cells exhibited 21 common proteins whereas the biological replicas of anaphase arrested cell exhibited 7. When we look at the significant hits separately, in metaphase overall pulled down protein number is more than the protein pulled down in anaphase. Metaphase I and Anaphase I also overlapped in 20 proteins. We expected more overlapping between groups and between anaphase and metaphase arrested cells. However, many factor may affect the mass spectrometry results and certain protein groups being pulled down and being so abundant may mask the other proteins which are less abundant. Overall, when we look at the common proteins in at least two groups, the significant protein hit list becomes more stringent and reliable. Especially the hits which came in at least three groups such as Hsv2, Spt5, SCP160 and DBP3 can be investigated even further (Fig3.8).

Then with the help of STRING.db their GO (gene ontology) analysis was performed (Szklarczyk et al., 2021). In our common hits, Hsv2 was an expected protein since it is a known binding partner of $PI(3,5)P_2$ (Junya Hasegawa et al., 2017). Surprisingly, we did not encounter Atg18 among out significant hits. This may be due to low abundance issue. In mass spectrometry, high abundant proteins may mask the low abundant proteins. To minimize this problem, we have fractionated our gel however still Atg18 was not achieved as a significant hit.

When we look at the proteins that came as a hit, strikingly lot of the proteins were involved in ribosomal biogenesis and translation. $PI(3,5)P_2$ is also related to ribosomes as it is involved in nuclear export and maturation of ribosomal subunit (Milkereit et al., 2003) (Johnson et al., 2002). Usually, ribosomal proteins may be ignored and classified as non-significant due to their abundance and stickiness. However, since $PI(3,5)P_2$ is shown to be involved in RNA granules docking to endosomes/vacuoles/lysosomes (Junya Hasegawa et al., 2017). It is tempting to speculate that the interactions with ribosome and translation components may be real and relevant. In addition to ribosome components, Noc1p-Noc2p complex came with high enrichment in our analysis.

Other than being indicated on the Venn Diagram, $PI(3,5)P_2$ is shown to be interacting a lot of cytoplasmic stress granule component such as; SSD1, NPL3, PAB1, GUS1, TIF4631, SBP1, YEF3, CLU1, DED1 and RBG1. It is known that stress granule formation is a needed process to promote cell survival, they try to keep the stress-related damage to a minimum (Wek et al., 2006). Also, the stress granules are non-translating pools of RNA granules and their fundamental role is in degradation and inhibition of host mRNAs (Lloyd, 2012).The malfunction in stress granule assembly usually results in diseases such as cancer, neurodegenerative diseases (Mahboubi and Stochaj 2017). It is also known that lack of $PI(3,5)P_2$ and the malfunctioning of its kinase Fab1 leads to neurodegenerative disorders as well.

One of the proteins that came significantly is Net1 protein which is a part of RENT complex (Net1-Cdc14) (Shou et al., 1999), it is involved in keeping the Cdc14 in the nucleolus until mitotic exit and ending of the mitosis is dependent on Cdc14 release. Considering the functional link between mitotic exit and P35p2, this interaction is particularly interesting to further follow up due to its direct link with mitotic exit.

Also, $PI(3,5)P_2$ is seen to be pulling down CKA2 which is a casein kinase 2 and it has a role in cell growth and proliferation. Nowadays CKA2 is now being targeted for many neurodegenerative disorders and viral infections such as COVID-19 (Borgo et al., 2021). Also, it is known that CKA2 together with TORC1 regulate ribosome biogenesis in post-transcriptional level(Kos-Braun et al., 2017). CKA2 also regulates stress response in yeast by

direct phosphorylation of Msn2/4 (general stress response transcriptional activator) (Cho & Hahn, 2017).

BBC1 and MYO3 are part of biological component of actin cortical patch. In budding yeast, the actin cortical patch assembles and disassembles very rapidly in cell cycle (Waddle et al., 1996). Even though, BBC1 and MYO3 along with MYO5 were first introduced as the components of actin cortical patch, it is also seen that in yeast BBC1 and MYO5 is also involved in endocytosis process (Goode et al., 2015). It was indicated earlier that $PI(3,5)P_2$ has a role in endosome maturation and cargo selection in endocytosis (Dong, Shen, et al., 2010). It may be a possibility for $PI(3,5)P_2$ to interact with BBC1 in functioning endocytosis.

$PI(3,5)P_2$ is also seen to be interacting with BSH1 which is involved clathrin-coated vesicle (S L Schmid, 1997). It is known that $PI(4,5)P_2$ is involved in clathrin-coated vesicle and cargo sorting however recent findings also revealed that $PI(3,5)P_2$ is also involved in cargo selection so this may indicate PPIs working together (Fig7).

It is worth to emphasize that these interactions should further be validated through other experimental set ups, such as using lipid arrays to show the specificity of the interaction towards PI3,5P2. Nevertheless, our suggests that, $PI(3,5)P_2$ may work together with various different proteins and so may be involved in many pathways from ribosome biogenesis and from cell cycle regulations and dynamics to translation.

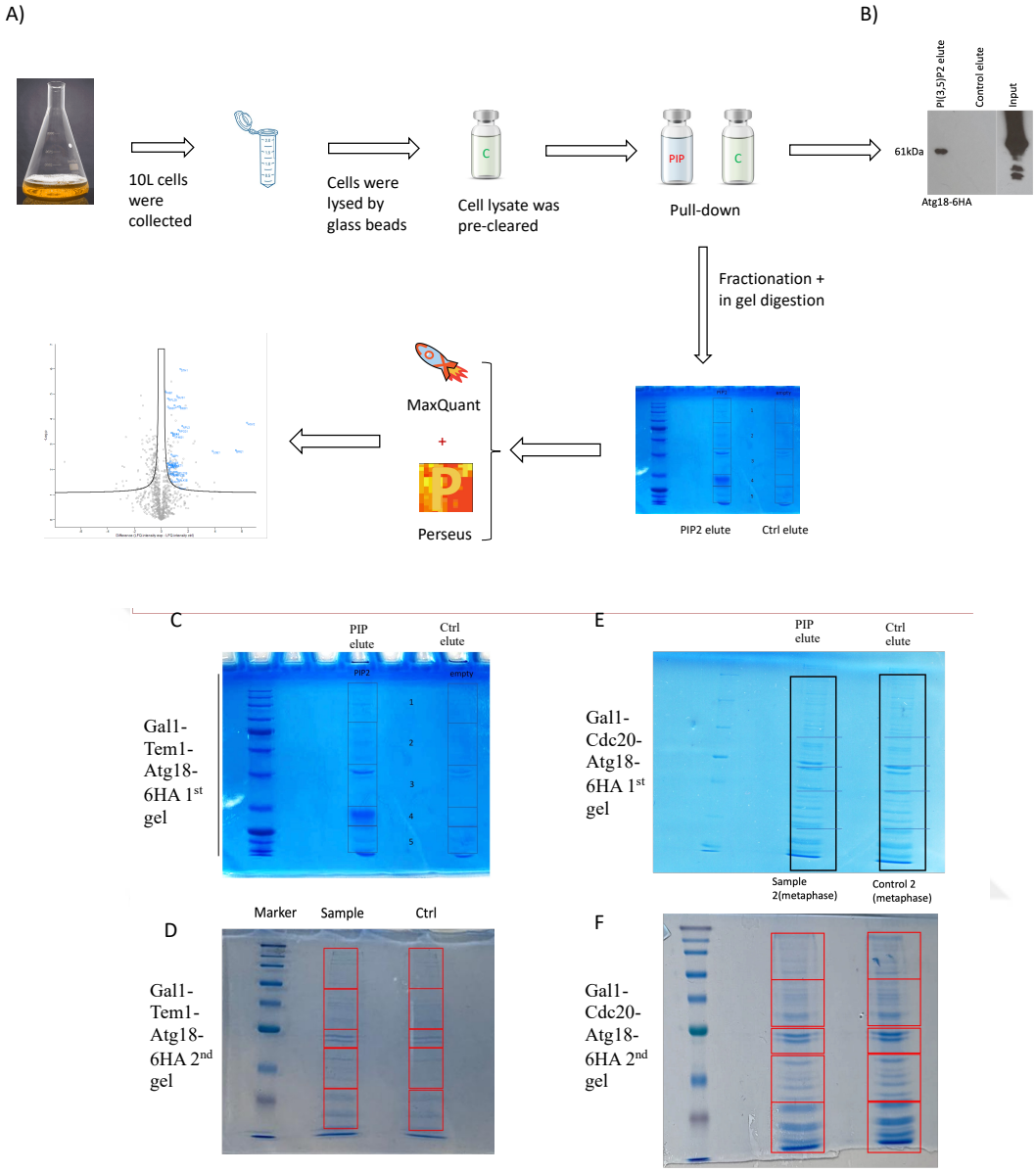

Figure 3. 5. Schematic representation of large scale pull down after optimizing small scale pull-down assay by using Atg18-6HA as a known effector protein

A. Small-scale optimization of pull-down assay was performed with using Atg18-6HA as effector protein and PI(3,5)P_2 covered beads along with control beads. 30µl slurry was used for 1ml 100OD cells. Before pull-down, pre-clear step was applied to whole cell lysate with 30µl slurry. **B.** Schematic design to explain large-scale pull-down assay. Atg18-6HA was collected in large flasks to obtain 5000OD cells to be incubated with 125µl slurry later. Before pull-down, pre-clear step was applied to whole cell lysate with 150µl slurry. After the pull-down samples were eluted with HU-DTT buffer and loaded on the 10% SDS-PAGE gel. **C-D-E-F.** PAGE

BLUE dyed gels of all four replicas; **C-D** is two biological replicas of Gal1-Tem1-Upl-Atg18-6HA (anaphase arrested) with being fractionated in 5 pieces, first lane being PI(3,5)P_2 elutes and second lane being control elutes. **E-F** is two biological replicas of Gal1-Cdc20-Upl-Atg18-6HA (metaphase arrested) with being fractionated in 5 pieces, first lane being PI(3,5)P_2 elutes and second lane being control elutes. All samples with their 5 fractions were sent to LC-MS/MS

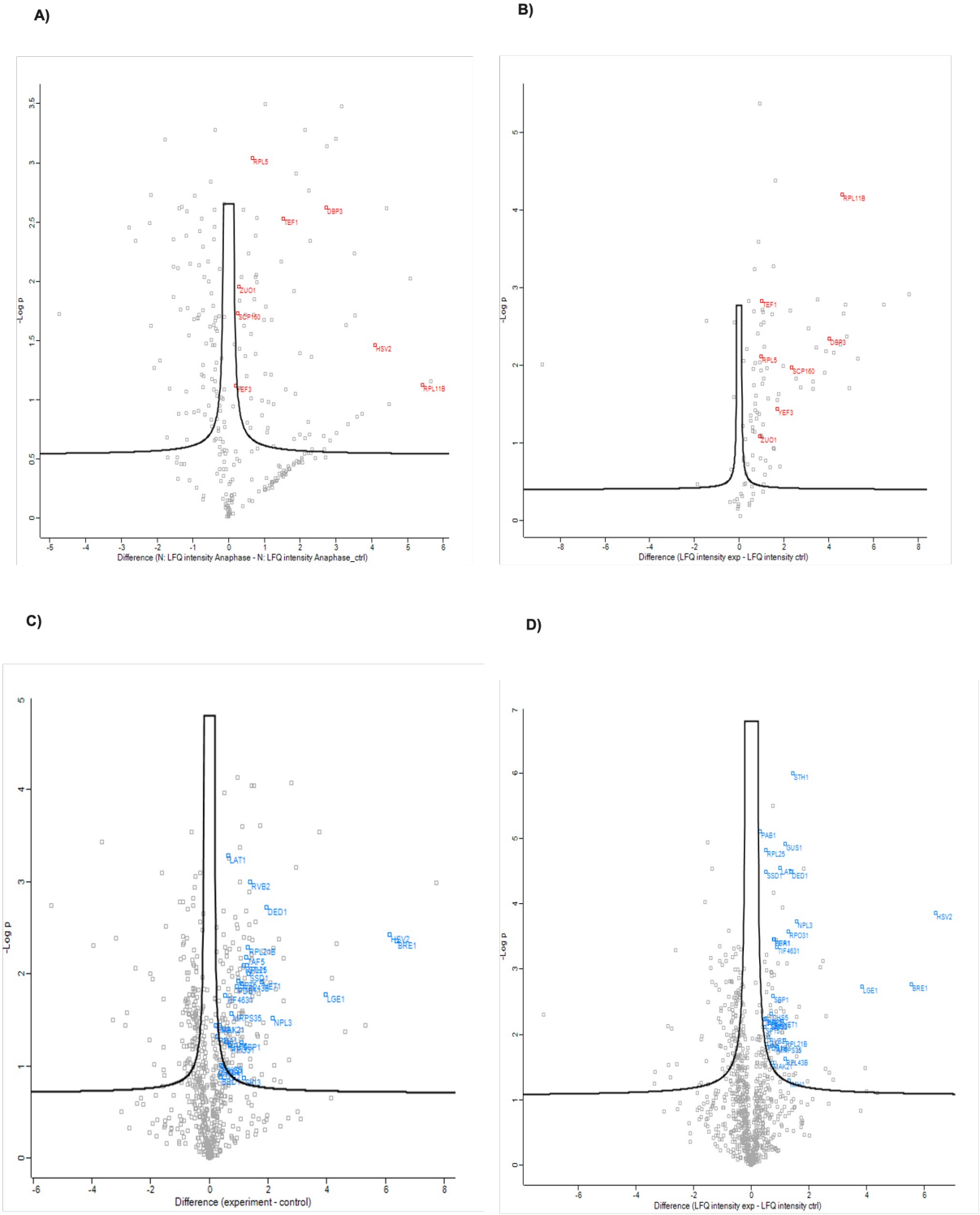

Figure 3. 6. The volcano plot of each biological replica.

HSV2 (known effector protein of PI(3,5)P_2 in three groups) **A-B.** represent the anaphase arrested biological replicas, first replica resulted in 86 significant proteins and second replica resulted in 82 based on the analysis done by MaxQuant and Perseus. Red colored proteins are the ones that resulted significant in both anaphase replicas. **C-D.** represent the metaphase arrested biological replicas, first replica resulted in 208 and second replica resulted in 98 significant proteins based on the analysis done by MaxQuant and Perseus. Blue colored proteins are the ones that resulted significant in both metaphase replicas.

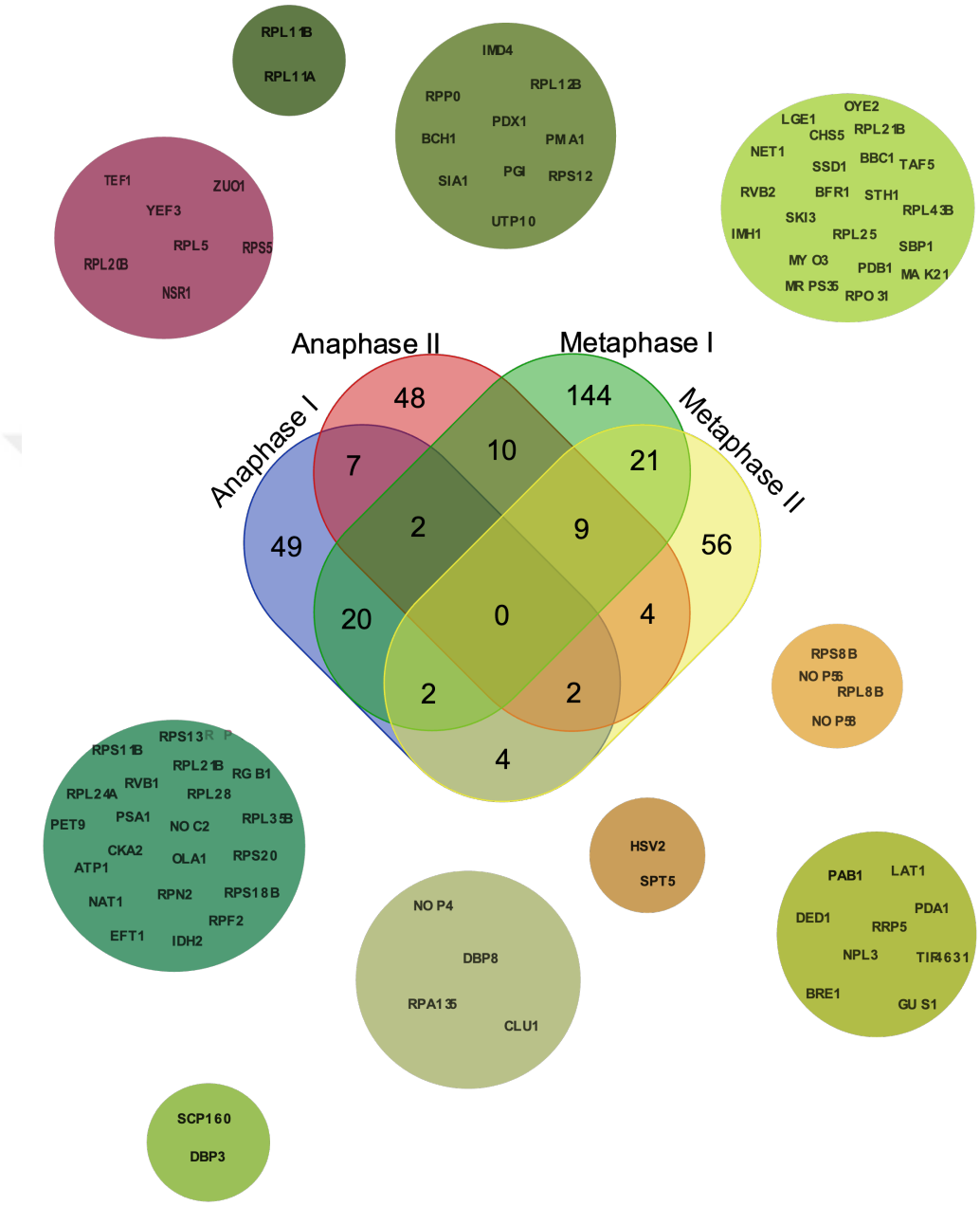

Figure 3. 7. All four replicas are represented in schemes. The common proteins are indicated using Venn Diagram.

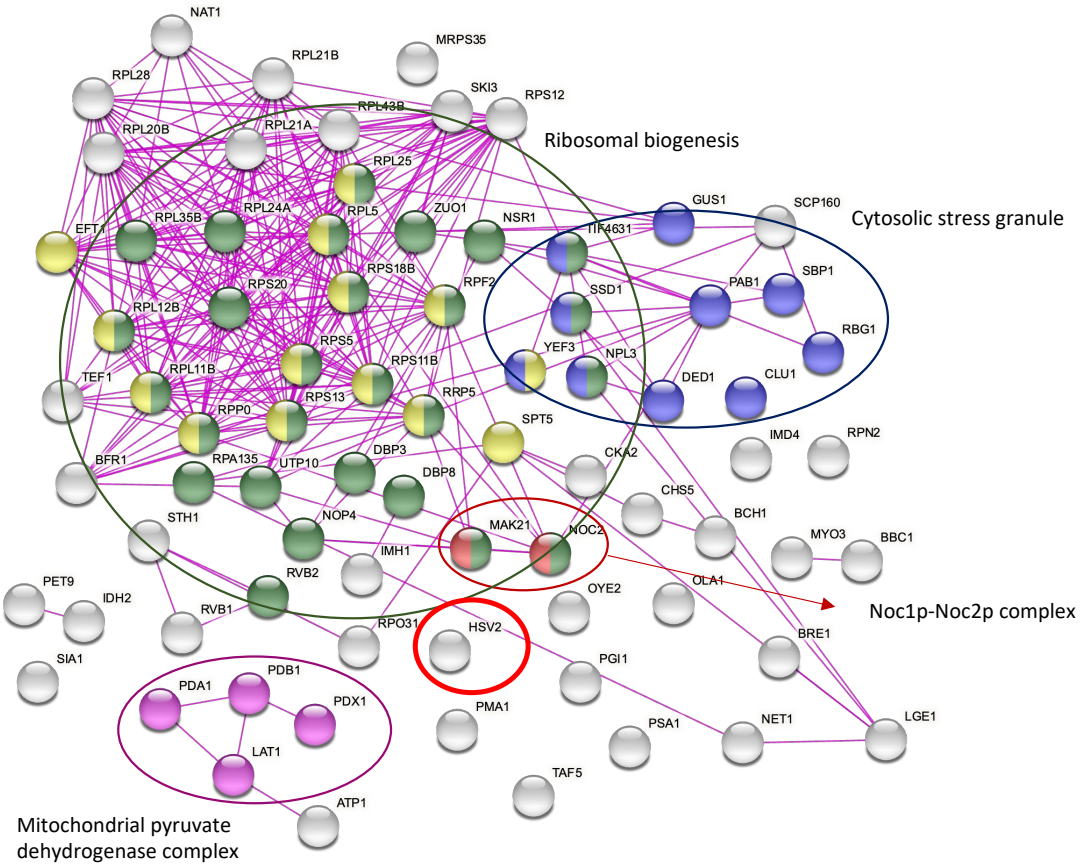

Figure 3. 8. Common significant proteins in at least two biological replicas of each anaphase arrested and metaphase arrested sets.

STRING database was used to identify the physical interactions and gene ontology analysis between the common significant proteins. Only the physical interactions are being represented. Green color indicates: Biological process- ribosomal biogenesis, blue color indicates: biological component-cytosolic stress granule, red color indicates, Noc2p-Noc1p component, pink color indicates mitochondrial pyruvate dehydrogenase complex and yellow color indicates, molecular function, rRNA binding. Hsv2 is a known protein of PI(3,5)P_2 came as a significant hit for three replicas.

DISCUSSION

In this study we aimed to characterize PI(3,5)P_2 localization and its interacting partners during mitosis.

In the first part of the thesis, we used Atg18 as a known effector protein of PI(3,5)P_2 (Jin et al., 2016). Of course, there are other effector proteins such as TRPML1 (Dong, Shen, et al., 2010). We sticked to Atg18 a potential *in vivo* sensor. There were no established sensors for PI(3,5)P_2 so we first asked whether Atg18 makes a good sensor for PI(3,5)P_2. Atg18 vacuole membrane localization correlated well with PI(3,5)P_2 levels. First, Atg18 vacuole membrane localization increased under conditions that increases PI(3,5)P_2 production (hyperosmotic shock and *fab1-hyp* expression). Second, Atg18 vacuole membrane localization diminished in mutants that are unable to synthesize PI(3,5)P_2 (*vac7*Δ and *fab1*Δ) and in *vac14*Δ mutant which has reduced PI(3,5)P_2 production. Importantly, it has been shown by others that hyperosmotic shock do not affect levels of Vac7, Vac14 and Fab1 at the vacuole membrane (J. E. Duex et al., 2006), yet it increases PI(3,5)P_2 (J. E. Duex et al., 2006)and Atg18 localization. This is in favor of Atg18 vacuole membrane localization reflecting PI(3,5)P_2 levels, rather than levels of PAS complex proteins on the vacuole. Third, under conditions when PI(3,5)P_2 levels were increased in *vac14*Δ mutant (upon hyperosmotic shock or *fab1-hyp* expression) Atg18 vacuole membrane localization was restored to wild type levels thus Atg18 vacuole membrane localization is not via Vac14 but via PI(3,5)P_2. However, our data also showed that Atg18 vacuole localization requires Vac7. Atg18 vacuole membrane localization disappeared in *vac7*Δ cells. Upon *fab1-hyp* expression, which was shown to increase PI3,5P2 levels in *vac7*Δ cells, Atg18 was still not able to localize to the vacuole membrane. However, when hyperosmotic shock was applied to *fab1-hyp* expressing *vac7*Δ cells, Atg18 vacuole localization was slightly increased (Fig3.1). Although we do not know how the combination of hyperosmotic shock and *fab1-hyp* affect PI3,5P2 levels, this data indicate that Atg18 is able to localize to the vacuole membrane in the absence of Vac7. It is worth mentioning here that the *fab1-hyp* mutant which is *fab1-14* (J. E. Duex et al., 2006) do not fully restore PI(3,5)P_2 levels in *vac7*Δ cells although it rescues the large vacuole phenotype. Thus, the reason for Vac7 requirement of Atg18 vacuole membrane localization could be the essential role of Vac7 in Fab1 activation. It would be worth to investigate using a different *fab1-hyp* mutant such as *fab1-5* (Botelho et al., 2008) that fully restores PI3,5P2 levels in *vac7*Δ cells to investigate the contribution of Vac7 to Atg18 vacuole membrane localization.

Atg18 was shown to physically interact with Fab1 (Efe et al., 2007). Our data does not exclude the possibility that Atg18 may localize to the vacuole membrane via Fab1. However, Atg18 vacuole localization increased under hyperosmotic conditions which does not change the vacuolar levels of Fab1 (C Malia et al., 2018) but promotes its ability to synthesize $PI(3,5)P_2$. This data supports that the change in Atg18 levels at the vacuole membrane correlates with $PI(3,5)P_2$ rather than Fab1 levels. Nevertheless, analysis of Fab1 levels as level as Vac7 levels at the vacuole membrane is necessary to confirm this in our experimental setup.

We next showed that under basal conditions Atg18-GFP localizes preferentially to the vacuole that moved to the daughter cell rather than the vacuole that stayed in the mother cell. Fig3.2 A).This localization was also dependent on $PI(3,5)P_2$ rather than PI3P based on analysis of Atg18-Sloop mutant. This asymmetric localization of Atg18 was largely dependent on Vac7 and Vac14. Hyperactivation of $PI(3,5)P_2$ production increased Atg18 localization on both vacuoles, increased overall vacuole localization but did not significantly affect the percentage of cells with Atg18 only daughter vacuole localization. We think that increased $PI(3,5)P_2$ synthesis may have converted "no signal" to "only daughter" or "both daughter and mother vacuole" localization. Meanwhile some of the only daughter localizations may be converted to "both daughter and mother vacuole" localization. It could as well be that cells with segregated vacuoles may activate mechanisms that down regulate $PI(3,5)P_2$ production or Atg18 localization in the mother vacuole.

Our interest peaked to understand the functional significance of the daughter cell specific Atg18 localization. Asymmetric protein localization to the daughter or to the mother only is common to many proteins in budding yeast. Since budding yeast divides through asymmetric cell division, mother and daughter cell differs in their fate. For example, daughter-specific transcription is mediated by the daughter-specific transcription factor Ace2 and transcriptional regulator Ash1 (Di Talia et al., 2009). Ash1 mRNA is localized and translated at the bud. Ace2 nuclear import/export is controlled in a compartment specific manner and is localized to the nucleus that segregated to the bud. Considering the role of $PI(3,5)P_2$ in transcriptional regulation and RNA granule transport, daughter cell specific increase in $PI(3,5)P_2$ may be linked to daughter specific transcription. It may work through Ace2 and Ash1 or unknown proteins and mRNA.(Han & Emr, 2011; Liao et al., 2019). Whether Ace2 and Ash1 asymmetry is downstream of PI3,5P2 or Atg18 can easily be investigated.

$PI(3,5)P_2$ is located in vacuolar membrane and late endosomes, and it regulates vacuolar homeostasis by regulating V-ATPase pump on vacuolar membrane (Li et al., 2014). Vacuolar pH Is more elevated in mother cell whereas in daughter cell the vacuolar pH is more acidic. This is linked to the renewed lifespans of daughters. It is believed that the pH difference is reducing the lifespan in mother cells while increasing the rejuvenation of the daughter cell (Henderson et al., 2014). Thus, $PI(3,5)P_2$'s daughter specific localization may be the cause for pH differences between mother and daughter cell vacuole.

Using tubulin as cell cycle indicator, we observed Atg18-GFP appeared on the daughter vacuole in mitosis before anaphase and signal persisted through anaphase. Many mitotic exit regulators localize asymmetrically to the daughter or mother cell (i.e. Bfa1-Bub2, Tem1, Lte1, Ste20, Kin4). Considering the preliminary data from our lab that show $PI(3,5)P_2$ has a mitotic exit promoting role, it is tempting to speculate that this asymmetric localization of Atg18 or asymmetric synthesis of $PI(3,5)P_2$ may be linked to the mitotic exit promoting role of $PI(3,5)P_2$. $PI(3,5)P_2$ may be involved in maintenance of daughter/mother asymmetry of mitotic exit related proteins.

To sum up, asymmetric localization of Atg18 or asymmetric synthesis of $PI(3,5)P_2$might indicate an important role of $PI(3,5)P_2$ in several aspects related to asymmetric cell division including cell polarity, cell cycle, aging and daughter specific transcription.

In the second part of the thesis, we identified proteins that are able to bind $PI(3,5)P_2$ in mitosis. Our analysis yielded 68 proteins. Intriguingly, most of these proteins were ribosome, RNA, and translation related proteins. Since we know that $PI(3,5)P_2$ has a role in transcription and on-site translation by ensuring RNA granule docking (Liao et al., 2019), we think that these interactions may be relevant in understanding $PI(3,5)P_2$'s role in transcription and RNA processing. Other than those proteins we have found Net1 to be pulled down with $PI(3,5)P_2$ covered beads. Net1 is involved in capturing Cdc14 in nucleolus until mitotic exit network activation (Jiménez et al., 2020). Considering $PI(3,5)P_2$'s ability to promote mitotic exit, this interaction may be important for regulating Cdc14 and thus mitotic exit. Yet, this interaction may not reflect the in vivo situation as it is unlikely for a nucleolar protein to interact with a vacuole membrane protein. Yet, a portion of Net1 may be cytoplasmic at certain stages of cell cycle. Nevertheless, our results must be validated through other interaction assays (such as using lipid strips) before further functional assay. For further confirmations and understanding the importance of daughter specific localization of $PI(3,5)P_2$, microscopy-based approaches can be used and mother and daughter cells can be investigated separately to understand better. Also, inhibiting

Fab1 specifically in daughter cell by using its inhibitor *Ivy1* can be an approach to illuminate the role of daughter specific localization.

Chapter 5: REFERENCES

Achiriloaie, M., Barylko, B., & Albanesi, J. P. (1999). Essential Role of the Dynamin Pleckstrin Homology Domain in Receptor-Mediated Endocytosis. *Molecular and Cellular Biology*, *19*(2), 1410-1415. https://doi.org/doi:10.1128/MCB.19.2.1410

Agarwal, R., & Cohen-Fix, O. (2002). Phosphorylation of the mitotic regulator Pds1/securin by Cdc28 is required for efficient nuclear localization of Esp1/separase. *Genes & development*, *16*, 1371-1382. https://doi.org/10.1101/gad.971402

Aikawa, Y., & Martin, T. F. J. (2005). ADP-Ribosylation Factor 6 Regulation of Phosphatidylinositol-4,5-Bisphosphate Synthesis, Endocytosis, and Exocytosis. In *Methods in Enzymology* (Vol. 404, pp. 422-431). Academic Press. https://doi.org/https://doi.org/10.1016/S0076-6879(05)04037-1

Akhtar, A., & Sah, S. P. (2020). Insulin signaling pathway and related molecules: Role in neurodegeneration and Alzheimer's disease. *Neurochemistry International*, *135*, 104707. https://doi.org/https://doi.org/10.1016/j.neuint.2020.104707

Alberghina, L., Mariani, L., & Martegani, E. (1986). Cell cycle modelling. *Biosystems*, *19*(1), 23-44. https://doi.org/https://doi.org/10.1016/0303-2647(86)90032-8

Alcázar-Román, A. R., & Wente, S. R. (2008). Inositol polyphosphates: a new frontier for regulating gene expression. *Chromosoma*, *117*(1), 1-13. https://doi.org/10.1007/s00412-007-0126-4

Alghamdi, T. A., Ho, C. Y., Mrakovic, A., Taylor, D., Mao, D., & Botelho, R. J. (2013). Vac14 protein multimerization is a prerequisite step for Fab1 protein complex assembly and function. *J Biol Chem*, *288*(13), 9363-9372. https://doi.org/10.1074/jbc.M113.453712

Andrews, B., & Measday, V. (1998). The cyclin family of budding yeast: abundant use of a good idea. *Trends Genet*, *14*(2), 66-72. https://doi.org/10.1016/s0168-9525(97)01322-x

Ann, K., Kowalchyk, J. A., Loyet, K. M., & Martin, T. F. J. (1997). Novel Ca²⁺-binding Protein (CAPS) Related to UNC-31 Required for Ca²⁺-activated Exocytosis *. *Journal of Biological Chemistry*, *272*(32), 19637-19640. https://doi.org/10.1074/jbc.272.32.19637

Auger, K. R., Serunian, L. A., Soltoff, S. P., Libby, P., & Cantley, L. C. (1989). PDGF-dependent tyrosine phosphorylation stimulates production of novel polyphosphoinositides in intact cells. *Cell*, *57*(1), 167-175. https://doi.org/https://doi.org/10.1016/0092-8674(89)90182-7

Bakin, A. V., Tomlinson, A. K., Bhowmick, N. A., Moses, H. L., & Arteaga, C. L. (2000). Phosphatidylinositol 3-kinase function is required for transforming growth factor β-mediated epithelial to mesenchymal transition and cell migration. *Journal of Biological Chemistry*, *275*(47), 36803-36810.

Balderhaar, H., Arlt, H., Ostrowicz, C., Bröcker, C., Sündermann, F., Brandt, R., Babst, M., & Ungermann, C. (2010). The Rab GTPase Ypt7 is linked to retromer-mediated receptor recycling and fusion at the yeast late endosome. *Journal of cell science*, *123*, 4085-4094. https://doi.org/10.1242/jcs.071977

Balla, T. (2013). Phosphoinositides: tiny lipids with giant impact on cell regulation. *Physiol Rev*, *93*(3), 1019-1137. https://doi.org/10.1152/physrev.00028.2012

Barneda, D., Cosulich, S., Stephens, L., & Hawkins, P. (2019). How is the acyl chain composition of phosphoinositides created and does it matter? *Biochem Soc Trans*, *47*(5), 1291-1305. https://doi.org/10.1042/bst20190205

Baskaran, S., Ragusa, Michael J., Boura, E., & Hurley, James H. (2012). Two-Site Recognition of Phosphatidylinositol 3-Phosphate by PROPPINs in Autophagy. *Molecular cell*, *47*(3), 339-348. https://doi.org/https://doi.org/10.1016/j.molcel.2012.05.027

Beach, D., Durkacz, B., & Nurse, P. (1982). Functionally homologous cell cycle control genes in budding and fission yeast. *Nature*, *300*(5894), 706-709. https://doi.org/10.1038/300706a0

Bloom, J., & Cross, F. R. (2007). Multiple levels of cyclin specificity in cell-cycle control. *Nature Reviews Molecular Cell Biology*, *8*(2), 149-160. https://doi.org/10.1038/nrm2105

Bonangelino, C. J., Catlett, N. L., & Weisman, L. S. (1997). Vac7p, a novel vacuolar protein, is required for normal vacuole inheritance and morphology. *Mol Cell Biol*, *17*(12), 6847-6858. https://doi.org/10.1128/mcb.17.12.6847

Bonangelino, C. J., Nau, J. J., Duex, J. E., Brinkman, M., Wurmser, A. E., Gary, J. D., Emr, S. D., & Weisman, L. S. (2002). Osmotic stress-induced increase of phosphatidylinositol 3,5-bisphosphate requires Vac14p, an activator of the lipid kinase Fab1p. *J Cell Biol*, *156*(6), 1015-1028. https://doi.org/10.1083/jcb.200201002

Botelho, R. J., Efe, J. A., Teis, D., & Emr, S. D. (2008). Assembly of a Fab1 phosphoinositide kinase signaling complex requires the Fig4 phosphoinositide phosphatase. *Mol Biol Cell*, *19*(10), 4273-4286. https://doi.org/10.1091/mbc.e08-04-0405

Bridges, D., Ma, J.-T., Park, S., Inoki, K., Weisman, L. S., & Saltiel, A. R. (2012). Phosphatidylinositol 3, 5-bisphosphate plays a role in the activation and subcellular localization of mechanistic target of rapamycin 1. *Molecular Biology of the Cell*, *23*(15), 2955-2962.

Bryant, N. J., & Stevens, T. H. (1998). Vacuole biogenesis in Saccharomyces cerevisiae: protein transport pathways to the yeast vacuole. *Microbiol Mol Biol Rev*, *62*(1), 230-247. https://doi.org/10.1128/mmbr.62.1.230-247.1998

Burke, D. J. (2009). Interpreting spatial information and regulating mitosis in response to spindle orientation. *Genes Dev*, *23*(14), 1613-1618. https://doi.org/10.1101/gad.1826409

C Malia, P., Numrich, J., Nishimura, T., González Montoro, A., Stefan, C., & Ungermann, C. (2018). Control of vacuole membrane homeostasis by a resident PI-3,5-kinase inhibitor. *Proceedings of the National Academy of Sciences*, *115*, 201722517. https://doi.org/10.1073/pnas.1722517115

Catimel, B., Schieber, C., Condron, M., Patsiouras, H., Connolly, L., Catimel, J., Nice, E. C., Burgess, A. W., & Holmes, A. B. (2008). The PI(3,5)P2 and PI(4,5)P2 Interactomes. *Journal of Proteome Research*, *7*(12), 5295-5313. https://doi.org/10.1021/pr800540h

Caydasi, A. K., Ibrahim, B., & Pereira, G. (2010). Monitoring spindle orientation: Spindle position checkpoint in charge. *Cell Division*, *5*(1), 28. https://doi.org/10.1186/1747-1028-5-28

Caydasi, A. K., Khmelinskii, A., Duenas-Sanchez, R., Kurtulmus, B., Knop, M., & Pereira, G. (2017). Temporal and compartment-specific signals coordinate mitotic exit with spindle position. *Nature Communications*, *8*(1), 14129. https://doi.org/10.1038/ncomms14129

Caydasi, A. K., Lohel, M., Grünert, G., Dittrich, P., Pereira, G., & Ibrahim, B. (2012). A dynamical model of the spindle position checkpoint. *Molecular Systems Biology*, *8*(1), 582. https://doi.org/https://doi.org/10.1038/msb.2012.15

Caydasi, A. K., Micoogullari, Y., Kurtulmus, B., Palani, S., & Pereira, G. (2014). The 14-3-3 protein Bmh1 functions in the spindle position checkpoint by breaking Bfa1 asymmetry

at yeast centrosomes. *Mol Biol Cell*, *25*(14), 2143-2151. https://doi.org/10.1091/mbc.E14-04-0890

Chant, J., & Pringle, J. R. (1995). Patterns of bud-site selection in the yeast Saccharomyces cerevisiae. *Journal of Cell Biology*, *129*(3), 751-765. https://doi.org/10.1083/jcb.129.3.751

Cherry, J. M., Hong, E. L., Amundsen, C., Balakrishnan, R., Binkley, G., Chan, E. T., Christie, K. R., Costanzo, M. C., Dwight, S. S., Engel, S. R., Fisk, D. G., Hirschman, J. E., Hitz, B. C., Karra, K., Krieger, C. J., Miyasato, S. R., Nash, R. S., Park, J., Skrzypek, M. S., . . . Wong, E. D. (2012). Saccharomyces Genome Database: the genomics resource of budding yeast. *Nucleic Acids Res*, *40*(Database issue), D700-705. https://doi.org/10.1093/nar/gkr1029

Chevalier-Larsen, E., & Holzbaur, E. L. (2006). Axonal transport and neurodegenerative disease. *Biochim Biophys Acta*, *1762*(11-12), 1094-1108. https://doi.org/10.1016/j.bbadis.2006.04.002

Cho, B.-R., & Hahn, J.-S. (2017). CK2-dependent phosphorylation positively regulates stress-induced activation of Msn2 in Saccharomyces cerevisiae. *Biochimica et Biophysica Acta (BBA) - Gene Regulatory Mechanisms*, *1860*(6), 695-704. https://doi.org/https://doi.org/10.1016/j.bbagrm.2017.03.003

Choi, S., Houdek, X., & Anderson, R. A. (2018). Phosphoinositide 3-kinase pathways and autophagy require phosphatidylinositol phosphate kinases. *Adv Biol Regul*, *68*, 31-38. https://doi.org/10.1016/j.jbior.2018.02.003

Chow, C. Y., Landers, J. E., Bergren, S. K., Sapp, P. C., Grant, A. E., Jones, J. M., Everett, L., Lenk, G. M., McKenna-Yasek, D. M., Weisman, L. S., Figlewicz, D., Brown, R. H., & Meisler, M. H. (2009). Deleterious variants of FIG4, a phosphoinositide phosphatase, in patients with ALS. *Am J Hum Genet*, *84*(1), 85-88. https://doi.org/10.1016/j.ajhg.2008.12.010

Choy, C. H., Saffi, G., Gray, M. A., Wallace, C., Dayam, R. M., Ou, Z. A., Lenk, G., Puertollano, R., Watkins, S. C., & Botelho, R. J. (2018). Lysosome enlargement during inhibition of the lipid kinase PIKfyve proceeds through lysosome coalescence. *J Cell Sci*, *131*(10). https://doi.org/10.1242/jcs.213587

Ciosk, R., Zachariae, W., Michaelis, C., Shevchenko, A., Mann, M., & Nasmyth, K. (1998). An ESP1/PDS1 complex regulates loss of sister chromatid cohesion at the metaphase to anaphase transition in yeast. *Cell*, *93*(6), 1067-1076. https://doi.org/10.1016/s0092-8674(00)81211-8

Colacurcio, D. J., Pensalfini, A., Jiang, Y., & Nixon, R. A. (2018). Dysfunction of autophagy and endosomal-lysosomal pathways: Roles in pathogenesis of Down syndrome and Alzheimer's Disease. *Free Radic Biol Med*, *114*, 40-51. https://doi.org/10.1016/j.freeradbiomed.2017.10.001

Costanzo, M., Kuzmin, E., van Leeuwen, J., Mair, B., Moffat, J., Boone, C., & Andrews, B. (2019). Global Genetic Networks and the Genotype-to-Phenotype Relationship. *Cell*, *177*(1), 85-100. https://doi.org/10.1016/j.cell.2019.01.033

Cox, J., & Mann, M. (2008). MaxQuant enables high peptide identification rates, individualized p.p.b.-range mass accuracies and proteome-wide protein quantification. *Nature Biotechnology*, *26*(12), 1367-1372. https://doi.org/10.1038/nbt.1511

Csikász-Nagy, A., Battogtokh, D., Chen, K. C., Novák, B., & Tyson, J. J. (2006). Analysis of a generic model of eukaryotic cell-cycle regulation. *Biophys J*, *90*(12), 4361-4379. https://doi.org/10.1529/biophysj.106.081240

Di Talia, S., Wang, H., Skotheim, J. M., Rosebrock, A. P., Futcher, B., & Cross, F. R. (2009). Daughter-specific transcription factors regulate cell size control in budding yeast. *PLoS Biol*, *7*(10), e1000221. https://doi.org/10.1371/journal.pbio.1000221

Ding, L., Cao, J., Lin, W., Chen, H., Xiong, X., Ao, H., Yu, M., Lin, J., & Cui, Q. (2020). The Roles of Cyclin-Dependent Kinases in Cell-Cycle Progression and Therapeutic Strategies in Human Breast Cancer. *Int J Mol Sci*, *21*(6). https://doi.org/10.3390/ijms21061960

Dong, X.-p., Shen, D., Wang, X., Dawson, T., Li, X., Zhang, Q., Cheng, X., Zhang, Y., Weisman, L. S., Delling, M., & Xu, H. (2010). PI(3,5)P2 controls membrane trafficking by direct activation of mucolipin Ca2+ release channels in the endolysosome. *Nature Communications*, *1*(1), 38. https://doi.org/10.1038/ncomms1037

Dong, X.-P., Wang, X., & Xu, H. (2010). TRP channels of intracellular membranes. *Journal of Neurochemistry*, *113*(2), 313-328. https://doi.org/https://doi.org/10.1111/j.1471-4159.2010.06626.x

Dooley, H. C., Razi, M., Polson, H. E., Girardin, S. E., Wilson, M. I., & Tooze, S. A. (2014). WIPI2 links LC3 conjugation with PI3P, autophagosome formation, and pathogen clearance by recruiting Atg12-5-16L1. *Mol Cell*, *55*(2), 238-252. https://doi.org/10.1016/j.molcel.2014.05.021

Dove, S. K., Piper, R. C., McEwen, R. K., Yu, J. W., King, M. C., Hughes, D. C., Thuring, J., Holmes, A. B., Cooke, F. T., Michell, R. H., Parker, P. J., & Lemmon, M. A. (2004). Svp1p defines a family of phosphatidylinositol 3,5-bisphosphate effectors. *Embo j*, *23*(9), 1922-1933. https://doi.org/10.1038/sj.emboj.7600203

Dubouloz, F., Deloche, O., Wanke, V., Cameroni, E., & De Virgilio, C. (2005). The TOR and EGO Protein Complexes Orchestrate Microautophagy in Yeast. *Molecular cell*, *19*, 15-26. https://doi.org/10.1016/j.molcel.2005.05.020

Duex, J. E., Nau, J. J., Kauffman, E. J., & Weisman, L. S. (2006). Phosphoinositide 5-phosphatase Fig4p is required for both acute rise and subsequent fall in stress-induced phosphatidylinositol 3, 5-bisphosphate levels. *Eukaryotic cell*, *5*(4), 723-731.

Duex, J. E., Tang, F., & Weisman, L. S. (2006). The Vac14p-Fig4p complex acts independently of Vac7p and couples PI3,5P2 synthesis and turnover. *J Cell Biol*, *172*(5), 693-704. https://doi.org/10.1083/jcb.200512105

Efe, J., Botelho, R., & Emr, S. (2005). Efe JA, Botelho RJ, Emr SD. The Fab1 phosphatidylinositol kinase pathway in the regulation of vacuole morphology. Curr Opin Cell Biol 17: 402-408. *Current opinion in cell biology*, *17*, 402-408. https://doi.org/10.1016/j.ceb.2005.06.002

Efe, J. A., Botelho, R. J., & Emr, S. D. (2007). Atg18 regulates organelle morphology and Fab1 kinase activity independent of its membrane recruitment by phosphatidylinositol 3,5-bisphosphate. *Mol Biol Cell*, *18*(11), 4232-4244. https://doi.org/10.1091/mbc.e07-04-0301

Fagarasanu, A., Fagarasanu, M., & Rachubinski, R. A. (2007). Maintaining Peroxisome Populations: A Story of Division and Inheritance. *Annual Review of Cell and Developmental Biology*, *23*(1), 321-344. https://doi.org/10.1146/annurev.cellbio.23.090506.123456

Falkenburger, B. H., Jensen, J. B., Dickson, E. J., Suh, B. C., & Hille, B. (2010). Phosphoinositides: lipid regulators of membrane proteins. *J Physiol*, *588*(Pt 17), 3179-3185. https://doi.org/10.1113/jphysiol.2010.192153

Foti, D. M., Welihinda, A., Kaufman, R. J., & Lee, A. S. (1999). Conservation and Divergence of the Yeast and Mammalian Unfolded Protein Response: ACTIVATION OF

SPECIFIC MAMMALIAN ENDOPLASMIC RETICULUM STRESS ELEMENT OF THE grp78/BiP PROMOTER BY YEAST Hac1 *. *Journal of Biological Chemistry*, *274*(43), 30402-30409. https://doi.org/10.1074/jbc.274.43.30402

Gary, J. D., Sato, T. K., Stefan, C. J., Bonangelino, C. J., Weisman, L. S., & Emr, S. D. (2002). Regulation of Fab1 phosphatidylinositol 3-phosphate 5-kinase pathway by Vac7 protein and Fig4, a polyphosphoinositide phosphatase family member. *Mol Biol Cell*, *13*(4), 1238-1251. https://doi.org/10.1091/mbc.01-10-0498

Gary, J. D., Wurmser, A. E., Bonangelino, C. J., Weisman, L. S., & Emr, S. D. (1998). Fab1p is essential for PtdIns(3)P 5-kinase activity and the maintenance of vacuolar size and membrane homeostasis. *J Cell Biol*, *143*(1), 65-79. https://doi.org/10.1083/jcb.143.1.65

Goffeau, A., Barrell, B. G., Bussey, H., Davis, R. W., Dujon, B., Feldmann, H., Galibert, F., Hoheisel, J. D., Jacq, C., Johnston, M., Louis, E. J., Mewes, H. W., Murakami, Y., Philippsen, P., Tettelin, H., & Oliver, S. G. (1996). Life with 6000 genes. *Science*, *274*(5287), 546, 563-547. https://doi.org/10.1126/science.274.5287.546

Goode, B. L., Eskin, J. A., & Wendland, B. (2015). Actin and endocytosis in budding yeast. *Genetics*, *199*(2), 315-358. https://doi.org/10.1534/genetics.112.145540

Gopaldass, N., Fauvet, B., Lashuel, H., Roux, A., & Mayer, A. (2017). Membrane scission driven by the PROPPIN Atg18. *Embo j*, *36*(22), 3274-3291. https://doi.org/10.15252/embj.201796859

Guimaraes, S. C., Schuster, M., Bielska, E., Dagdas, G., Kilaru, S., Meadows, B. R., Schrader, M., & Steinberg, G. (2015). Peroxisomes, lipid droplets, and endoplasmic reticulum "hitchhike" on motile early endosomes. *J Cell Biol*, *211*(5), 945-954. https://doi.org/10.1083/jcb.201505086

Han, B. K., & Emr, S. D. (2011). Phosphoinositide [PI(3,5)P2] lipid-dependent regulation of the general transcriptional regulator Tup1. *Genes Dev*, *25*(9), 984-995. https://doi.org/10.1101/gad.1998611

Han, Y. (2019). Analysis of the role of the Hippo pathway in cancer. *Journal of Translational Medicine*, *17*(1), 116. https://doi.org/10.1186/s12967-019-1869-4

Hanson, P. K. (2018). Saccharomyces cerevisiae: A Unicellular Model Genetic Organism of Enduring Importance. *Current Protocols Essential Laboratory Techniques*, *16*(1), e21. https://doi.org/https://doi.org/10.1002/cpet.21

Harrison, D. E., Strong, R., Sharp, Z. D., Nelson, J. F., Astle, C. M., Flurkey, K., Nadon, N. L., Wilkinson, J. E., Frenkel, K., Carter, C. S., Pahor, M., Javors, M. A., Fernandez, E., & Miller, R. A. (2009). Rapamycin fed late in life extends lifespan in genetically heterogeneous mice. *Nature*, *460*(7253), 392-395. https://doi.org/10.1038/nature08221

Hartwell, L. H. (1967). Macromolecule synthesis in temperature-sensitive mutants of yeast. *J Bacteriol*, *93*(5), 1662-1670. https://doi.org/10.1128/jb.93.5.1662-1670.1967

Hartwell, L. H. (1974). Saccharomyces cerevisiae cell cycle. *Bacteriol Rev*, *38*(2), 164-198. https://doi.org/10.1128/br.38.2.164-198.1974

Hartwell, L. H., Culotti, J., Pringle, J. R., & Reid, B. J. (1974). Genetic control of the cell division cycle in yeast. *Science*, *183*(4120), 46-51. https://doi.org/10.1126/science.183.4120.46

Hartwell, L. H., & Unger, M. W. (1977). Unequal division in Saccharomyces cerevisiae and its implications for the control of cell division. *J Cell Biol*, *75*(2 Pt 1), 422-435. https://doi.org/10.1083/jcb.75.2.422

Harvey, K. F., & Hariharan, I. K. (2012). The hippo pathway. *Cold Spring Harb Perspect Biol*, *4*(8), a011288. https://doi.org/10.1101/cshperspect.a011288

Hasegawa, J., Strunk, B., & Weisman, L. (2017). PI5P and PI(3,5)P2: Minor, but essential phosphoinositides. *Cell Structure and Function*, *42*. https://doi.org/10.1247/csf.17003

Hasegawa, J., Strunk, B. S., & Weisman, L. S. (2017). PI5P and PI(3,5)P(2): Minor, but Essential Phosphoinositides. *Cell Struct Funct*, *42*(1), 49-60. https://doi.org/10.1247/csf.17003

Hassan, B. A., Prokopenko, S. N., Breuer, S., Zhang, B., Paululat, A., & Bellen, H. J. (1998). skittles, a Drosophila phosphatidylinositol 4-phosphate 5-kinase, is required for cell viability, germline development and bristle morphology, but not for neurotransmitter release. *Genetics*, *150*(4), 1527-1537.

Henderson, K. A., Hughes, A. L., & Gottschling, D. E. (2014). Mother-daughter asymmetry of pH underlies aging and rejuvenation in yeast. *Elife*, *3*, e03504. https://doi.org/10.7554/eLife.03504

Ho, C. Y., Alghamdi, T. A., & Botelho, R. J. (2012). Phosphatidylinositol-3,5-Bisphosphate: No Longer the Poor PIP2. *Traffic*, *13*(1), 1-8. https://doi.org/https://doi.org/10.1111/j.1600-0854.2011.01246.x

Ho, C. Y., Choy, C. H., Wattson, C. A., Johnson, D. E., & Botelho, R. J. (2015). The Fab1/PIKfyve phosphoinositide phosphate kinase is not necessary to maintain the pH of lysosomes and of the yeast vacuole. *J Biol Chem*, *290*(15), 9919-9928. https://doi.org/10.1074/jbc.M114.613984

Hornig, N. C., Knowles, P. P., McDonald, N. Q., & Uhlmann, F. (2002). The dual mechanism of separase regulation by securin. *Curr Biol*, *12*(12), 973-982. https://doi.org/10.1016/s0960-9822(02)00847-3

Huotari, J., & Helenius, A. (2011). Endosome maturation. *Embo j*, *30*(17), 3481-3500. https://doi.org/10.1038/emboj.2011.286

Hutchison, H. T., & Hartwell, L. H. (1967). Macromolecule Synthesis in Yeast Spheroplasts. *Journal of Bacteriology*, *94*(5), 1697-1705. https://doi.org/doi:10.1128/jb.94.5.1697-1705.1967

Jaber, N., & Zong, W. X. (2013). Class III PI3K Vps34: essential roles in autophagy, endocytosis, and heart and liver function. *Ann N Y Acad Sci*, *1280*, 48-51. https://doi.org/10.1111/nyas.12026

Jiménez, J., Queralt, E., Posas, F., & de Nadal, E. (2020). The regulation of Net1/Cdc14 by the Hog1 MAPK upon osmostress unravels a new mechanism regulating mitosis. *Cell Cycle*, *19*(17), 2105-2118. https://doi.org/10.1080/15384101.2020.1804222

Jin, M., He, D., Backues, S. K., Freeberg, M. A., Liu, X., Kim, J. K., & Klionsky, D. J. (2014). Transcriptional regulation by Pho23 modulates the frequency of autophagosome formation. *Current Biology*, *24*(12), 1314-1322.

Jin, N., Chow, C. Y., Liu, L., Zolov, S. N., Bronson, R., Davisson, M., Petersen, J. L., Zhang, Y., Park, S., Duex, J. E., Goldowitz, D., Meisler, M. H., & Weisman, L. S. (2008). VAC14 nucleates a protein complex essential for the acute interconversion of PI3P and PI(3,5)P(2) in yeast and mouse. *Embo j*, *27*(24), 3221-3234. https://doi.org/10.1038/emboj.2008.248

Jin, N., Jin, Y., & Weisman, L. S. (2017). Early protection to stress mediated by CDK-dependent PI3,5P(2) signaling from the vacuole/lysosome. *J Cell Biol*, *216*(7), 2075-2090. https://doi.org/10.1083/jcb.201611144

Jin, N., Lang, M. J., & Weisman, L. S. (2016). Phosphatidylinositol 3,5-bisphosphate: regulation of cellular events in space and time. *Biochem Soc Trans*, *44*(1), 177-184. https://doi.org/10.1042/bst20150174

Jin, Y., & Weisman, L. S. (2015). The vacuole/lysosome is required for cell-cycle progression. *Elife*, *4*, e08160.

Johnston, G. C., Ehrhardt, C. W., Lorincz, A., & Carter, B. L. (1979). Regulation of cell size in the yeast Saccharomyces cerevisiae. *J Bacteriol*, *137*(1), 1-5. https://doi.org/10.1128/jb.137.1.1-5.1979

Johnston, G. C., Pringle, J. R., & Hartwell, L. H. (1977). Coordination of growth with cell division in the yeast Saccharomyces cerevisiae. *Exp Cell Res*, *105*(1), 79-98. https://doi.org/10.1016/0014-4827(77)90154-9

Justice, R. W., Zilian, O., Woods, D. F., Noll, M., & Bryant, P. J. (1995). The Drosophila tumor suppressor gene warts encodes a homolog of human myotonic dystrophy kinase and is required for the control of cell shape and proliferation. *Genes Dev*, *9*(5), 534-546. https://doi.org/10.1101/gad.9.5.534

Katzmann, D. J., Sarkar, S., Chu, T., Audhya, A., & Emr, S. D. (2004). Multivesicular body sorting: ubiquitin ligase Rsp5 is required for the modification and sorting of carboxypeptidase S. *Mol Biol Cell*, *15*(2), 468-480. https://doi.org/10.1091/mbc.e03-07-0473

Ketel, K., Krauss, M., Nicot, A.-S., Puchkov, D., Wieffer, M., Müller, R., Subramanian, D., Schultz, C., Laporte, J., & Haucke, V. (2016). A phosphoinositide conversion mechanism for exit from endosomes. *Nature*, *529*(7586), 408-412. https://doi.org/10.1038/nature16516

Kim, Y. J., Guzman-Hernandez, M. L., & Balla, T. (2011). A highly dynamic ER-derived phosphatidylinositol-synthesizing organelle supplies phosphoinositides to cellular membranes. *Dev Cell*, *21*(5), 813-824. https://doi.org/10.1016/j.devcel.2011.09.005

Kindler, S., Wang, H., Richter, D., & Tiedge, H. (2005). RNA transport and local control of translation. *Annu Rev Cell Dev Biol*, *21*, 223-245. https://doi.org/10.1146/annurev.cellbio.21.122303.120653

Knop, M., Siegers, K., Pereira, G., Zachariae, W., Winsor, B., Nasmyth, K., & Schiebel, E. (1999). Epitope tagging of yeast genes using a PCR-based strategy: more tags and improved practical routines. *Yeast*, *15*(10b), 963-972. https://doi.org/10.1002/(sici)1097-0061(199907)15:10b<963::Aid-yea399>3.0.Co;2-w

Kohler, V., Aufschnaiter, A., & Büttner, S. (2020). Closing the Gap: Membrane Contact Sites in the Regulation of Autophagy. *Cells*, *9*(5). https://doi.org/10.3390/cells9051184

Komarnitsky, S. I., Chiang, Y. C., Luca, F. C., Chen, J., Toyn, J. H., Winey, M., Johnston, L. H., & Denis, C. L. (1998). DBF2 protein kinase binds to and acts through the cell cycle-regulated MOB1 protein. *Mol Cell Biol*, *18*(4), 2100-2107. https://doi.org/10.1128/mcb.18.4.2100

Konopka, J. B. (2022). Plasma Membrane Phosphatidylinositol 4-Phosphate Is Necessary for Virulence of Candida albicans. *Mbio*, e00366-00322.

Kos-Braun, I. C., Jung, I., & Koš, M. (2017). Tor1 and CK2 kinases control a switch between alternative ribosome biogenesis pathways in a growth-dependent manner. *PLoS Biol*, *15*(3), e2000245. https://doi.org/10.1371/journal.pbio.2000245

Kotani, T., Kirisako, H., Koizumi, M., Ohsumi, Y., & Nakatogawa, H. (2018). The Atg2-Atg18 complex tethers pre-autophagosomal membranes to the endoplasmic reticulum for autophagosome formation. *Proceedings of the National Academy of Sciences*, *115*(41), 10363-10368. https://doi.org/doi:10.1073/pnas.1806727115

Kunkl, M., Porciello, N., Mastrogiovanni, M., Capuano, C., Lucantoni, F., Moretti, C., Persson, J. L., Galandrini, R., Buzzetti, R., & Tuosto, L. (2017). isa-2011B, a Phosphatidylinositol 4-Phosphate 5-Kinase α inhibitor, impairs cD28-Dependent

costimulatory and Pro-inflammatory signals in human T lymphocytes. *Frontiers in Immunology*, *8*, 502.

Lenk, G. M., Berry, I. R., Stutterd, C. A., Blyth, M., Green, L., Vadlamani, G., Warren, D., Craven, I., Fanjul-Fernandez, M., Rodriguez-Casero, V., Lockhart, P. J., Vanderver, A., Simons, C., Gibb, S., Sadedin, S., White, S. M., Christodoulou, J., Skibina, O., Ruddle, J., . . . Meisler, M. H. (2019). Cerebral hypomyelination associated with biallelic variants of FIG4. *Hum Mutat*, *40*(5), 619-630. https://doi.org/10.1002/humu.23720

Lennon, G. G., & Lehrach, H. (1992). Gene database for the fission yeast Schizosaccharomyces pombe. *Current Genetics*, *21*(1), 1-11. https://doi.org/10.1007/BF00318646

Lew, D. J., & Reed, S. I. (1995). Cell cycle control of morphogenesis in budding yeast. *Curr Opin Genet Dev*, *5*(1), 17-23. https://doi.org/10.1016/s0959-437x(95)90048-9

Li, S., Tiab, L., Jiao, X., Munier, F., Zografos, L., Frueh, B., Sergeev, Y., Smith, J., Rubin, B., Meallet, M., Forster, R., Hejtmancik, J., & Schorderet, D. (2005). Mutations in PIP5K3 Are Associated with François-Neetens Mouchetée Fleck Corneal Dystrophy. *American journal of human genetics*, *77*, 54-63. https://doi.org/10.1086/431346

Li, S. C., Diakov, T. T., Xu, T., Tarsio, M., Zhu, W., Couoh-Cardel, S., Weisman, L. S., & Kane, P. M. (2014). The signaling lipid PI(3,5)P_2 stabilizes V_1-V(o) sector interactions and activates the V-ATPase. *Mol Biol Cell*, *25*(8), 1251-1262. https://doi.org/10.1091/mbc.E13-10-0563

Liao, Y. C., Fernandopulle, M. S., Wang, G., Choi, H., Hao, L., Drerup, C. M., Patel, R., Qamar, S., Nixon-Abell, J., Shen, Y., Meadows, W., Vendruscolo, M., Knowles, T. P. J., Nelson, M., Czekalska, M. A., Musteikyte, G., Gachechiladze, M. A., Stephens, C. A., Pasolli, H. A., . . . Ward, M. E. (2019). RNA Granules Hitchhike on Lysosomes for Long-Distance Transport, Using Annexin A11 as a Molecular Tether. *Cell*, *179*(1), 147-164.e120. https://doi.org/10.1016/j.cell.2019.08.050

Lines, M., Ito, Y., Kernohan, K., Mears, W., Hurteau, J., Venkateswaran, S., Ward, L., Khatchadourian, K., McClintock, J., Bhola, P., Campeau, P., Boycott, K., Michaud, J., Kuilenburg, A., Ferdinandusse, S., & Dyment, D. (2017). Yunis-Varón syndrome caused by biallelic VAC14 mutations. *European journal of human genetics : EJHG*, *25*. https://doi.org/10.1038/ejhg.2017.99

Liu, X., McLeod, I., Anderson, S., Yates, J. R., 3rd, & He, X. (2005). Molecular analysis of kinetochore architecture in fission yeast. *Embo j*, *24*(16), 2919-2930. https://doi.org/10.1038/sj.emboj.7600762

Lloyd, R. E. (2012). How do viruses interact with stress-associated RNA granules? *PLoS pathogens*, *8*(6), e1002741.

Loewith, R., & Hall, M. N. (2011). Target of rapamycin (TOR) in nutrient signaling and growth control. *Genetics*, *189*(4), 1177-1201. https://doi.org/10.1534/genetics.111.133363

Malave, T. M., & Dent, S. Y. (2006). Transcriptional repression by Tup1–Ssn6. *Biochemistry and cell biology*, *84*(4), 437-443.

Malumbres, M., & Barbacid, M. (2009). Cell cycle, CDKs and cancer: a changing paradigm. *Nat Rev Cancer*, *9*(3), 153-166. https://doi.org/10.1038/nrc2602

Manna, P., & Jain, S. K. (2015). Phosphatidylinositol-3, 4, 5-triphosphate and cellular signaling: implications for obesity and diabetes. *Cellular Physiology and Biochemistry*, *35*(4), 1253-1275.

Martínez-Reyes, I., & Chandel, N. S. (2020). Mitochondrial TCA cycle metabolites control physiology and disease. *Nat Commun*, *11*(1), 102. https://doi.org/10.1038/s41467-019-13668-3

Mayhew, M. B., Iversen, E. S., & Hartemink, A. J. (2017). Characterization of dependencies between growth and division in budding yeast. *Journal of The Royal Society Interface*, *14*(127), 20160993.

McCartney, A. J., Zhang, Y., & Weisman, L. S. (2014). Phosphatidylinositol 3,5-bisphosphate: Low abundance, high significance. *BioEssays*, *36*(1), 52-64. https://doi.org/https://doi.org/10.1002/bies.201300012

McCubrey, J. A., Steelman, L. S., Chappell, W. H., Abrams, S. L., Wong, E. W., Chang, F., Lehmann, B., Terrian, D. M., Milella, M., & Tafuri, A. (2007). Roles of the Raf/MEK/ERK pathway in cell growth, malignant transformation and drug resistance. *Biochimica et Biophysica Acta (BBA)-Molecular Cell Research*, *1773*(8), 1263-1284.

Michaelis, C., Ciosk, R., & Nasmyth, K. (1997). Cohesins: chromosomal proteins that prevent premature separation of sister chromatids. *Cell*, *91*(1), 35-45. https://doi.org/10.1016/s0092-8674(01)80007-6

Miner, G. E., Sullivan, K. D., Guo, A., Jones, B. C., Hurst, L. R., Ellis, E. C., Starr, M. L., & Fratti, R. A. (2019). Phosphatidylinositol 3,5-bisphosphate regulates the transition between trans-SNARE complex formation and vacuole membrane fusion. *Mol Biol Cell*, *30*(2), 201-208. https://doi.org/10.1091/mbc.E18-08-0505

Morgan, D. O. (1995). Principles of CDK regulation. *Nature*, *374*(6518), 131-134. https://doi.org/10.1038/374131a0

Murray, A. W. (2004). Recycling the Cell Cycle: Cyclins Revisited. *Cell*, *116*(2), 221-234. https://doi.org/https://doi.org/10.1016/S0092-8674(03)01080-8

Musacchio, A., & Salmon, E. D. (2007). The spindle-assembly checkpoint in space and time. *Nature Reviews Molecular Cell Biology*, *8*(5), 379-393. https://doi.org/10.1038/nrm2163

Nagano, M., Toshima, J. Y., Siekhaus, D. E., & Toshima, J. (2019). Rab5-mediated endosome formation is regulated at the trans-Golgi network. *Communications Biology*, *2*(1), 419. https://doi.org/10.1038/s42003-019-0670-5

Newport, J. W., & Forbes, D. J. (1987). THE NUCLEUS: STRUCTURE, FUNCTION, AND DYNAMICS. *Annual Review of Biochemistry*, *56*(1), 535-565. https://doi.org/10.1146/annurev.bi.56.070187.002535

Novak, B., & Tyson, J. J. (1993). Modeling the cell division cycle: M-phase trigger, oscillations, and size control. *Journal of Theoretical Biology*, *165*(1), 101-134.

Numrich, J., Péli-Gulli, M. P., Arlt, H., Sardu, A., Griffith, J., Levine, T., Engelbrecht-Vandré, S., Reggiori, F., De Virgilio, C., & Ungermann, C. (2015). The I-BAR protein Ivy1 is an effector of the Rab7 GTPase Ypt7 involved in vacuole membrane homeostasis. *J Cell Sci*, *128*(13), 2278-2292. https://doi.org/10.1242/jcs.164905

Nurse, P., & Thuriaux, P. (1980). REGULATORY GENES CONTROLLING MITOSIS IN THE FISSION YEAST SCHIZOSACCHAROMYCES POMBE. *Genetics*, *96*(3), 627-637. https://doi.org/10.1093/genetics/96.3.627

Obara, K., Noda, T., Niimi, K., & Ohsumi, Y. (2008). Transport of phosphatidylinositol 3-phosphate into the vacuole via autophagic membranes in Saccharomyces cerevisiae. *Genes to Cells*, *13*(6), 537-547. https://doi.org/https://doi.org/10.1111/j.1365-2443.2008.01188.x

Odorizzi, G., Babst, M., & Emr, S. D. (1998). Fab1p PtdIns(3)P 5-kinase function essential for protein sorting in the multivesicular body. *Cell*, *95*(6), 847-858. https://doi.org/10.1016/s0092-8674(00)81707-9

Ohashi, P. S. (2002). T-cell signalling and autoimmunity: molecular mechanisms of disease. *Nature Reviews Immunology*, *2*(6), 427-438.

Orr-Weaver, T. L., Szostak, J. W., & Rothstein, R. J. (1981). Yeast transformation: a model system for the study of recombination. *Proceedings of the National Academy of Sciences*, *78*(10), 6354-6358. https://doi.org/doi:10.1073/pnas.78.10.6354

Ou, X., Liu, Y., Lei, X., Li, P., Mi, D., Ren, L., Guo, L., Guo, R., Chen, T., Hu, J., Xiang, Z., Mu, Z., Chen, X., Chen, J., Hu, K., Jin, Q., Wang, J., & Qian, Z. (2020). Characterization of spike glycoprotein of SARS-CoV-2 on virus entry and its immune cross-reactivity with SARS-CoV. *Nature Communications*, *11*(1), 1620. https://doi.org/10.1038/s41467-020-15562-9

Pan, D. (2010). The hippo signaling pathway in development and cancer. *Dev Cell*, *19*(4), 491-505. https://doi.org/10.1016/j.devcel.2010.09.011

Pavletich, N. P. (1999). Mechanisms of cyclin-dependent kinase regulation: structures of Cdks, their cyclin activators, and Cip and INK4 inhibitors. *J Mol Biol*, *287*(5), 821-828. https://doi.org/10.1006/jmbi.1999.2640

Pellicioli, A., Lee, S. E., Lucca, C., Foiani, M., & Haber, J. E. (2001). Regulation of Saccharomyces Rad53 Checkpoint Kinase during Adaptation from DNA Damage–Induced G2/M Arrest. *Molecular cell*, *7*(2), 293-300. https://doi.org/https://doi.org/10.1016/S1097-2765(01)00177-0

Pereira, G., & Schiebel, E. (2001). The role of the yeast spindle pole body and the mammalian centrosome in regulating late mitotic events. *Curr Opin Cell Biol*, *13*(6), 762-769. https://doi.org/10.1016/s0955-0674(00)00281-7

Pereira, G., Tanaka, T. U., Nasmyth, K., & Schiebel, E. (2001). Modes of spindle pole body inheritance and segregation of the Bfa1p-Bub2p checkpoint protein complex. *Embo j*, *20*(22), 6359-6370. https://doi.org/10.1093/emboj/20.22.6359

Proikas-Cezanne, T., Waddell, S., Gaugel, A., Frickey, T., Lupas, A., & Nordheim, A. (2004). WIPI-1alpha (WIPI49), a member of the novel 7-bladed WIPI protein family, is aberrantly expressed in human cancer and is linked to starvation-induced autophagy. *Oncogene*, *23*(58), 9314-9325. https://doi.org/10.1038/sj.onc.1208331

Puray-Chavez, M., LaPak, K. M., Schrank, T. P., Elliott, J. L., Bhatt, D. P., Agajanian, M. J., Jasuja, R., Lawson, D. Q., Davis, K., Rothlauf, P. W., Jo, H., Lee, N., Tenneti, K., Eschbach, J. E., Mugisha, C. S., Vuong, H. R., Bailey, A. L., Hayes, D. N., Whelan, S. P. J., . . . Kutluay, S. B. (2021). Systematic analysis of SARS-CoV-2 infection of an ACE2-negative human airway cell. *bioRxiv*. https://doi.org/10.1101/2021.03.01.433431

Qiao, R., Weissmann, F., Yamaguchi, M., Brown, N. G., VanderLinden, R., Imre, R., Jarvis, M. A., Brunner, M. R., Davidson, I. F., Litos, G., Haselbach, D., Mechtler, K., Stark, H., Schulman, B. A., & Peters, J.-M. (2016). Mechanism of APC/C^{CDC20} activation by mitotic phosphorylation. *Proceedings of the National Academy of Sciences*, *113*(19), E2570-E2578. https://doi.org/doi:10.1073/pnas.1604929113

Renicke, C., Allmann, A. K., Lutz, A. P., Heimerl, T., & Taxis, C. (2017). The Mitotic Exit Network Regulates Spindle Pole Body Selection During Sporulation of Saccharomyces cerevisiae. *Genetics*, *206*(2), 919-937. https://doi.org/10.1534/genetics.116.194522

Rieter, E., Vinke, F., Bakula, D., Cebollero, E., Ungermann, C., Proikas-Cezanne, T., & Reggiori, F. (2012). Atg18 function in autophagy is regulated by specific sites within its -propeller. *Journal of cell science*, *126*. https://doi.org/10.1242/jcs.115725

Rieter, E., Vinke, F., Bakula, D., Cebollero, E., Ungermann, C., Proikas-Cezanne, T., & Reggiori, F. (2013). Atg18 function in autophagy is regulated by specific sites within its β-propeller. *J Cell Sci*, *126*(Pt 2), 593-604. https://doi.org/10.1242/jcs.115725

Rivero-Ríos, P., & Weisman, L. S. (2022). Roles of PIKfyve in multiple cellular pathways. *Current opinion in cell biology*, *76*, 102086. https://doi.org/https://doi.org/10.1016/j.ceb.2022.102086

Rudge, S. A., Anderson, D. M., & Emr, S. D. (2004). Vacuole size control: regulation of PtdIns(3,5)P2 levels by the vacuole-associated Vac14-Fig4 complex, a PtdIns(3,5)P2-specific phosphatase. *Mol Biol Cell*, *15*(1), 24-36. https://doi.org/10.1091/mbc.e03-05-0297

Sancak, Y., Peterson, T. R., Shaul, Y. D., Lindquist, R. A., Thoreen, C. C., Bar-Peled, L., & Sabatini, D. M. (2008). The Rag GTPases bind raptor and mediate amino acid signaling to mTORC1. *Science*, *320*(5882), 1496-1501. https://doi.org/10.1126/science.1157535

Schmitt, M. E., & Clayton, D. A. (1993). Conserved features of yeast and mammalian mitochondrial DNA replication. *Curr Opin Genet Dev*, *3*(5), 769-774. https://doi.org/10.1016/s0959-437x(05)80097-8

Shen, D., Wang, X., Li, X., Zhang, X., Yao, Z., Dibble, S., Dong, X.-p., Yu, T., Lieberman, A. P., Showalter, H. D., & Xu, H. (2012). Lipid storage disorders block lysosomal trafficking by inhibiting a TRP channel and lysosomal calcium release. *Nature Communications*, *3*(1), 731. https://doi.org/10.1038/ncomms1735

Shou, W., Seol, J., Shevchenko, A., Baskerville, C., Moazed, D., Chen, Z. W. S., Jang, J., Charbonneau, H., & Deshaies, R. (1999). Exit from Mitosis Is Triggered by Tem1-Dependent Release of the Protein Phosphatase Cdc14 from Nucleolar RENT Complex. *Cell*, *97*, 233-244. https://doi.org/10.1016/S0092-8674(00)80733-3

Sikorski, R. S., & Hieter, P. (1989). A system of shuttle vectors and yeast host strains designed for efficient manipulation of DNA in Saccharomyces cerevisiae. *Genetics*, *122*(1), 19-27. https://doi.org/10.1093/genetics/122.1.19

Siller, K. H., & Doe, C. Q. (2009). Spindle orientation during asymmetric cell division. *Nat Cell Biol*, *11*(4), 365-374. https://doi.org/10.1038/ncb0409-365

Sironi, L., Mapelli, M., Knapp, S., De Antoni, A., Jeang, K. T., & Musacchio, A. (2002). Crystal structure of the tetrameric Mad1-Mad2 core complex: implications of a 'safety belt' binding mechanism for the spindle checkpoint. *Embo j*, *21*(10), 2496-2506. https://doi.org/10.1093/emboj/21.10.2496

Steensels, J., Snoek, T., Meersman, E., Nicolino, M., Voordeckers, K., & Verstrepen, K. (2014). Improving industrial yeast strains: Exploiting natural and artificial diversity. *FEMS Microbiology Reviews*, *38*. https://doi.org/10.1111/1574-6976.12073

Strunk, B. S., Steinfeld, N., Lee, S., Jin, N., Muñoz-Rivera, C., Meeks, G., Thomas, A., Akemann, C., Mapp, A. K., MacGurn, J. A., & Weisman, L. S. (2020). Roles for a lipid phosphatase in the activation of its opposing lipid kinase. *Mol Biol Cell*, *31*(17), 1835-1845. https://doi.org/10.1091/mbc.E18-09-0556

Stutterd, C., Diakumis, P., Bahlo, M., Fernandez, M., Leventer, R., Delatycki, M., Amor, D., Chow, C., Stephenson, S., Meisler, M., McLean, C., & Lockhart, P. (2017). Neuropathology of childhood-onset basal ganglia degeneration caused by mutation of VAC14. *Annals of Clinical and Translational Neurology*, *4*. https://doi.org/10.1002/acn3.487

Szklarczyk, D., Gable, A. L., Nastou, K. C., Lyon, D., Kirsch, R., Pyysalo, S., Doncheva, N. T., Legeay, M., Fang, T., Bork, P., Jensen, L. J., & von Mering, C. (2021). The STRING database in 2021: customizable protein-protein networks, and functional characterization of user-uploaded gene/measurement sets. *Nucleic Acids Res*, *49*(D1), D605-d612. https://doi.org/10.1093/nar/gkaa1074

Takatori, S., Tatematsu, T., Cheng, J., Matsumoto, J., Akano, T., & Fujimoto, T. (2016). Phosphatidylinositol 3,5-Bisphosphate-Rich Membrane Domains in Endosomes and Lysosomes. *Traffic*, *17*(2), 154-167. https://doi.org/https://doi.org/10.1111/tra.12346

Takeda, E., Jin, N., Itakura, E., Kira, S., Kamada, Y., Weisman, L. S., Noda, T., & Matsuura, A. (2018). Vacuole-mediated selective regulation of TORC1-Sch9 signaling following oxidative stress. *Mol Biol Cell*, *29*(4), 510-522. https://doi.org/10.1091/mbc.E17-09-0553

Takeshige, K., Baba, M., Tsuboi, S., Noda, T., & Ohsumi, Y. (1992). Autophagy in yeast demonstrated with proteinase-deficient mutants and conditions for its induction. *J Cell Biol*, *119*(2), 301-311. https://doi.org/10.1083/jcb.119.2.301

Throm, E., & Duntze, W. (1970). Mating-Type-Dependent Inhibition of Deoxyribonucleic Acid Synthesis in Saccharomyces cerevisiae. *Journal of Bacteriology*, *104*(3), 1388-1390. https://doi.org/doi:10.1128/jb.104.3.1388-1390.1970

Tyanova, S., Temu, T., Carlson, A., Sinitcyn, P., Mann, M., & Cox, J. (2015). Visualization of LC-MS/MS proteomics data in MaxQuant. *PROTEOMICS*, *15*(8), 1453-1456. https://doi.org/https://doi.org/10.1002/pmic.201400449

Tyanova, S., Temu, T., Sinitcyn, P., Carlson, A., Hein, M. Y., Geiger, T., Mann, M., & Cox, J. (2016). The Perseus computational platform for comprehensive analysis of (prote)omics data. *Nature Methods*, *13*(9), 731-740. https://doi.org/10.1038/nmeth.3901

Vaccari, I., Dina, G., Tronchère, H., Kaufman, E., Chicanne, G., Cerri, F., Wrabetz, L., Payrastre, B., Quattrini, A., Weisman, L. S., Meisler, M. H., & Bolino, A. (2011). Genetic interaction between MTMR2 and FIG4 phospholipid phosphatases involved in Charcot-Marie-Tooth neuropathies. *PLoS Genet*, *7*(10), e1002319. https://doi.org/10.1371/journal.pgen.1002319

Valerio-Santiago, M., & Monje-Casas, F. (2011). Tem1 localization to the spindle pole bodies is essential for mitotic exit and impairs spindle checkpoint function. *J Cell Biol*, *192*(4), 599-614. https://doi.org/10.1083/jcb.201007044

Vinod, P. K., Freire, P., Rattani, A., Ciliberto, A., Uhlmann, F., & Novak, B. (2011). Computational modelling of mitotic exit in budding yeast: the role of separase and Cdc14 endocycles. *Journal of The Royal Society Interface*, *8*(61), 1128-1141. https://doi.org/doi:10.1098/rsif.2010.0649

Visintin, R., Craig, K., Hwang, E. S., Prinz, S., Tyers, M., & Amon, A. (1998). The phosphatase Cdc14 triggers mitotic exit by reversal of Cdk-dependent phosphorylation. *Mol Cell*, *2*(6), 709-718. https://doi.org/10.1016/s1097-2765(00)80286-5

Wallroth, A., & Haucke, V. (2018). Phosphoinositide conversion in endocytosis and the endolysosomal system. *J Biol Chem*, *293*(5), 1526-1535. https://doi.org/10.1074/jbc.R117.000629

Wang, Y.-X., Catlett, N. L., & Weisman, L. S. (1998). Vac8p, a Vacuolar Protein with Armadillo Repeats, Functions in both Vacuole Inheritance and Protein Targeting from the Cytoplasm to Vacuole. *Journal of Cell Biology*, *140*(5), 1063-1074. https://doi.org/10.1083/jcb.140.5.1063

Watson, A. D. (2006). Thematic review series: Systems Biology Approaches to Metabolic and Cardiovascular Disorders. Lipidomics: a global approach to lipid analysis in biological systems. *Journal of Lipid Research*, *47*(10), 2101-2111. https://doi.org/10.1194/jlr.R600022-JLR200

Watt, S. A., Kular, G., Fleming, I. N., Downes, C. P., & Lucocq, J. M. (2002). Subcellular localization of phosphatidylinositol 4,5-bisphosphate using the pleckstrin homology

domain of phospholipase C delta1. *Biochem J*, *363*(Pt 3), 657-666. https://doi.org/10.1042/0264-6021:3630657

Waugh, M. G. (2012). Phosphatidylinositol 4-kinases, phosphatidylinositol 4-phosphate and cancer. *Cancer Letters*, *325*(2), 125-131. https://doi.org/https://doi.org/10.1016/j.canlet.2012.06.009

Weber, S. C., & Brangwynne, C. P. (2012). Getting RNA and protein in phase. *Cell*, *149*(6), 1188-1191. https://doi.org/10.1016/j.cell.2012.05.022

Weisman, L. S., Bacallao, R., & Wickner, W. (1987). Multiple methods of visualizing the yeast vacuole permit evaluation of its morphology and inheritance during the cell cycle. *Journal of Cell Biology*, *105*(4), 1539-1547. https://doi.org/10.1083/jcb.105.4.1539

Wloka, C., & Bi, E. (2012). Mechanisms of cytokinesis in budding yeast. *Cytoskeleton*, *69*(10), 710-726. https://doi.org/https://doi.org/10.1002/cm.21046

Wong, K. H., & Struhl, K. (2011). The Cyc8-Tup1 complex inhibits transcription primarily by masking the activation domain of the recruiting protein. *Genes Dev*, *25*(23), 2525-2539. https://doi.org/10.1101/gad.179275.111

Wu, X., & Malkova, A. (2021). Break-induced replication mechanisms in yeast and mammals. *Curr Opin Genet Dev*, *71*, 163-170. https://doi.org/10.1016/j.gde.2021.08.002

Yamashiro, C. T., Kane, P. M., Wolczyk, D. F., Preston, R. A., & Stevens, T. H. (1990). Role of vacuolar acidification in protein sorting and zymogen activation: a genetic analysis of the yeast vacuolar proton-translocating ATPase. *Mol Cell Biol*, *10*(7), 3737-3749. https://doi.org/10.1128/mcb.10.7.3737-3749.1990

Ye, P., Peyser, B. D., Pan, X., Boeke, J. D., Spencer, F. A., & Bader, J. S. (2005). Gene function prediction from congruent synthetic lethal interactions in yeast. *Mol Syst Biol*, *1*, 2005.0026. https://doi.org/10.1038/msb4100034

Yellman, C. M., & Roeder, G. S. (2015). Cdc14 Early Anaphase Release, FEAR, Is Limited to the Nucleus and Dispensable for Efficient Mitotic Exit. *PloS one*, *10*(6), e0128604. https://doi.org/10.1371/journal.pone.0128604

Yorimitsu, T., & Klionsky, D. (2005). Autophagy: Molecular machinery for self-eating. *Cell death and differentiation*, *12 Suppl 2*, 1542-1552. https://doi.org/10.1038/sj.cdd.4401765

Zurita-Martinez, S. A., Puria, R., Pan, X., Boeke, J. D., & Cardenas, M. E. (2007). Efficient Tor signaling requires a functional class C Vps protein complex in Saccharomyces cerevisiae. *Genetics*, *176*(4), 2139-2150. https://doi.org/10.1534/genetics.107.072835

Chapter 6: Appendix

6.1 Table of Strains

Table 6. 1: Table showing the strains used in this thesis.

Strain Name	Description	Reference
ESM356	*MATa ura3-52 leu2Δ1 his3Δ200 trp1Δ63.,*	*(Pereira & Schiebel, 2001; Pereira et al., 2001)*
SEY063	*ESM356-1 VPH1-3xmCherry- KanMX6*	*This study*
SEY082	*ESM356-1 VPH1-3xmCherry- KanMX6 ATG18-GFP-klTRP1*	*This study*
CDY001	*ESM356-1 ATG18-6HA-klTRP1*	*This study*
CDY20	*ESM356-1 ATG18-GFP-klTRP3 mCherry-LEU2*	*This study*
CDY24	*ESM356VPH1-3xmcherry-kanATG18-GFP-klTRP1 vac7Δ::HIS3MX6*	*This study*
CDY47	*ESM356-1 VPH1-3xmCherry- KanMX6 ATG18-GFP-klTRP1-fab1hyperactive-LEU2*	*This study*
CDY53	*ESM356-1 VPH13x-mCherry- KanMX6 atg18Δ::hphNT1*	*This study*
CDY56	*ESM356VPH1-3xmcherry-kanATG18-GFP-klTRP1 vac7Δ::HIS3MX6 fab1hyperactive-LEU2*	*This study*
CDY57	*ESM356VPH1-3xmcherry-kanATG18-GFP-klTRP1 vac14Δ::hphNT1*	*This study*
CDY58	*ESM356VPH1-3xmcherry-kanATG18-GFP-klTRP1 vac14Δ::hphNT1 fab1hyperactive-LEU2*	*This study*
CDY59	*ESM356-1 VPH1-3xmCherry- KanMX6 atg18Δ::hphNT1 ATG18-GFP-klTRP1*	*This study*
CDY60-	*ESM356-1 VPH1-3xmCherry- KanMX6 atg18Δ::hphNT1 ATG18-FGGG-GFP-klTRP1*	*This study*
CDY61	*ESM356-1 VPH1-3xmCherry- KanMX6 atg18Δ::hphNT1 ATG18-SLOOP-GFP-klTRP1*	*This study*
CDY68	*ESM356-1 VPH1-3xmCherry- KanMX6 fab1Δ-klTRP1 ATG18-GFP-HIS*	*This study*
CDY25	*MBY20-1 MATa ura3-52 leu2Δ1 his3Δ200 trp1Δ63 ESM356 pWS103 GAL1-UPL-TEM1::klTRP1 Atg18-6HA-HIS*	*(Sikorski & Hieter, 1989)*
CDY26	*ESM356 Nat-Gal1-Cdc20 Atg18-6HA-HIS*	*This study*

6.2 Table of Plasmids

Table 6. 2: Table showing the plasmids used in this thesis.

Plasmid Name	Description	Reference
pYM3	*6HA-kITRP1*	(Knop et al., 1999)
pBK067-1	*mCherry-TUB1-LEU2-containing integration plasmid*	(Knop et al., 1999)
pFA6a	*pSM471 NcoI/EcoRV+ HIS5*	(Knop et al., 1999)
pYM24	*3HA-hphNT1*	(Knop et al., 1999)
pRS305	LEU2-dependent yeast integration plasmid	(Caydasi et al., 2017; Caydasi et al., 2014)

6.3 Table of Primers

Table 6. 3: Table showing the primers used in this thesis.

Primer name	Description
Atg18-S1	AATAGTGTTCCAGTTAACTCTGTATCCTTTTCTTCTTCGGCCTGACAATGcgtacgctgcaggtcgac
Atg18-S2	GTGTATGCGTTGTGACGTACGGAAGGCAGCGCGAGACACTTCCGTGATCAatcgatgaattcgagctcg
Atg18-S3	AGAGAGGCGGCGATTGCTTAATATTGTCACAGTATTCCATCTTGATGGATcgtacgctgcaggtcgac
Vac7-S1	TTATCGTTTCATCTCAGGCAAGTTAAAGCATTTGGGAAACGTGCTAGATGCGTACGCTGCAGGTCGAC
Vac7-S2	AAAAAGAAAAATACCCAGCTTTGACGAAAAAGCTACATTCTTAACACTCAATCGATGAATTCGAGCTCG
Vac14-S1	TTGATGCTGCTGTGCTTATCTGCTCAGGCTACAACAGGAACTGGAACATGCGTACGCTGCAGGTCGAC

6.4 Table of Reagent, Buffer, and Chemicals

Table 6. 4: Table showing the reagents, buffers and chemicals used in this thesis.

Name	Description
TY agar with selective antibiotics (Ampicillin or Kanamycin)	5 g of NaCl (Merck, #106498), 5 g of Yeast Extract (Conda, #1702), 10 g of Tryptone (Biolife, #4122902), 20 g of Agar (Carl Roth, #5210.2), ddH2O up to 1000 mL. 100 µg/mL Ampicillin or 50 Kanamycin µg/mL
10X PCR Buffer	500mM Tris-HCl pH: 9.2 (Sigma, #T1503), 160mM (NH4)2SO4, 17.5mM MgCl2 (Fisher BioReagents, #BP214)
1X Blotting Buffer	25mM Tris, 190mM Glycine (AppliChem, #A1067), 0.025% SDS (Sigma, #75746), 20% methanol (Sigma, #32213)
1X Laemmli Running Buffer	25mM Tris, 192mM Glycine, 0.1% SDS, adjust pH to 8.3
1X PBS	137mM NaCl, 2.7mM KCl (Merck, #104936), 10mM Na2HPO4 (Merck, #106575), 1.76mM KH2PO4 (Fisher BioReagents, #BP362). Adjust pH to 7.2-7.4
1X PBS-T	137mM NaCl, 2.7mM KCl, 10mM Na2HPO4, 1.76mM KH2PO4. Adjust pH to 7.2-7.4 and add Tween-20 in final concentration of 0.02% (AppliChem, #A4974)
1X TAE Buffer	4.84 g of Tris, 1.14 mL of Glacial acetic acid (Isolab, #901016), 2 mL of 0.5M EDTA pH:8.0 (Sigma, #E5134), ddH2O up to 1000 mL.
2mM dNTPs mix	20 µL of dATP (100 mM), 20 µL dCTP (100 mM), 20 µL dTTP (100 mM) and 20 µL dGTP (100 mM), 920 µL ddH2O
Homemade ECL Solutions	Solution 1: 20 mL of 1M Tris-HCI pH: 8.5, 2 mL of 250mM Luminol (in DMSO, Sigma # A-8511), 889 µL of 90mM p-Coumaric acid (in DMSO, Sigma # C-9008), 178 mL of ddH2O Solution 2: 20 mL of 1M Tris-HCI pH: 8.5, 180 mL of ddH2O, 123 µL of 30% Hydrogen peroxide (H2O2, Sigma # H-1009)
HU-DTT	8M Urea (MP Biomedicals, #823048), 5% SDS, 200mM Tris-HCl pH: 6.8, 0.1mM EDTA, Bromophenol blue, 100mM 15 mg/mL DTT (Fisher BioReagnets, #BP172)

LiPEG	100mM LiOAc (Sigma, #L6883), 10mM Tris pH: 8.0, 1mM EDTA pH 8.0, 40% PEG3350 (Sigma, #P4338) ddH2O to complete the desired volume. Filter to sterilize.
LiSORB	100mM Lithium Acetate (LiOAc), 10mM Tris pH: 8.0, 1mM EDTA pH: 8.0, 1M Sorbitol (Merck, #107758), ddH2O to complete the desired volume. Filter to sterilize
P1 Buffer	50mM Tris-HCl pH:8.0, 10mM EDTA pH 8.0, 0.1 mg/mL RNase A
P2 Buffer	200mM NaOH, 1% SDS
P3 Buffer	3M KAc pH: 5.5
Ponceau S	0.2% (w/w) Ponceau S (Sigma #P3504) 3% (w/w) TCA in ddH2O
SC-X (X= URA, LEU, HIS or TRP)	3.4 g of Bacto Yeast Nitrogen Base (YNB) without amino acids with ammonium sulfate, 1 g of SC-X dropout amino acid mix, 10 g of D- (+)-Glucose, 0.05 g of Adenine hemisulfate salt (Sigma # A9126), ddH2O up to 500 mL
SC-X with selective antibiotics (Geneticin, Nourseothricin, or Hygromycin)	1.7 g of Yeast Nitrogen Base without amino acids without ammonium sulfate (Conda, #1553), 1 g of monosodium glutamic acid, 2 g of dropout amino acid mix, 20 g of D-(+)-Glucose, 20 g of Agar, ddH2O up to 500 mL were mixed and autoclaved, then mixed with 20 g of sterile agar in 500 mL ddH2O. 200 mg/L G418, 100 mg/L Nourseothricin or 300 mg/L Hygromycin into autoclaved agar
TY agar	5 g of NaCl, 5 g of Yeast Extract, 10 g of Tryptone, 20 g of Agar, ddH2O up to 1000 mL
TY medium	5 g of NaCl, 5 g of Yeast Extract, 10 g of Tryptone, ddH2O up to 1000 mL
TY medium with selective antibiotics (Ampicillin or Kanamycin)	5 g of NaCl, 5 g of Yeast Extract, 10 g of Tryptone, ddH2O up to 1000 mL. 100 µg/mL Ampicillin or 50 Kanamycin µg/mL
YPAD	5 g of Yeast Extract, 10 g of Peptone (Conda, #1616), 10 g of D-(+)- Glucose, 0.05 g of Adenine hemisulfate salt, ddH2O up to 500 mL

YPD with selective antibiotics (Geneticin, Nourseothricin, or Hygromycin)	10 g of Yeast Extract, 20 g of Peptone, 20 g of D-(+)-Glucose, 20 g of Agar, ddH2O up to 1000 mL. 200 mg/L G418, 100 mg/L Nourseothricin or 300 mg/L Hygromycin in autoclaved agar

6.5. Table of Selected Hits from MS Analysis

Table 6. 5: Table of Selected Hits from MS Analysis

Gene name	Name Description	Description
TEF1	Translation Elongation Factor	GTP-bound active form, binds to and delivers aminoacylated tRNA to the A-site of ribosomes for elongation of nascent polypeptides
RPL20B	Ribosomal Protein of the Large subunit	Ribosomal 60S subunit protein L20B
YEF3	Yeast Elongation Factor	Binds and hydrolyzes ATP
RPL5	Ribosomal Protein of the Large subunit	Ribosomal 60S subunit protein L5
RPS5	Ribosomal Protein of the Small subunit	Protein component of the small (40S) ribosomal subunit
NSR1	-	Nucleolin, nucleolar protein that binds nuclear localization sequences;

		required for pre-rRNA processing and ribosome biogenesis
ZUO1	ZUOtin	Ribosome-associated chaperone; zuotin functions in ribosome biogenesis and as a chaperone for nascent polypeptide chains in partnership with Ssz1p and SSb1/2
RPS11B	Ribosomal Protein of the Small subunit	Protein component of the small (40S) ribosomal subunit
RPL24A	Ribosomal Protein of the Large subunit	Ribosomal 60S subunit protein L24A; forms two bridges within ribosome, stimulates translation initiation and elongation
RPS13	Ribosomal Protein of the Small subunit	Protein component of the small (40S) ribosomal subunit
RPL21A	Ribosomal Protein of the Large subunit	Ribosomal 60S subunit protein L21A
RPL28	Ribosomal Protein of the Large subunit	Ribosomal 60S subunit protein L28

RPL35B	Ribosomal Protein of the Large subunit	Ribosomal 60S subunit protein L35B;
RPS20	Ribosomal Protein of the Small subunit	Protein component of the small (40S) ribosomal subunit
RPS18B	Ribosomal Protein of the Small subunit	Protein component of the small (40S) ribosomal subunit
IDH2	socitrate DeHydrogenase	Subunit of mitochondrial NAD(+)-dependent isocitrate dehydrogenase; complex catalyzes the oxidation of isocitrate to alpha-ketoglutarate in the TCA cycle; phosphorylated
PET9	PETite	Major ADP/ATP carrier of the mitochondrial inner membrane
PSA1	-	GDP-mannose pyrophosphorylase, required for normal cell wall structure
NOC2	NucleOlar Complex associated	Protein involved in ribosome biogenesis

OLA1	Obg-Like ATPase	Specifically interacting with the proteasome
RPN2	Regulatory Particle Non-ATPase	Subunit of the 26S proteasome
ATP1	ATP synthase	Evolutionarily conserved enzyme complex required for ATP synthesis
CKA2	Casein Kinase Alpha' subunit	lpha' catalytic subunit of casein kinase 2 (CK2); CK2 is a Ser/Thr protein kinase with roles in cell growth and proliferation
NAT1	N-terminal AcetylTransferase	N-terminally acetylates many proteins to influence multiple processes such as cell cycle progression
EFT1	Elongation Factor Two	catalyzes ribosomal translocation during protein synthesis
RBG1	Ribosome interacting Gtpase	Associates with translating ribosomes
RVB1	RuVB-like	Involved in multiple processes such as chromatin remodeling, box C/D

		snoRNP assembly, and RNA polymerase II assembly
RPF2	Ribosome Production Factor	Essential protein involved in rRNA maturation and ribosomal assembly
LGE1	LarGE cells	Protein involved in histone H2B ubiquitination; acts as cofactor for Bre1p
NET1	Nucleolar silencing Establishing factor and Telophase regulator	Core subunit of the RENT complex; involved in nucleolar silencing and telophase exit
RVB2	RuVB-like	Involved in multiple processes such as chromatin remodeling, box C/D snoRNP assembly, and RNA polymerase II assembly
SSD1	Suppressor of SIT4 Deletion	Translational repressor; involved in polar growth, wall integrity. Interacts with TOR pathway components; nucleocytoplasmic shuttling appears to be critical to Ssd1p function

RPL21B	Ribosomal Protein of the Large subunit	Ribosomal 60S subunit protein L21B
STH1	SNF Two Homolog	ATPase component of the RSC chromatin remodeling complex; required for expression of early meiotic genes
TAF5	TATA binding protein-Associated Factor	Involved in RNA polymerase II transcription initiation
SKI3	SuperKIller	Ski complex component and TPR protein; mediates 3'-5' RNA degradation by the cytoplasmic exosome
RPL25	Ribosomal Protein of the Large subunit	Ribosomal 60S subunit protein L25
RPL43B	Ribosomal Protein of the Large subunit	Ribosomal 60S subunit protein L43B
SBP1		Protein that binds eIF4G and has a role in repression of translation
PDB1	Pyruvate Dehydrogenase Beta subunit	E1 beta subunit of the pyruvate dehydrogenase (PDH) complex

MRPS35	Mitochondrial ribosomal protein of the small subunit	Mitochondrial Ribosomal Protein, Small subunit
MYO3	MYOsin	One of two type I myosins; localizes to actin cortical patches
RPO31	RNA POlymerase	RNA polymerase III largest subunit C160
IMH1	shares with Integrins and Myosins significant Homology	Protein involved in vesicular transport; mediates transport between an endosomal compartment and the Golgi
BFR1	BreFeldin A Resistance	Component of mRNP complexes associated with polyribosomes; involved in localization of mRNAs to P bodies
CHS5	CHitin Synthase-related	Component of the exomer complex
BBC1	Bni1 synthetic lethal and Bee1 (las17) Complex member	Protein possibly involved in assembly of actin patches
OYE2	Old Yellow Enzyme	Conserved NADPH oxidoreductase containing flavin mononucleotide

MAK21	MAintenance of Killer	Constituent of 66S pre-ribosomal particles; required for large (60S) ribosomal subunit biogenesis
NOP4	NucleOlar Protein	Nucleolar protein; essential for processing and maturation of 27S pre-rRNA and large ribosomal subunit biogenesis
DBP8	Dead Box Protein	ATPase, putative RNA helicase of the DEAD-box family
RPA135	RNA Polymerase A	RNA polymerase I second largest subunit A135
CLU1	CLUstered mitochondria	Subunit of the eukaryotic translation initiation factor 3 (eIF3)
PMA1	Plasma Membrane ATPase	Plasma membrane P2-type H+-ATPase; pumps protons out of cell; major regulator of cytoplasmic pH and plasma membrane potential
RPP0	Ribosomal Protein P0	Conserved ribosomal protein P0 of the ribosomal stalk

RPL12B	Ribosomal Protein of the Large subunit	Ribosomal 60S subunit protein L12B
PGI1	PhosphoGlucoIsomerase	Glycolytic enzyme phosphoglucose isomerase; catalyzes the interconversion of glucose-6-phosphate and fructose-6-phosphate; required for cell cycle progression
PDX1	Pyruvate Dehydrogenase complex protein X	E3-binding protein of the mitochondrial pyruvate dehydrogenase complex
RPL11B	Ribosomal Protein of the Large subunit	Ribosomal 60S subunit protein L11B
HSV2	Homologous with SVP	Phosphoinositide (PI) binding protein; involved in micronucleophagy; belongs to the PROPPIN family of proteins defined by a seven-bladed beta-propeller fold and FRRG motif required for PI binding
SPT5	SuPpressor of Ty's	Spt4p/5p (DSIF) transcription elongation factor complex subunit

SCP160	S. cerevisiae protein involved in the Control of Ploidy	Essential RNA-binding G protein effector of mating response pathway
DBP3	Dead Box Protein	RNA-Dependent ATPase, member of DExD/H-box family
PAB1	Poly(A) Binding protein	Mediates interactions between the 5' cap structure and the 3' mRNA poly(A) tail
DED1	Defines Essential Domain	ATP-dependent DEAD-box RNA helicase with strand-annealing activity
LAT1	-	Dihydrolipoamide acetyltransferase component (E2) of the PDC
PDA1	Pyruvate Dehydrogenase Alpha	E1 alpha subunit of the pyruvate dehydrogenase (PDH) complex
TIF4631	Translation Initiation Factor	Translation initiation factor eIF4G and scaffold protein
GUS1	GlUtamyl-tRNA Synthetase	Glutamyl-tRNA synthetase (GluRS)

NPL3	Nuclear Protein Localization	RNA-binding protein; promotes elongation, regulates termination, and is involved in nuclear export of poly(A) mRNA
RRP5	Ribosomal RNA Processing	RNA binding protein involved in synthesis of 18S and 5.8S rRNAs

All the information in this table was collected from SGD (Saccharomyces Genome Database) (Cherry et al., 2012)